

COOPERATIVE SENSING SCHEDULING STRATEGIES FOR COGNITIVE
RADIO NETWORKS

by

Salim Eryiğit

B.S., Industrial Engineering, Boğaziçi University, 2003

M.S., Computer Engineering, Boğaziçi University, 2008

Submitted to the Institute for Graduate Studies in
Science and Engineering in partial fulfillment of
the requirements for the degree of
Doctor of Philosophy

Graduate Program in Computer Engineering
Boğaziçi University

2014

ACKNOWLEDGEMENTS

First of all, I would like to thank my thesis supervisor Assoc. Prof. Tuna Tuğcu not only for his guidance during this thesis but also for his endless support, kindness, and patience. His helpful comments and brilliant ideas made this possible.

I also would like to express my gratitude to Prof. Fatih Alagöz and Assoc. Prof. Albert Levi for their insightful and leading comments in my progress presentations and for being in my thesis committee. I am grateful to Prof. Cem Ersoy for being in my committee and our wonderful academical and social conversations. Finally, I would like to thank Prof. Sema Oktuğ for her participation in my thesis committee.

I am indebted to Suzan Bayhan for her ideas, collaboration and support. Without her, it would be more challenging to finish this thesis. I also like to thank Gürkan, Ali, Birkan, Şükrü and all other members of SATLAB and NETLAB for their support and friendship.

I would like to express my sincere thanks to my close friends, namely Erinç, Deniz, Umut, Derya, Alper, Baki and Alber. I always felt refreshed and happy after meeting them.

Finally, I am really thankful to my family, and especially my spouse Özge. She always made me feel special by being caring, supportive and bearing me in my ups and downs.

This thesis is partially supported by the Scientific and Technical Research Council of Turkey (TUBITAK) under BIDEB 2111 (National Ph.D. Scholarship) and grant number 112E011, Boğaziçi University Research fund under grant number BAP-7437, and State Planning Organization of Turkey under grant number 07K120610.

ABSTRACT

COOPERATIVE SENSING SCHEDULING STRATEGIES FOR COGNITIVE RADIO NETWORKS

In this thesis, our main focus is on cooperative sensing scheduling (CSS) for cognitive radio networks (CRNs). We first consider the joint scheduling of sensing and transmission for a multi-channel CRN with varying sensing accuracy among secondary users (SUs). We give the optimization model that maximizes the expected throughput together with our solution methodology. Then, we turn our attention to the trade-offs involved in providing energy efficiency (EE) in CRNs. We analyze how these trade-offs affect each other and energy consumption of CRNs. Furthermore, we also explore future research directions that are related to the EE of CRNs. After discussing the factors regarding EE, we focus on the EE of CSS for two cases. For the first case, we consider the energy consumption of CSS in terms of sensing and reporting energy components. For the second case, we also take the energy consumption due to channel switching into account. We provide the optimization models together with optimal solution methods for both cases. Our models support heterogeneous channel conditions, which allows us to adjust the sensing durations based on the signal strength. Moreover, we also propose time efficient suboptimal heuristic methods. We observe that sacrificing little transmission time results in huge energy savings in the long run. Finally, we delve into the CSS problem in a social CRN setting where SUs cooperate probabilistically based on their social ties. In this scenario, we first formulate the cooperative detection and false alarm probabilities in addition to a simple trust mechanism. Subsequently, we give a multi-objective optimization model that maximizes expected throughput and accuracy of sensing results together. Numerical evaluations show that our method performs very close to the expected throughput optimal solution when there are no malicious SUs and outperforms it in case of a misbehaving SU.

ÖZET

BİLİŞSEL RADYO AĞLARI İÇİN YARDIMLAŞMALI ALGILAMA ÇİZELGELEME STRATEJİLERİ

Bu tezde ana ilgi alanımız bilişsel radyo ağları (BRAlar) için yardımlaşmalı algılama çizelgelemesidir (YAÇ). Öncelikle çok kanallı ve ikincil kullanıcıların (İK) algılama doğruluklarının farklı olduğu bir BRA'da algılama ve iletişimin ortak çizelgelemesine odaklanıyoruz. Beklenen üretilen işi en büyüten en iyileme modelini, kullandığımız çözüm yöntemi ile birlikte sunuyoruz. Daha sonra, dikkatimizi BRA'larda enerji verimliliği (EV) sağlamak için verilen ödünlere çeviriyoruz. Bu ödünlerin birbirlerini ve BRA'ların enerji tüketimini nasıl etkilediğini analiz ediyoruz. Ayrıca, BRA'ların EV ile ilgili araştırma konularını keşfediyoruz. EV ile ilgili faktörleri tartıştıktan sonra YAÇ'lerinin EV'ne iki farklı durum için yoğunlaşıyoruz. Birinci durumda YAÇ'nin enerji tüketiminin algılama ve raporlama bileşenlerini düşünüyoruz. İkinci durum için ise kanal değiştirmenin de enerji tüketimini hesaba katıyoruz. İki durum için de en iyileme modellerini ve en iyi çözüm bulma metotlarını sağlıyoruz. Modellerimiz heterojen kanal şartlarını destekliyor ve sinyal gücüne göre algılama süresini değiştirmemize imkan veriyor. Ayrıca zaman etkin, idealin altında keşifsel metotlar öneriyoruz. İletişim zamanından çok az feragat etmenin uzun vadede büyük enerji tasarrufunu getirdiğini gözlemliyoruz. Son olarak, İK'ların olasılıksal olarak yardımlaştığı sosyal bir BRA'da YAÇ problemine bakıyoruz. Bu senaryoda ilk önce yardımlaşmalı tespit etme ve yanlış alarm olasılıklarına ek olarak basit bir güven mekanizması formülleştireyoruz. Daha sonra, beklenen üretilen işi ve algılama sonuçlarının doğruluğunu birlikte en büyüten çok amaçlı bir en iyileme modeli veriyoruz. Sayısal değerlendirmeler metodumuzun kötü niyetli İK'ların olmadığı en iyi beklenen üretilen iş çözümüne çok yakın olduğunu, ve kötü davranan bir İK olması durumunda ise çok üstün olduğunu göstermektedir.

TABLE OF CONTENTS

ACKNOWLEDGEMENTS	iii
ABSTRACT	iv
ÖZET	v
LIST OF FIGURES	ix
LIST OF TABLES	xiii
LIST OF SYMBOLS	xiv
LIST OF ACRONYMS/ABBREVIATIONS	xviii
1. INTRODUCTION	1
1.1. Key Contributions	2
1.2. Thesis Outline	4
2. RELATED WORK	7
2.1. Joint Sensing and Transmission Scheduling for Cognitive Radio Networks	8
2.2. Energy Efficient Cooperative Sensing Scheduling for Cognitive Radio Networks	10
2.3. Social Aware Cooperative Sensing Scheduling for Cognitive Radio Net- works	13
3. JOINT CHANNEL AND USER SELECTION FOR TRANSMISSION AND SENSING IN COGNITIVE RADIO NETWORKS	15
3.1. Joint Optimization of Channel and User Selection	16
3.1.1. System Model	16
3.1.2. Optimization Model	17
3.2. Using Genetic Algorithm for Tackling Non-linearity in the Optimization Model	21
3.2.1. Encoding	21
3.2.2. Fitness Function	22
3.2.3. Initial Population	22
3.2.4. Crossover	22
3.2.5. Mutation	25
3.2.6. Replacement	25

3.3.	Evaluation of the Method	26
3.4.	Chapter Summary	28
4.	ENERGY EFFICIENCY: FUNDAMENTAL TRADE-OFFS FOR COGNITIVE RADIO NETWORKS	30
4.1.	Fundamental Trade-offs For Energy Efficiency in Cognitive Radio Net- works	31
4.1.1.	Energy Efficiency vs. QoS	31
4.1.2.	Energy Efficiency vs. Fairness	33
4.1.3.	Energy Efficiency vs. Primary User Interference	35
4.1.4.	Energy Efficiency vs. Network Architecture	37
4.1.5.	Energy Efficiency vs. Security	40
4.2.	Future Research Directions	41
4.2.1.	Social Network Analysis (SNA)	42
4.2.2.	User Behavior	44
4.2.3.	Energy Harvesting	45
4.3.	Chapter Summary	46
5.	ENERGY-EFFICIENT MULTI-CHANNEL COOPERATIVE SENSING SCHED- ULING WITH HETEROGENEOUS CHANNEL CONDITIONS FOR COGNI- TIVE RADIO NETWORKS	47
5.1.	Contributions	48
5.2.	System Model	48
5.3.	Optimization Model and Solution Methodology	51
5.3.1.	Energy Consumption Model	51
5.3.2.	Optimization Model for Energy-Efficient Sensing	53
5.3.3.	Outer Linearization	55
5.3.4.	Transmission Time Maximization (TXT)	57
5.4.	Heuristic Approaches	58
5.4.1.	Sensing Energy Minimization Heuristic (SEM)	58
5.4.2.	Reporting Energy Minimization Heuristic (RPEM)	60
5.5.	Results	60
5.6.	Chapter Summary	66
6.	CHANNEL SWITCHING AWARE AND ENERGY-EFFICIENT COOPERA-	

TIVE SENSING SCHEDULING FOR COGNITIVE RADIO NETWORKS	67
6.1. System Model	67
6.2. Problem Formulation	69
6.3. Outer Linearization (OL)	73
6.3.1. A Low Complexity Heuristic Algorithm: Energy Aware Sensing schEduling (EASE)	73
6.4. Performance Evaluation	74
6.5. Chapter Summary	78
7. OPTIMAL COOPERATOR SET SELECTION IN SOCIAL COGNITIVE RA- DIO NETWORKS	80
7.1. System Model	82
7.1.1. Notations and Assumptions	82
7.1.2. Frame Structure	84
7.1.3. Trust	87
7.1.4. Sensing Accuracy of Social-aware Cooperative Sensing	88
7.2. Cooperator Set Selection	90
7.2.1. Objectives	90
7.2.2. Problem Formulation	91
7.3. Evolutionary Multi-objective Optimization	93
7.4. Numerical Analysis	97
7.5. Chapter Summary	109
8. CONCLUSIONS AND FUTURE RESEARCH DIRECTIONS	111
8.1. Summary of Contributions	111
8.2. Future Research Directions	112
APPENDIX A: PROOF OF THEOREM 5.1.	114
A.1. Proof of Lemma 5.1.	115
APPENDIX B: PROOF OF THEOREM 5.2.	116
REFERENCES	118

LIST OF FIGURES

Figure 3.1.	Frame Structure.	16
Figure 3.2.	Expected throughput and transmitter count for TPM ($N = 100$, $\beta = 0.6$).	27
Figure 3.3.	Expected throughput and transmitter count for TXM ($N = 100$, $\beta = 0.6$).	27
Figure 3.4.	Expected throughput and transmitter count for TPM ($N = 100$, $\mu_{SNR} = 6\text{dB}$).	28
Figure 3.5.	Expected throughput and transmitter count for TXM ($N = 100$, $\mu_{SNR} = 6\text{dB}$).	28
Figure 4.1.	Interaction between EE related concepts for CR.	31
Figure 4.2.	EE and QoS interaction.	34
Figure 4.3.	A CR can control its interference on a PU by adjusting its sensing accuracy and power adaptation along with relaying and channel aggregation. $P^{tx,rx} > P^{tx,1}$ and $P^{tx,rx} > P^{1,rx}$	36
Figure 4.4.	Three dimensions of CRN protocol design.	40
Figure 4.5.	A CRN as a social network with different social ties.	42
Figure 5.1.	A frame starts with a sensing period followed by reporting and transmission periods.	50

Figure 5.2.	Sensing Energy Minimization Heuristic.	59
Figure 5.3.	Reporting Energy Minimization Heuristic.	61
Figure 5.4.	Energy consumption profiles with $N = 200$, $\delta^{min} = 3$, $\alpha = 2$	63
Figure 5.5.	Effect of μ^{SNR} on total sensing energy consumption with $N = 200$, $\delta^{min} = 3$, $\alpha = 2$	63
Figure 5.6.	Effect of number of SUs on total sensing energy consumption with $\mu^{SNR} = -5$ dB, $\delta^{min} = 3$, $\alpha = 2$	64
Figure 5.7.	Energy consumption profiles with $N = 200$, $\delta^{min} = 3$, $\alpha = 2$, $f_s =$ 10 kHz, $\mu^{SNR} = -5$ dB.	64
Figure 5.8.	Effect of sensing duration (T_s) under low and high SNR values with $N = 200$, $\delta^{min} = 3$	65
Figure 6.1.	Frame organization.	68
Figure 6.2.	Channel sensing sequence.	70
Figure 6.3.	EASE algorithm.	75
Figure 6.4.	Energy vs μ^{SNR} with $t^{cs}=1\text{ms}/100\text{kHz}$	76
Figure 6.5.	Energy consumption profiles with $t^{cs} = 1\text{ms}/100\text{kHz}$	77
Figure 6.6.	Energy vs t^{cs}	77
Figure 6.7.	Energy consumption profiles with $\mu^{SNR}=-3\text{dB}$	78

Figure 7.1.	Two layered view of a network.	80
Figure 7.2.	System model: A CR and $N - 1$ CRs in its transmission range. Only some representative links are depicted. The link between CR_i and CR_j is marked with the social tie, cooperation probability, and trust information $(w_{i,j}^{soc}, p_{i,j}, s_{i,j})$ from CR_i 's viewpoint.	83
Figure 7.3.	Steps of the proposed sensing scheme and the time period corresponding to each step in the frame structure. Steps in shaded boxes (cooperation decision and sensing/reporting) are performed by the requested CR, CR_j	85
Figure 7.4.	Steps of social-aware cooperative sensing. Steps in the figure correspond to the steps depicted in Figure 7.3.	85
Figure 7.5.	Evolutionary multi-objective optimization algorithm (EMOA). . .	94
Figure 7.6.	Example solutions for EMOA.	95
Figure 7.7.	Crowding distance assignment algorithm.	97
Figure 7.8.	An example Pareto front found by EMOA. The marked solution is the selected final solution with the highest hypervolume.	98
Figure 7.9.	Physical location of CRs and social graphs	100
Figure 7.10.	Performance evaluation for different scenarios.	103
Figure 7.11.	Performance values per CR for selected scenarios.	106

Figure 7.12. CR properties: node degree, aggregate social tie (with and excluding tie with CR_0), and average social tie. In the figures, CRs are sorted according to their property in decreasing order. 107

LIST OF TABLES

Table 3.1.	Model parameters.	17
Table 3.2.	Parameters for the genetic algorithm.	25
Table 3.3.	Model parameters.	26
Table 4.1.	Future directions and their interactions with the trade-offs.	42
Table 5.1.	Parameter values.	62
Table 6.1.	Model parameters.	76
Table 7.1.	Possible cases for sensing accuracy evaluation.	87
Table 7.2.	Simulation parameters.	99
Table 7.3.	EMOA parameters.	100
Table 7.4.	Realized throughput decrease (percent) in case of an SSDF attack (Scenarios F and H).	108

LIST OF SYMBOLS

a_m	Probability that channel m is available for transmission
b_{final}	Final solution
B_{size}	Population size
\mathcal{B}_t	Population at iteration t
c	Speed of light
C	Throughput
C_m	Number of bits that can be sent in a slot using channel
C_{min}	Minimum of all C_m values
C_n	Ordered set of frequencies sensed by secondary user n
C_{size}	Offspring population size
C_t	Offspring population at iteration t
$d_{PU,j}$	Distance between the primary user and secondary user j
E^{rep}	Total energy consumed for reporting
E_n^{rep}	Reporting energy for secondary user n
E^s	Total energy consumed for sensing
$E_{m,n}^s$	Energy dissipated by secondary user n for sensing channel m
f_m	Frequency of channel m
f_n^0	Initial frequency of secondary user n
f_s	Sampling frequency
G_j	Antenna gain of secondary user j
G_{PU}	Antenna gain of primary user
h	Complex gain of an ideal channel
H	Actual state of the channel
H_i	Final decision of secondary user i
$H_{j,i}$	Sensing outcome of secondary user j
K^T	Number of time slots reserved for transmission in a frame
l	Path loss exponent
L_j	Path loss between the primary user and secondary user j
M	Number of channels

N	Number of secondary users
n_i	Degree of secondary user i
\mathcal{N}^{req}	Set of requested secondary users
\mathcal{N}_k^{req}	Set of cooperating secondary users
N_{th}	Noise floor
$n(t)$	Additive white Gaussian noise
$o_{i,j,k}$	k^{th} interaction between secondary users i and j
P^{cs}	Channel switching power
P^D	Probability of detection
$P_{m,n}^D$	Detection probability of secondary user n for channel m
$P_m^{D,coop}$	Cooperative detection probability for channel m
$_{th}P^{D,coop}$	Threshold for cooperative detection probability
$P_{\mathcal{N}^{req}}^{D,soc}$	Social-aware probability of detection
P^F	Probability of false alarm
$P_{m,n}^F$	False alarm probability of secondary user n for channel m
$P_m^{F,coop}$	Cooperative false alarm probability for channel m
$_{th}P^{F,coop}$	Threshold for cooperative false alarm probability
$P_{\mathcal{N}^{req}}^{F,soc}$	Social-aware probability of false alarm
$p_{i,j}$	Probability that user j complies with the request of user i
p_m	Mutation probability
P^{on}	Probability that the primary user is active
P^s	Sensing power
P^{tx}	Transmission power
P_{PU}^{tx}	Transmission power of primary user
Q	Complementary cumulative distribution of a Gaussian
r	Number of channels that can be sensed
R	Shannon capacity
R_n	Number of bits for user n that need to be sent at next frame
R_{min}^+	Minimum positive R_n value
S	Trust
\mathcal{S}	Set of sensing secondary users

$s_{i,j}$	Trust of secondary user i towards secondary user j
\mathcal{S}_m	Set of secondary users sensing channel m
\mathcal{S}^{rep}	Set of reporting secondary users
T	Frame length
t^{cs}	Time required to switch to the adjacent channel
T^{cs}	Duration of channel switching
T_n^{rem}	Remaining sensing time of secondary user n
T^{rep}	Duration of reporting period
T^{req}	Duration of request period
T^s	Duration of quiet sensing period
T_{opt}^s	Optimal duration of quiet sensing period
T^{tx}	Duration of transmission period
$w_{i,j}^{peer}$	Peer willingness of secondary user j for secondary user i
$w_{i,j}^{soc}$	Strength of the social tie between secondary users i and j
w_j^{sys}	System willingness for secondary user j
$X(t)$	Signal received by the secondary user
α	Scaling factor for the optimal quiet sensing period
β	Activity ratio
$\gamma_{m,n}$	Signal-to-noise ratio for secondary user n over channel m
δ	Required number of sensing users for a channel
δ_i	Sum of social tie strengths for secondary user i
$\tilde{\delta}_i$	Average social tie strength for secondary user i
δ^{max}	Maximum number of sensing users for a channel
δ^{min}	Minimum number of sensing users for a channel
ΔE_n	Additional energy consumption of secondary user n
θ	Percentage of recent observations
λ	Weight of recent observations
μ_{SNR}	Mean value of signal-to-noise ratio
τ_j	Sensing time required by secondary user j
$\tau_{m,n}$	Length of time that secondary user n senses channel m

$\tau_{m,n}^{min}$	Minimum sensing time required by user n for channel m
ϕ	Virtual terminal channel

LIST OF ACRONYMS/ABBREVIATIONS

BINLP	Binary integer nonlinear problem
CBS	Cognitive base station
CR	Cognitive radio
CRN	Cognitive radio network
CSS	Cooperative sensing scheduling
DSA	Dynamic spectrum access
DTN	Delay tolerant network
EASE	Energy aware spectrum sensing
EE	Energy efficiency
EMOA	Evolutionary multi-objective optimization algorithm
ET	Expected throughput
EXP-THR-OPT	Expected throughput optimal
MOP	Multi-objective optimization problem
OL	Outer linearization
PLL	Phase locked loop
POMDP	Partially observable Markovian decision process
PSK	Phase shift keying
PU	Primary user
QoS	Quality of service
REM	Radio environment map
RPEM	Reporting energy minimization
SAP	Small cell access point
SEM	Sensing energy minimization
SNA	Social network analysis
SSDF	Spectrum sensing data falsification
SU	Secondary user
SNR	Signal-to-noise ratio
TC	Transmitter count
TPM	Throughput maximization

TXM	Transmitter maximization
TXT	Transmission time maximization
VCO	Voltage-controlled oscillator

1. INTRODUCTION

Sharing economy — be it a car, a flat, or a network infrastructure [1], emerges as a new approach to services if the commodity of interest is utilized during non-contiguous periods. Such an approach is imperative not only to meet the demand for a restricted pool of resources but also for environmental sustainability. Spectrum sharing can be considered in this line: *secondary users* (SUs) equipped with cognitive radio (CR) capabilities access the spectrum when they need it without holding the exclusive rights for the band. Dynamic spectrum access (DSA) provides the spectrum etiquette for a number of users to share the spectrum *efficiently*, e.g., in terms of throughput or energy, or fairly. In this context, commodity is the *white spectrum* that is not used by the licensed users of the band, *primary users* (PUs). First, SUs have to locate these white spectra by high accuracy spectrum sensing techniques and release it quickly whenever a PU appears in the band. Hence, a sensing period is reserved at the beginning of each frame for the spectrum sensing task. Accuracy of spectrum sensing is measured by the PU detection probability (P^D) and PU false alarm probability (P^F). While achieving high P^D is crucial for not interfering with the PUs, low P^F is essential to harvest the unused spectrum resources for SU transmission.

Previous works [2,3] have shown that *cooperative spectrum sensing* improves the sensing performance, especially in environments where hidden nodes exist. In cooperative sensing, several SUs sense the spectrum and the final decision on the spectrum availability is given considering these individual sensing decisions. However, contrary to local sensing in which each SU senses only by itself, this approach requires communication among cooperating nodes. Therefore, the resulting overhead must be considered.

On the other hand, energy efficiency (EE), which used to be considered as an issue only for battery powered wireless sensors, has become one of the major design criteria for all types of networks. This can be attributed to three main factors: operators, increasing carbon emissions, and mobile users. Regarding operators, energy costs of running a network is reported to be almost 20-30 percent of the operational expenditure

[4]. As energy prices increase consistently, such an expense motivates the operators to take the EE as a principal performance criterion. Regarding carbon emissions, although currently Information and Communication Technologies emit only 2 percent of the global carbon emissions [5], it is naive to underestimate this amount considering the exponential increase in the data traffic. Apart from using renewable energy sources for electricity [6], increasing EE of the system is a viable solution for declining carbon emissions. Finally, regarding the mobile society, accessing the Internet from mobile devices is a daily practice. Power-hungry mobile video traffic has a significant share (i.e. more than 50 percent [7]) in total mobile traffic, which brings EE as an important measure for mobile users. Unfortunately, achieving high EE while preserving the user satisfaction is one of the major research questions [8]. Hence, EE should be considered as a basic design criterion at every scale - from hardware at the small scale to the design of the whole Internet in the large scale.

In this thesis, we approach the cooperative sensing scheduling (CSS) problem in cognitive radio networks (CRNs). Broadly speaking, CSS can be defined as deciding on the channels to sense, the SUs to sense those channels, and possibly their sensing durations. We consider the heterogeneous nature of signal-to-noise ratio (SNR) of individual SUs for each channel since sensing performed by SUs with higher SNR results in more sensing accuracy and less energy consumption.

1.1. Key Contributions

The methods proposed in this thesis cover CSS with the aim of either throughput maximization or EE. For the first objective, we consider the problem both in an infrastructure-based CRN with a cognitive base station (CBS) and an ad hoc CRN with social ties among SUs. For the second objective, our focus is on the infrastructure-based CRNs.

Main contributions of this thesis can be listed as:

- (i) *Joint channel and user selection for transmission and sensing*: In Chapter 3,

we analyze the case where there are insufficient number of SUs¹ to sense all channels. We propose a scheme to select the channels to be sensed together with the sensing assignment of users to selected channels. Our method also considers the transmission requirements of the SUs together with their differing sensing quality metrics. For this task, we propose a system model together with its optimization model for channel selection for transmission and cooperative sensing that maximizes expected throughput of the system. Subsequently, we solve the problem using genetic algorithm along with CPLEX software, and evaluate its performance for different operational parameters.

- (ii) *Fundamental trade-offs regarding the energy efficiency of CRN*: EE is now at the forefront of CR research, as networks become more and more energy-demanding. This demand has been under the spotlight due to the environmental concerns and rising energy costs. In Chapter 4, we provide insight into the major factors regarding EE in CRNs, i.e. how these factors affect EE and each other. Although there is significant research on EE in CRNs, the common approach is to analyze EE considering just a single trade-off, e.g. maximizing EE while satisfying a QoS constraint. To the best of our knowledge, this is the first work that combines these elements to investigate the subtle relations between these factors and EE while highlighting fundamental trade-offs, namely *QoS, fairness, PU interference, network architecture, and security*.
- (iii) *Energy-efficient cooperative sensing scheduling*: Subsequently, we focus on EE of cooperative spectrum sensing in a multi-channel CRN with heterogeneous PU channels in terms of received SNR values. Since scheduling the SUs to sense a number of channels in a CRN is a difficult task [9], we propose three schemes for energy-efficient CSS in Chapter 5. The first one uses outer linearization to find the optimal solution whereas the latter two are efficient heuristic methods. Apart from these three, we also analyze the problem from the transmission time point of view as time spent for sensing is also time lost for transmission. We also analyze the same problem in Chapter 6, but this time we incorporate the channel switching cost (in terms of time and energy) into our design, provide the optimal solution, and develop a heuristic algorithm with low complexity.

¹Throughout this thesis, we use the terms SU and CR interchangeably.

(iv) *Social-aware cooperative sensing*: Almost all of the previous works in CSS assume that an SU that is asked for cooperation is always willing to cooperate. However, this is not the case in reality as SUs may lack the incentives to spend their battery for the benefit of others. In Chapter 7, we study the CSS problem from this point of view by incorporating social ties among the nodes into our design. These social ties determine the willingness of an SU to sense for another SU. Furthermore, we also take into account the case where an SU may act maliciously.

1.2. Thesis Outline

First we propose a joint transmission and scheduling algorithm. Then, we discuss EE issues in CRN and explore future research directions. We also propose energy-efficient CSS methods for CRNs. This is followed by CSS in social CRNs. We give the outline of each chapter below.

We discuss the related works about CSS and EE to identify our contributions to the literature in Chapter 2.

Chapter 3 presents a scheduling scheme that jointly performs sensing and transmission scheduling for infrastructure-based CRNs. Our protocol employs cooperative sensing with hard decisions, and the decision fusion is performed at the CBS with MAJORITY rule. Our goal in this chapter is to maximize the expected throughput. Furthermore, our model accounts for the varying sensing reliability metrics (i.e. different detection and false alarm probabilities) among SUs. We compare this method with another method that maximizes the number of transmitters under different SNR values, SU activity ratios, and required number of cooperating SUs.

In Chapter 4, we discuss the implications of facilitating higher EE in CRNs from the perspective of fundamental trade-offs, i.e. what needs to be sacrificed to be energy-efficient. These trade-offs are identified as QoS, fairness, PU interference, network architecture, and security, which are also essential network design dimensions. We analyze these dimensions and their interactions from the perspective of EE. Furthermore,

future research directions related to the integration of CRN with other networking paradigms and EE are introduced and discussed.

Chapters 5 and 6 focus on the EE of CSS for CRNs. Cooperation in sensing is less error prone, but cooperation also increases the energy spent for sensing. Considering the periodic nature of sensing, even a small amount of saving in each sensing period leads to considerable improvement in the long run. In Chapter 5, we consider the problem of energy-efficient spectrum sensing scheduling with satisfactory primary user protection. Our model exploits the diversity of SUs in their received SNR value of the primary signal to determine the sensing duration for each user/channel pair for higher EE. We model the mentioned problem as an optimization problem with two different objectives. The first one minimizes the energy consumption whereas the second one minimizes the spectrum sensing duration in order to maximize the remaining time for data transmission. We solve both problems using outer linearization method. In addition, we present two sub-optimal but efficient heuristic methods. We provide an extensive performance analysis of our proposed methods under various number of SUs, average channel signal-to-noise-ratio, and channel sampling frequency. Our analysis reveals that all proposals with energy minimization perspective provide significant energy savings compared to a pure transmission time maximization technique. In Chapter 6, we also take the cost of channel switching into account since an SU also spends energy to switch to the next frequency in its sensing sequence. The scheduling scheme that we propose in this chapter discovers the appropriate set of SUs for each frequency by considering the sensing and channel switching energy as well as the energy consumed for reporting the sensing outcomes. We also present a polynomial time heuristic, Energy Aware Spectrum sEnsing (EASE), that performs close to the optimal solution.

In Chapter 7, we focus on a *social CRN* in which CRs cooperate for spectrum sensing based on the social ties among each other. In this network where CRs do not necessarily fulfill every cooperative sensing request, we focus on the cooperator set selection problem, i.e. which CRs to ask for cooperation so that the resulting throughput and sensing accuracy are maximized subject to detection and false alarm probability constraints. We devise a multi-objective optimization model and utilize an evolution-

ary multi-objective algorithm for obtaining the solution. Moreover, we propose various models for a CR's probability to sense for another CR that is asking for cooperation to represent a variety of operation scenarios. Our evaluations show that the proposed multi-objective solution is near-optimal in terms of throughput under legitimate operation, i.e., no malicious users, whereas it outperforms expected throughput-optimal scheme in case of attackers. Numerical analysis demonstrates the robustness of our proposal with little loss of performance when the network is subject to common spectrum sensing attacks.

Chapter 8 concludes this thesis with a summary of our contributions together with the possible research directions to explore.

2. RELATED WORK

Spectrum sensing is the task of deciding whether there exists a PU signal on the channel. It is usually formulated as the following hypotheses:

$$H_0 : X(t) = n(t)$$

$$H_1 : X(t) = hs(t) + n(t)$$

where $X(t)$ is the signal received by the SU, $n(t)$ is the additive white Gaussian noise, and h is the complex gain of an ideal channel.

The common method for spectrum sensing is transmitter detection by energy detection method. In this method, the energy of the received signal is squared and integrated over an observation interval. The resulting value is compared with a threshold value to decide on the existence of a signal. This is also the method that we use in the thesis.

In CSS, sensing results from different sensors are fused to obtain a more accurate sensing decision. Individual sensing results may be hard (0 or 1) or soft (a real number). Hard decisions are usually combined by using *k of N* rule. For instance, OR rule (1 of N) concludes the existence of a PU if at least one sensor reports 1. OR, MAJORITY, and AND are the most commonly used *k of N* rules. On the other hand, soft decisions are combined by making use of a weighted summation. Equal gain combining, maximal-ratio combining, switched combining and selection combining can be listed as well known soft decision fusion strategies.

In this thesis, we focus on the case where the individual sensing results of SUs are hard. We assume MAJORITY rule for fusion just in Chapter 3. All the remaining chapters (5, 6, and 7) employ OR rule.

2.1. Joint Sensing and Transmission Scheduling for Cognitive Radio Networks

Shen *et al.* optimize cooperative spectrum sensing in CR [10]. They introduced the randomized counting rule, that is to decide on the existence of a primary user signal whenever the number of SUs detecting the PU is above a predefined threshold. If the number is equal to the threshold, the decision is taken randomly. They also try to find the optimal value of the threshold under both Neyman-Pearson and Bayesian criteria. Shen *et al.* also try to maximize channel throughput by making use of cooperative sensing strategy [11]. They use energy detection for local sensing, and counting rule for cooperative decision. Their goal is to find the settings for sensing such that the channel throughput is maximized.

Jiang *et al.* investigates the problem on channel sensing order [12]. The problem is given a channel set to sense, in which order to perform sensing such that the time require to find a satisfactory channel is minimum. They observe that without adaptive modulation, intuitive sensing order is optimum where an SU senses the channels in descending order of availability probabilities. If adaptive modulation is used, intuitive sensing order may not be optimal. For this case, they developed a dynamic programming solution to find the optimum order. They also analyze the sensing orders for some special cases for which simple solutions are possible. Furthermore, they devise an algorithm for the case with channel sensing errors that bounds the probability of collisions with primary users.

Fan and Jiang try to find the ideal sensing setting for a multi-channel multi-user secondary network with cooperative sensing [13]. The sensing setting includes the time dedicated for the sensing task, and allocating that time to multiple channels. They aim to maximize the throughput of the secondary network by minimizing the time dedicated for sensing. Slotted-time sensing mode and continuous time sensing mode are investigated cases.

Zhang *et al.* use partially observable Markov decision process for scheduling of

cooperative spectrum sensing [14]. They employ the myopic policy, which may not always be optimal. Moreover, they analyze the properties of the optimal policy for some simple cases. Zhang *et al.* also look at the cooperative sensing scheduling problem from an energy point of view [15]. They maximize the useful energy consumption, and use bisection search to find the optimal solution. Peh *et al.* optimize throughput by employing cooperative sensing [16]. They consider a single channel, and obtain the ideal values of sensing time and type of logic to be used for hard decision combining. They decompose the main problem into two subproblems and obtain a local optimum solution. Song *et al.* also study the single channel case and find the ideal number of secondary users for sensing, and also ideal durations for transmission and sensing [17].

Qu *et al.* study the resource allocation problem for CR based mobile ad hoc networks that use CDMA modulation [18]. Their objective is to minimize the power consumption of the SUs subject to bit error rate and data rate constraints. For spectrum sensing, they employ multitaper spectrum estimation method together with singular value decomposition. They observe that the optimization problem is difficult to solve. Hence, they devise distributed sub-optimal algorithm. Cheng *et al.* propose an optimal solution for joint frequency, rate, and power allocation problem for OFDMA CRNs [19]. By using interference temperature model, they define two optimization problems, both of which are solved both in a centralized and distributed manner.

Hoang, Liang and Zeng focus on a different perspective, and study the problem of how to allocate the slots in a frame for sensing and data transmission such that total throughput is maximized [20]. First, they focus on the case where SUs have always data to send and experience time-varying channels. By making use of a reward function based on the action (transmission or sensing) of an SU, the problem is solved with dynamic programming techniques. Second, they study the more general problem when SUs have stochastic data arrival and deadline constraints. A suboptimal algorithm is developed that aims to reduce the packet loss due to deadline violation by giving more priority to packets with more stringent deadlines and higher sojourn time and have a higher data rate.

Rashid *et al.* studies opportunistic spectrum scheduling from a queuing perspective analytically for an infrastructure-based CRN [21]. PU activity is modeled as a two state Markov chain. Channel fading power gain is assumed to follow Nakagami-m distribution. Packet arrival process for SUs is modeled as a batch Bernoulli process. The system is analyzed as a Markov chain. In addition, based on steady state probabilities performance metrics such as packet queue length, delay distribution, packet loss rate, and average throughput are obtained.

Wang *et al.* proposes a joint cross-layer scheduling and sensing for OFDMA CRNs that limits the average interference on the PU that is closest to the CBS [22]. Their objective is to maximize the average system throughput based on channel state information and raw sensing information. After Lagrangian relaxation, they obtain two subproblems, that are power allocation and user scheduling. Those two problems are iteratively solved using sub-gradient optimization.

These approaches do not differentiate between sensing quality of different SUs. However, thanks to interference, noise and geographical location, an SU has different sensing quality for different channels. Moreover, they assume all channels can be sensed, which is not energy nor time efficient considering the spectrum and operating range of a typical CRN. In Chapter 3, we propose a joint sensing and transmission scheduling scheme that takes these factors into account.

2.2. Energy Efficient Cooperative Sensing Scheduling for Cognitive Radio Networks

EE of CRNs has recently gained interest and most of the initial works focus on the EE of spectrum sensing [23–28] and cooperative sensing [29–33].

Su *et al.* minimize the sensing energy consumption while meeting the constraint on undiscovered spectrum opportunities [24], and adapt the period of spectrum sensing in order to attain a balance between energy consumption and missed spectrum opportunities for a random access CRN [26]. Optimal sensing and transmission durations

for an SU under both high and low SU power capacity are analytically derived in [27]. The effect of transmission, idling, and sensing power consumption are analyzed in that work.

Pei *et al.* devise an optimal policy for a single SU to decide on the order of channels to be sensed as well as when to stop sensing and start transmission [28]. *While all these previous works have valuable contributions, they fall short of practicality.* In practical CRNs, there are multiple and most likely heterogeneous primary channels. In this setting, one of the major concern of the operator is to explore as many PU channels as possible meeting the PU detection and false alarm constraints. Therefore, we enforce the SUs to sense all PU channels collaboratively to maximize the discovered spectrum opportunities in Chapters 5 and 6.

Works in [31] and [32] consider the communication cost for determining the number of cooperating SUs. Maleki *et al.* find the minimum number of cooperating SUs that attains the required detection and false alarm probability performance [31]. The fewer SUs are engaged in sensing, the less time is spent for reporting the sensing outcomes, and thereby the more time is spent for transmission. Moreover, sensing reports from unreliable SUs may decrease the sensing performance. SUs with unreliable sensing information are refrained from reporting their sensing results to save energy in [32]. Each SU evaluates its own reliability by comparing its sensing outcome with the outcomes of other SUs. If it agrees with the results, the SU increases its confidence. Once confidence of an SU exceeds the threshold, it participates in the cooperative sensing.

In addition, a cluster-based decision collection instead of a high power-consuming broadcasting scheme, is also proposed in [32]. The cluster-based scheme adapts the transmission power considering the most distant node. The decision fusion rule (i.e., how the collected sensing information is processed to give the final decision on the existence of PU) at the fusion center also affects the EE. Peh *et al.* [33] tune the k parameter in k -out-of- N fusion rule at each frame as well as the threshold for energy detection scheme at the fusion center. *Heterogeneity of PU channels and SU link conditions* were ignored in these works making the investigated scenarios less realistic.

In addition, assigning the same sensing duration for all SUs regardless of their link conditions may result in waste of energy at SUs with good link conditions. In contrast to these works, we incorporate the effect of signal-to-noise ratios of SUs into our scheme to calculate appropriate sensing duration for each SU and frequency pair in Chapters 5 and 6.

Chen *et al.* observe that with a single channel, the optimal sensing decision is threshold based [34]. The SU senses the channel if the probability that the channel is idle conditioned on the past sensing and observation history, is larger than a threshold. For a channel with fading conditions, the channel access strategy also shows similar behavior. This time, SU accesses the channel if sensing result shows the channel is idle and its fading condition is better than a threshold.

Works in [35,36] and [37] present various solutions for improving the EE of CSS. Sensing scheduling is modeled as a utility maximization problem subject to a certain cooperative detection probability in [35]. In addition, a constraint on minimum discovered transmission time is imposed in order to ensure a certain QoS together with heterogeneous detection probability requirements. Similarly, Zhang *et al.* determine the number of SUs to sense each channel as well as the sensing duration in a slot [36] while Hao *et al.* study the optimal partition of the SUs into coalitions such that the total EE of all coalitions are maximized [37]. Work in [36] utilizes partially observable Markovian decision process (POMDP) framework and tunes the punishment parameter for higher EE. A distributed solution using coalition formation is proposed in [37]. Unlike these works, we consider a heterogeneous environment in terms of SNR of the primary signal at each SU. Using the relationship between SNR and sensing duration in [38], we determine the set of SUs for each primary channel together with the sensing duration. In Chapter 5, we provide the energy-optimal CSS scheme in a CRN with heterogeneous primary channels. Different from Chapter 5, we incorporate the channel switching cost into our design, provide the optimal solution, and develop a heuristic algorithm with low complexity in Chapter 6.

2.3. Social Aware Cooperative Sensing Scheduling for Cognitive Radio Networks

Vast majority of previous works on cooperative spectrum sensing pay attention on the physical layer properties, e.g., the wireless channel between PU and SU, with the goal of exploiting the multi-user diversity. Cooperation increases the information about the state of the channel by multiple measurements at various locations. However, as it entails additional overhead (i.e., communication cost as well as spectrum sensing energy), selection of the most informative nodes as well as avoiding redundant information is essential.

Cacciapuoti *et al.* [39] decrease the redundancy in sensing by exploiting the correlations among CRs and selecting the spatially uncorrelated ones. Reliability of CRs should also be accounted for avoiding (intentional or unintentional) erroneous sensing reports [40]. Zeng *et al.* [41] avoid cooperation with misbehaving CRs by tracking their reputation that reflects the consistency of this CR's decision with the global network decision. We also track the reputation of CRs via recording the sensing consistency of each cooperating CR in Chapter 7. Moreover, we account for the probabilistic nature of sensing and avoid CRs who are not very cooperative.

The use of social networking perspective is not a new research topic but has attracted relatively low interest in CR research. For example, pocket switched networks focus on human contact characteristics to discover the nodes who have higher probability to deliver a message to the destination or serve as a better relay. Degree centrality, betweenness centrality, community structure, social selfishness are all considered as metrics to be exploited in message dissemination in delay tolerant networks (DTNs) [42–44]. Similarly, this perspective has found application in content-centric networks [45] and ad hoc networks [46]. Simply, this approach is based on the idea that nodes in a network have unique characteristics in terms of their interactions with other nodes or their properties. Hence, this diversity of nodes should be exploited to take ultimate benefit from these characteristics. For instance, a mobile node meeting many other nodes may be a good relay as it can spread the message to a large number

of nodes. However, if the network has several sub-groups (e.g. communities), a node which is in contact with nodes from several groups may serve as a better relay to spread the message to diverse set of nodes compared to a node with high meeting rate but meeting only with the members of a single community.

In Chapter 7, we focus on cooperative spectrum sensing in a single collision domain (i.e., a mesh topology) and design a cooperation scheme to highlight how CRs can be aware of the others' cooperation behavior via considering their static (e.g., time invariant) social ties, i.e., friendship tie. However, we should stress that all aforementioned properties can also be applied to CRs, especially for routing similar to DTNs or other cooperative tasks such as relaying.

To the best of our knowledge, there are very few works in this line [47–49]. Güven *et al.* [47] devise a social-aware cooperation scheme that assesses each CR according to the friendship tie between the two CRs, the community the CR belongs to, and sensing history. Different from [47], we formulate the optimal cooperator selection policy and present an evolutionary multi-objective solution methodology for the formulated optimization problem. Chen *et al.* [48] extend the primary channel recommendation scheme among CRs that is proposed in [50]. In these works, a CR that finds a primary channel idle, recommends this channel to other CRs. As spectrum occupancy is time and space correlated, other CRs can benefit from these recommendations. However, since CRs may collide upon attempt to transmit, authors propose efficient access schemes. Bayhan *et al.* [49] emphasize the importance of social network tools for CRNs by listing its potentials for both the user, the operator, and the network designer.

3. JOINT CHANNEL AND USER SELECTION FOR TRANSMISSION AND SENSING IN COGNITIVE RADIO NETWORKS

Spectrum sensing is the biggest challenge in front of CR technology. Moreover, the spectrum is large and sensing all available channels with limited number of SUs is impossible. Hence, a clever mechanism to select channels that can be sensed more accurately is needed together with the assignments of SUs to those particular channels for sensing.

In addition, the transmission requirements of the SUs also affects the channel selection, and should be taken into account. If the channel capacities do not satisfy the user requirements, the utilization and throughput will be low, significantly affecting the performance.

In this chapter, we propose a system model together with its optimization model for channel selection for transmission and cooperative sensing that maximizes expected throughput of the system. Subsequently, we solve the problem using a genetic algorithm along with CPLEX software, and evaluate its performance for different operational parameters [51].

The rest of this chapter is organized as follows: In Section 3.1, we present the system model, define the decision variables and construct the optimization model. Section 3.2 discusses how non-linearity in the optimization problem is handled. The results of the performance analysis are given in Section 3.3. Finally, we conclude the chapter and explore future research directions in Section 3.4.

3.1. Joint Optimization of Channel and User Selection

In this section, we formulate and solve the CSS problem simultaneously with the transmission scheduling for infrastructure-based CR networks.

3.1.1. System Model

In our system model, we assume that all channels operate according to the frame structure given in Figure 3.1. A frame starts with the revision of the transmission schedule for the current frame. After the transmission schedule is revised, it is announced to SUs by the CBS. CBS gathers the requests for the next frame subsequently. Then, data transmission begins. We assume a TDMA scheme with K^T slots for all channels. During data transmission period, CBS works on the sensing and transmission schedule for the next frame. When transmission period ends, the sensing schedule is announced, which is followed by a quiet sensing period where the SUs sense the channels assigned to them. The CBS retrieves the sensing results from the SUs, and based on those results it revises the transmission schedule at the beginning of the next frame.

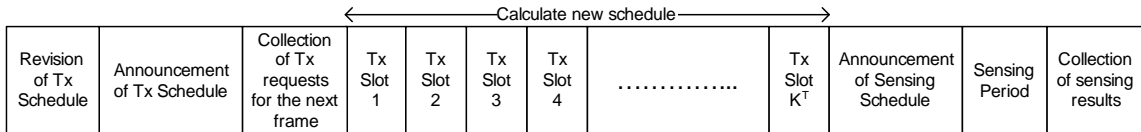


Figure 3.1. Frame Structure.

At the request collection phase, each SU that requires a transmission opportunity for the next frame, informs the CBS about the number of bits it needs to send during the next frame. That is to say, the CBS knows all requirements of the SUs and it tries to allocate channels based on those requirements. However, in order to select the channels for allocation, a subset of all the candidate channels must be sensed. In this chapter, we are mainly focused on the joint scheduling of cooperative sensing and transmission.

We employ a cooperative sensing mechanism with hard decision combining using majority logic since it is less error prone compared to individual sensing. Furthermore,

a couple of criteria should be met in order to use a channel for transmission. Firstly, the result of the sensing procedure should indicate that the channel is not occupied by a PU. Secondly, the channel should be sensed accurately. Let $P_m^{D,coop}$ and $P_m^{F,coop}$ denote the cooperative detection and false alarm probabilities for channel m , respectively. If channel m is to be employed for transmission, we require that $P_m^{D,coop} \geq {}_{th}P^{D,coop}$ and $P_m^{F,coop} \leq {}_{th}P^{F,coop}$ where ${}_{th}P^{D,coop}$ and ${}_{th}P^{F,coop}$ are threshold values for probability of detection and probability of false alarm, respectively. In our model, we assume that in order to successfully sense a channel δ SUs are needed. Moreover, we let individual detection and false alarm probabilities be different not only among SUs but also for different channels for each SU.

Table 3.1. Model parameters.

M	Number of channels
N	Number of SUs
K^T	Number of transmission slots in a frame
a_m	Estimated probability that channel m is available for transmission
R_n	Number of bits for user n that need to be sent at next frame
C_m	Number of bits that can be sent in a slot using channel m
$P_{m,n}^D$	Detection probability of user n for channel m
$P_{m,n}^F$	False alarm probability of user n for channel m
$P_m^{D,coop}$	Cooperative detection probability for channel m
$P_m^{F,coop}$	Cooperative false alarm probability for channel m
${}_{th}P^{D,coop}$	Threshold value for cooperative detection probability
${}_{th}P^{F,coop}$	Threshold value for cooperative false alarm probability

3.1.2. Optimization Model

During the operation of the CRN, we would like to sense as many channels as possible in order to obtain the maximum information about the status of the channels. Since there are many channels and the number of SUs is limited, sensing all channels is usually not an option. Moreover, we also have to keep the cooperative detection, and false alarm probabilities in compliance with their respective thresholds for the channels

that are used for transmission. Hence, we would like to successfully sense the channels that are more likely to be used for transmission by the SUs, and if there are still SUs unassigned for sensing, then sense other channels for updating our information about those channels.

The parameters for the system are given in Table 3.1. In this table, the parameter a_m deserves some explanation. It estimates the probability that channel m is not occupied by a PU. The value of a_m is calculated based on past data. To accommodate for trends such as peak hours of the day, an exponential smoothing procedure or a window based approach can be used. The former takes all of the past data into account whereas the latter takes only the last measurements within the window.

After discussing the parameters, we give the decision variables for the optimization model. Let

$$y_{m,n,t} = \begin{cases} 1, & \text{if channel } m \text{ is used for tx by } SU_n \text{ at slot } t \\ 0, & \text{o/w} \end{cases},$$

$r_{m,n,t}$ = number of bits that will be sent by SU_n using channel m at slot t in the next frame,

$$x_{m,n} = \begin{cases} 1, & \text{if channel } m \text{ is sensed by } SU_n \text{ in this frame} \\ 0, & \text{o/w} \end{cases},$$

$$v_n = \begin{cases} 1, & \text{if } SU_n \text{ transmits during next frame} \\ 0, & \text{o/w} \end{cases},$$

$$u_m = \begin{cases} 1, & \text{if channel } m \text{ is to be sensed in this frame} \\ 0, & \text{o/w} \end{cases},$$

$$z_m = \begin{cases} 1, & \text{if channel } m \text{ is used for tx in the next frame} \\ 0, & \text{o/w} \end{cases}.$$

Then our problem becomes:

$$\max w = \sum_{m=1}^M \sum_{n=1}^N \sum_{t=1}^{K^T} a_m r_{m,n,t} \quad (3.1)$$

subject to

$$\sum_{m=1}^M y_{m,n,t} \leq 1 \quad \forall n, t \quad (3.2)$$

$$\sum_{n=1}^N y_{m,n,t} \leq 1 \quad \forall m, t \quad (3.3)$$

$$\sum_{m=1}^M \sum_{t=1}^{K^T} y_{m,n,t} \leq \frac{R_n}{C_{\min}} v_n \quad \forall n \quad (3.4)$$

$$r_{m,n,t} \leq C_m y_{m,n,t} \quad \forall m, n, t \quad (3.5)$$

$$\sum_{m=1}^M \sum_{t=1}^{K^T} r_{m,n,t} = R_n v_n \quad \forall n \quad (3.6)$$

$$v_n \leq \frac{R_n}{R_{\min}^+} \quad \forall n \quad (3.7)$$

$$\sum_{m=1}^M x_{m,n} \leq 1 \quad \forall n \quad (3.8)$$

$$\sum_{n=1}^N \sum_{t=1}^{K^T} y_{m,n,t} \leq K^T z_m \quad \forall m \quad (3.9)$$

$$z_m \leq u_m \quad \forall m \quad (3.10)$$

$$\sum_{n=1}^N x_{m,n} = \delta u_m \quad \forall m \quad (3.11)$$

$${}_{th} P^{D,coop} z_m \leq P^{D,coop} \quad \forall m \quad (3.12)$$

$$P^{F,coop} \leq {}_{th} P^{F,coop} + (1 - z_m) \quad \forall m \quad (3.13)$$

$$P^{D,coop} = \sum_{A \in H_\delta} \sum_{k=\lceil \delta/2 \rceil}^{\delta} \sum_{B \in A_k} \left[\prod_{i \in B} P_{m,i}^D x_{m,i} \prod_{j \in A \setminus B} (1 - P_{m,j}^D) x_{m,j} \right] \quad \forall m \quad (3.14)$$

$$P^{F,coop} = \sum_{A \in H_\delta} \sum_{k=\lceil \delta/2 \rceil}^{\delta} \sum_{B \in A_k} \left[\prod_{i \in B} P_{m,i}^F x_{m,i} \prod_{j \in A \setminus B} (1 - P_{m,j}^F) x_{m,j} \right] \quad \forall m \quad (3.15)$$

$$y_{m,n,t}, x_{m,n}, v_n, u_m, z_m \in (0, 1) \quad \forall m, n, t \quad (3.16)$$

$$r_{m,n,t} \geq 0. \quad (3.17)$$

The objective in (3.1) maximizes the expected throughput of the system for a frame by favoring channels with large a_m values. Constraint (3.2) ensures that an SU can transmit in a single channel at any given slot since we assume that all SUs have a single transceiver. Constraint (3.3) denotes that at most one SU can transmit in a channel at a given slot. Constraint (3.4) forces v_n to be 1 if SU n transmits at least once during the next frame. In this constraint C_{min} denotes the minimum of all C_m values. Furthermore, this constraint also forces $y_{m,n,t}$ values of user n to zero if R_n is zero. Constraint (3.5) expresses that the number of bits sent over channel m at slot t should be less than or equal to the channel capacity. Constraint (3.6) makes sure that if a user transmits, its requirements are met. Constraint (3.7) forces v_n to 0 if $R_n = 0$. In this constraint, R_{min}^+ is defined as the minimum positive R_n value. Constraint (3.8) guarantees that an SU can sense at most one channel. Constraint (3.9) forces z_m to be 1 if some SU transmits on that channel during the frame. Constraint (3.10) expresses that if a channel is to be used for transmission, it has to be sensed. We ensure that a channel is sensed by exactly δ users by constraint (3.11). Constraints (3.12) and (3.13) are used for forcing cooperative detection and false alarm probabilities meet the specified threshold criteria if a channel is used for transmission.

The mathematical definitions of $P^{D,coop}$ and $P^{F,coop}$ for majority logic are given in constraints (3.14) and (3.15), respectively. Let us focus on constraint (3.14). Let H be the set $\{1, 2, \dots, N\}$, and let H_δ denote the set of all the subsets of H with δ elements. Similarly, A_k denotes the set of all the subsets of A with k elements. In constraint (3.14), we select a set B from A_k where k ranges from $\lceil \delta/2 \rceil$ to δ for majority logic. The elements in B are the ones that correctly sense the channel (success), and contribute $P_{m,i}^D$. The elements in $A \setminus B$ constitute the users that sense the channel incorrectly (failure), and contribute $(1 - P_{m,j}^D)$. We should state that in order for the product terms be different than zero, all $x_{m,i}$ and $x_{m,j}$ values should be 1. Hence, if

we perform this task over all the subsets of H with δ elements, we find the probability of successful detection of a given channel for the majority logic with the given set of SUs (with $x_{m,n} = 1$). The same arguments also apply for constraint (3.15). Finally, constraints (3.16) and (3.17) merely define the types of variables.

We also propose another problem with the same set of constraints but with a different objective, $\max w = \sum_{n=1}^N v_n$. This objective tries to maximize the number of transmitting SUs in a frame, that is to say it maximizes the number of satisfied users. In order to achieve this task, it favors SUs that has low R_n values whereas our first objective favors SUs with high R_n values to maximize throughput. For a given set of parameters, we solve both problems in order to compare the results.

The model given above is highly non-linear thanks to constraints (3.14) and (3.15) and cannot be solved to optimality by commercial solvers.

3.2. Using Genetic Algorithm for Tackling Non-linearity in the Optimization Model

In the given optimization model, once $x_{m,n}$ values are known, the problem becomes a standard binary linear problem that can be solved by commercial solvers. Knowing $x_{m,n}$ values also enables us to know u_m values. Furthermore, we can calculate corresponding $P^{D,coop}$ and $P^{F,coop}$ values easily. Based on those calculated $P^{D,coop}$ and $P^{F,coop}$ values, we set $z_m = 1$ if they satisfy the thresholds. Otherwise, $z_m = 0$, since that channel cannot be used for transmission. We employ a genetic algorithm to find the ideal $x_{m,n}$ and u_m values, and then solve for the other variables using CPLEX solver. We now discuss the details of the genetic algorithm.

3.2.1. Encoding

Encoding defines how we represent a solution. To represent a solution we store the corresponding $x_{m,n}$ values in matrix form and u_m values in a vector form. As an example, with 4 channels, 5 SUs, and a δ value of 2, a possible solution is:

$$x = \begin{bmatrix} 0 & 0 & 0 & 0 & 0 \\ 0 & 1 & 1 & 0 & 0 \\ 0 & 0 & 0 & 0 & 0 \\ 1 & 0 & 0 & 0 & 1 \end{bmatrix}, u = \begin{bmatrix} 0 \\ 1 \\ 0 \\ 1 \end{bmatrix}.$$

Since there are 5 users, at most 2 channels can be sensed. Hence, only two of the u_m values are 1 in this case. That would not be the case if δ was 3.

3.2.2. Fitness Function

We use the objective value of the optimization problem as the fitness value of an individual. As stated above, we employ CPLEX solver to find the optimal value for given x and u .

3.2.3. Initial Population

Before the algorithm starts, we find r , the number of channels that can be sensed, which is given by $\min\{\lfloor N/\delta \rfloor, M\}$. For each individual, we randomly select r channels among M channels, and construct the u vector by assigning u values to 1 for the selected channels. Then, for each channel to be sensed, that is $u_m = 1$, we randomly assign δ users from the set of unassigned ones for the sensing task and obtain z_m values. Then, we calculate the fitness value for each individual.

3.2.4. Crossover

Crossover operator produces offspring that will be added to the population for the next generation. In our algorithm, two parents are used for producing two children. We use roulette wheel selection together with 3-tournament strategy. In other words, for each parent three candidate individuals are inspected. The selection of candidates is done randomly, but candidates with better fitness values have more chance to be selected. Among the three candidates, the best one is selected as the parent.

After the parents are selected, the actual crossover procedure begins. We first select r channels to be sensed among the channels sensed by either the first or the second parent. That is to say, we first form the u vector. Then, for each $u_m = 1$ for the new child, we look at the u_m value of the parents. There are two cases to consider:

- Only one of the parents have $u_m = 1$: We directly copy the $x_{m,n}$ values of that parent at row m to the child.
- Both parents have $u_m = 1$: This time, we randomly select a parent and perform the same procedure.

For instance, let p_1 and p_2 be two parents defined by x_1 and u_1 , x_2 and u_2 , respectively as follows:

$$x_1 = \begin{bmatrix} 0 & 0 & 0 & 0 & 0 \\ 0 & 1 & 1 & 0 & 0 \\ 0 & 0 & 0 & 0 & 0 \\ 1 & 0 & 0 & 0 & 1 \end{bmatrix}, u_1 = \begin{bmatrix} 0 \\ 1 \\ 0 \\ 1 \end{bmatrix};$$

$$x_2 = \begin{bmatrix} 1 & 0 & 0 & 0 & 1 \\ 0 & 0 & 0 & 0 & 0 \\ 0 & 0 & 1 & 1 & 0 \\ 0 & 0 & 0 & 0 & 0 \end{bmatrix}, u_2 = \begin{bmatrix} 1 \\ 0 \\ 1 \\ 0 \end{bmatrix}.$$

Then their children c_3 that is defined by x_3 and u_3 , and c_4 that is defined by x_4 and u_4 may look like:

$$x_3 = \begin{bmatrix} 1 & 0 & 0 & 0 & 1 \\ 0 & 1 & 1 & 0 & 0 \\ 0 & 0 & 0 & 0 & 0 \\ 0 & 0 & 0 & 0 & 0 \end{bmatrix}, u_3 = \begin{bmatrix} 1 \\ 1 \\ 0 \\ 0 \end{bmatrix};$$

$$x_4 = \begin{bmatrix} 0 & 0 & 0 & 0 & 0 \\ 0 & 1 & 1 & 0 & 0 \\ 0 & 0 & 1 & 1 & 0 \\ 0 & 0 & 0 & 0 & 0 \end{bmatrix}, u_4 = \begin{bmatrix} 0 \\ 1 \\ 1 \\ 0 \end{bmatrix}.$$

We observe that c_3 is a feasible child whereas c_4 is not, since SU_3 needs to sense two channels at the same time. Let's now focus on how an infeasible child is transformed into a feasible one.

- Step 1: An SU may be assigned to 0, 1, or 2 channels for sensing. We find the SUs that are assigned to 2 channels and randomly reverse one of those assignments. Thus, after this step c_4 may look like:

$$x_4 = \begin{bmatrix} 0 & 0 & 0 & 0 & 0 \\ 0 & 1 & 1 & 0 & 0 \\ 0 & 0 & 0 & 1 & 0 \\ 0 & 0 & 0 & 0 & 0 \end{bmatrix}, u_4 = \begin{bmatrix} 0 \\ 1 \\ 1 \\ 0 \end{bmatrix}.$$

- Step 2: Even though we solve the double assignment problem, this time there may be channels with less than δ users for sensing. To alleviate the problem, we randomly select from unassigned SUs and assign them to those channels until there are δ users for each channel that is to be sensed. After this step c_4 may look like:

$$x_4 = \begin{bmatrix} 0 & 0 & 0 & 0 & 0 \\ 0 & 1 & 1 & 0 & 0 \\ 0 & 0 & 0 & 1 & 1 \\ 0 & 0 & 0 & 0 & 0 \end{bmatrix}, u_4 = \begin{bmatrix} 0 \\ 1 \\ 1 \\ 0 \end{bmatrix}.$$

After these two steps, a child is guaranteed to be feasible since each SU is assigned to at most one channel, and all channels to be sensed have δ users assigned to them.

3.2.5. Mutation

When we generate offspring population, we perform mutation operation on each new member with some probability p_m . Mutation operation is defined as randomly exchanging two rows of the child. For instance, mutation operator applied to c_4 may result in:

$$x_4 = \begin{bmatrix} 0 & 0 & 0 & 0 & 0 \\ 0 & 1 & 1 & 0 & 0 \\ 0 & 0 & 0 & 0 & 0 \\ 0 & 0 & 0 & 1 & 1 \end{bmatrix}, u_4 = \begin{bmatrix} 0 \\ 1 \\ 0 \\ 1 \end{bmatrix}.$$

3.2.6. Replacement

We use the elitist strategy to perform replacement. We add all offspring to the current population and we discard the ones with worse fitness values such that the original population size is maintained in order to form the next generation. However; when adding an offspring to population, we check that if there is an individual with the same chromosome. If that is the case, we do not include that offspring in the population even if it has a good fitness value, to preserve the diversity.

The algorithm runs for a predefined number of iterations. The parameters that are used for the genetic algorithm are given in Table 3.2.

Table 3.2. Parameters for the genetic algorithm.

Population Size	100
Number of Iterations	100
Offspring Population Size	20
p_m	0.1

3.3. Evaluation of the Method

For the performance evaluation of the proposed method, we assign a uniform random value between (0, 1) for a_m values. $P_{m,n}^F$ is also uniform random between (0.1, 0.4) for each channel-user pair. We assume a Rayleigh channel model with mean SNR, μ_{SNR} . Then for each user and channel, we assign an exponential random SNR value. Based on that value and $P_{m,n}^F$, we calculate the corresponding detection threshold (Δ) and $P_{m,n}^D$. Furthermore, we assign a random channel capacity (C_m) to each channel that is uniformly distributed between (0.125, 2) Mb. Each SU generates traffic for a given frame randomly based on an activity ratio, β . If the random number is smaller than β , we also assign a uniform random R_n value between (0.125, 5) Mb. The same R_n , C_m , a_m , $P_{m,n}^F$ values are used throughout the runs for consistency. In addition, the same SNR value is used for each channel-user pair for a given μ_{SNR} . The other parameters are given in Table 3.3. All values shown in the figures are the average of ten runs.

Table 3.3. Model parameters.

M	20
N	100
K^T	10
${}_{th}P^{D,coop}$	0.9
${}_{th}P^{F,coop}$	0.1
δ	{5, 7, 9, 11, 13}
β	{0.2, 0.4, 0.6, 0.8, 1}
μ_{SNR}	{4dB, 5dB, 6dB, 7dB, 8dB}

The effect of μ_{SNR} on expected throughput (ET) and transmitter count (TC) for different values of δ for throughput maximization (TPM) and transmitter maximization (TXM) is shown in Figures 3.2, and 3.3, respectively. For a given $P_{m,n}^F$, higher SNR implies higher $P_{m,n}^D$. Both performance metrics favor large δ values when μ_{SNR} is low. However, as μ_{SNR} increases both metrics increase for different δ values, the rate of increase for smaller δ being more significant. This is due to the fact that with higher

$P_{m,n}^D$, more channels can be sensed accurately when δ is low. For instance, for a μ_{SNR} of 4dB, taking $\delta = 5$ leads to zero ET since no channel is sensed with adequate accuracy. On the other hand, when $\mu_{SNR} = 8$ dB, a δ value of 5 leads to the maximum ET. Thus, selection of the ideal δ value heavily depends on μ_{SNR} . Another point to note is that, even though ET does not differ significantly for the two objectives, the same argument does not apply to TC, especially for low values of μ_{SNR} .

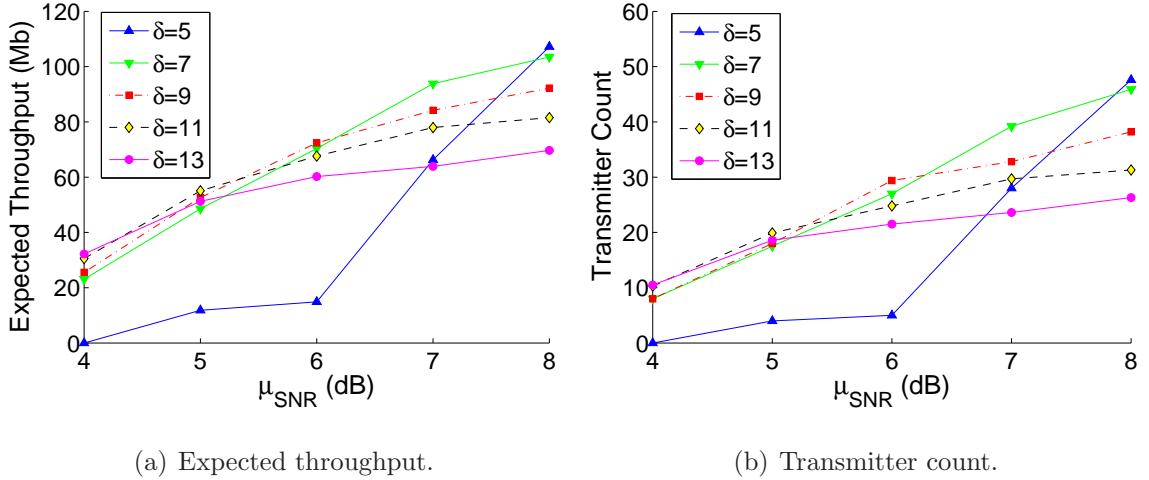


Figure 3.2. Expected throughput and transmitter count for TPM ($N = 100$, $\beta = 0.6$).

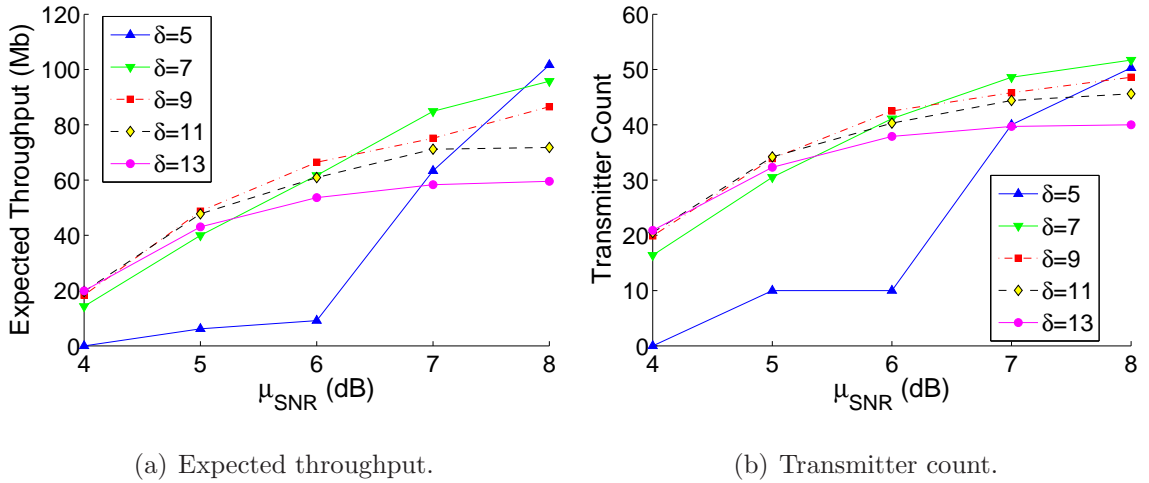


Figure 3.3. Expected throughput and transmitter count for TXM ($N = 100$, $\beta = 0.6$).

The performance metrics for changing β and δ values are given in Figures 3.4, and 3.5. As we can see from Figure 3.4a, ET almost saturates after $\beta = 0.6$ for TPM. On the other hand, ET first increases then slightly decreases for increasing β values for TXM as shown in Figure 3.5a. This can be attributed to the fact that beyond a

saturation point, increasing β adds more users with small R_n values. By favoring those users, although ET slightly decreases, TXM objective increases TC. This fact is also observed from Figure 3.5b. It should be noted that for this case $\delta = 9$ always achieves the best performance.

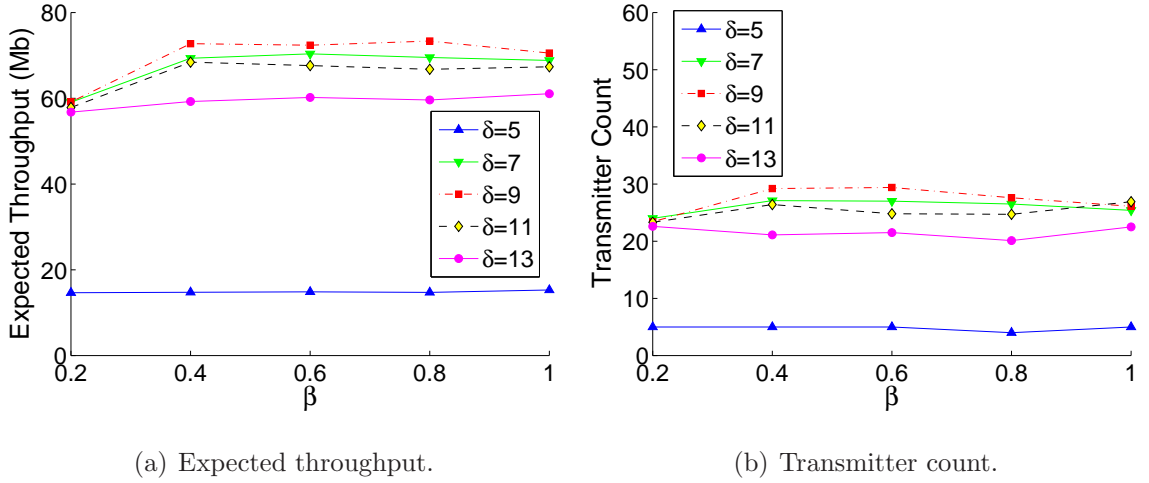


Figure 3.4. Expected throughput and transmitter count for TPM ($N = 100$,

$\mu_{SNR} = 6\text{dB}$).

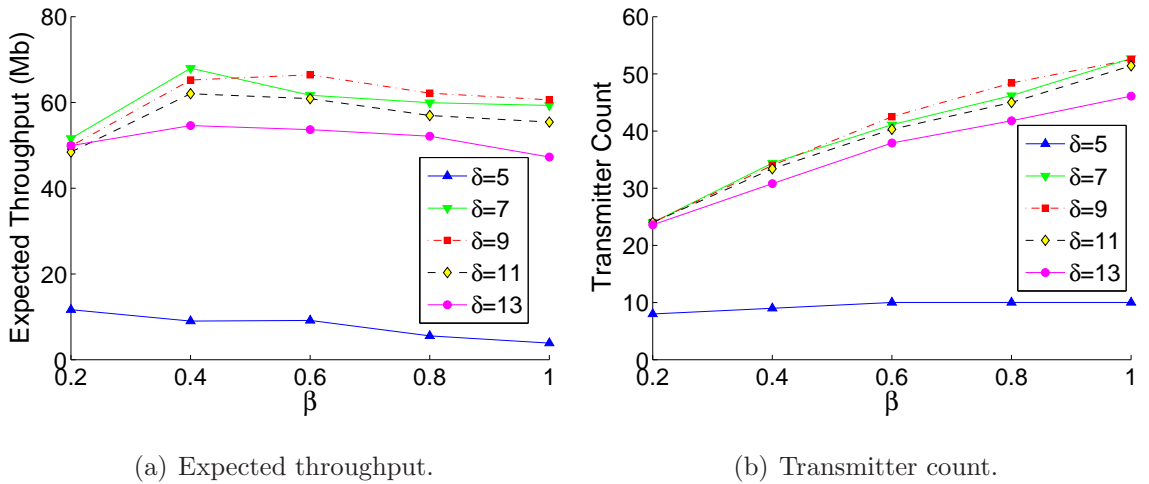


Figure 3.5. Expected throughput and transmitter count for TXM ($N = 100$,

$\mu_{SNR} = 6\text{dB}$).

3.4. Chapter Summary

In this chapter a joint transmission and sensing scheduling problem is defined in terms of its mathematical model together with two alternative objectives. Due to

its non-linear nature, the optimization problem is solved by using genetic algorithm together with CPLEX. For this task, building blocks of the genetic algorithm such as crossover and mutation strategy are defined. Then, both problems are solved for varying set of parameters.

For future work, we plan to model the same problem for a general case by incorporating δ and the decision logic into the model. Hence, it will be possible to select the ideal δ and the decision logic for each channel.

4. ENERGY EFFICIENCY: FUNDAMENTAL TRADE-OFFS FOR COGNITIVE RADIO NETWORKS

Ensuring high EE in a CRN is formidable due to the difficulty in satisfying the competing demands of different stakeholders such as PUs, CRs, and the CR operator. For example, the PUs put strict requirements on the interference and the channel usage of CRs while CRs expect high QoS from the operator, and the operator desires low operating and management costs. This multifaceted challenge constitutes the essence of this chapter: how to provide EE in CRNs while meeting the expectations of different actors and elements in the system. Taking this question as our motivation, we focus on five fundamental trade-offs which are paramount since they affect all the constituents of CRN design and implementation: *QoS*, *fairness*, *PU interference*, *network architecture*, and *security* [52]. Although we elaborate on each trade-off separately, we should note that the relations among these trade-offs are inextricably intertwined. For example, relaying as a potential solution for balancing the EE vs. PU interference trade-off also affects the EE vs. the network architecture trade-off, e.g. complexity and deployment cost.

The investigated trade-offs are depicted in Figure 4.1 from a cognitive map perspective. Deployment and network level factors can be decomposed into various items such as offloading, heterogeneous network architecture, and relaying. Cooperation mechanisms in that domain affect all deployment and network level items in the figure. Security establishes another trade-off, which affects the cooperation item due to the trust mechanisms. It is a critical system-wide attribute that might override EE concerns. On the other hand, PU interference is a CR-native factor, which is crucial for feasibility of CRNs. It interacts with QoS factor, which in turn complicates the fairness trade-off. There are also general issues such as learning, complexity, and dynamism, which emerge when elaborating on the EE trade-offs. Therefore, the distinction among these trade-offs is not that clear-cut.

4.1. Fundamental Trade-offs For Energy Efficiency in Cognitive Radio Networks

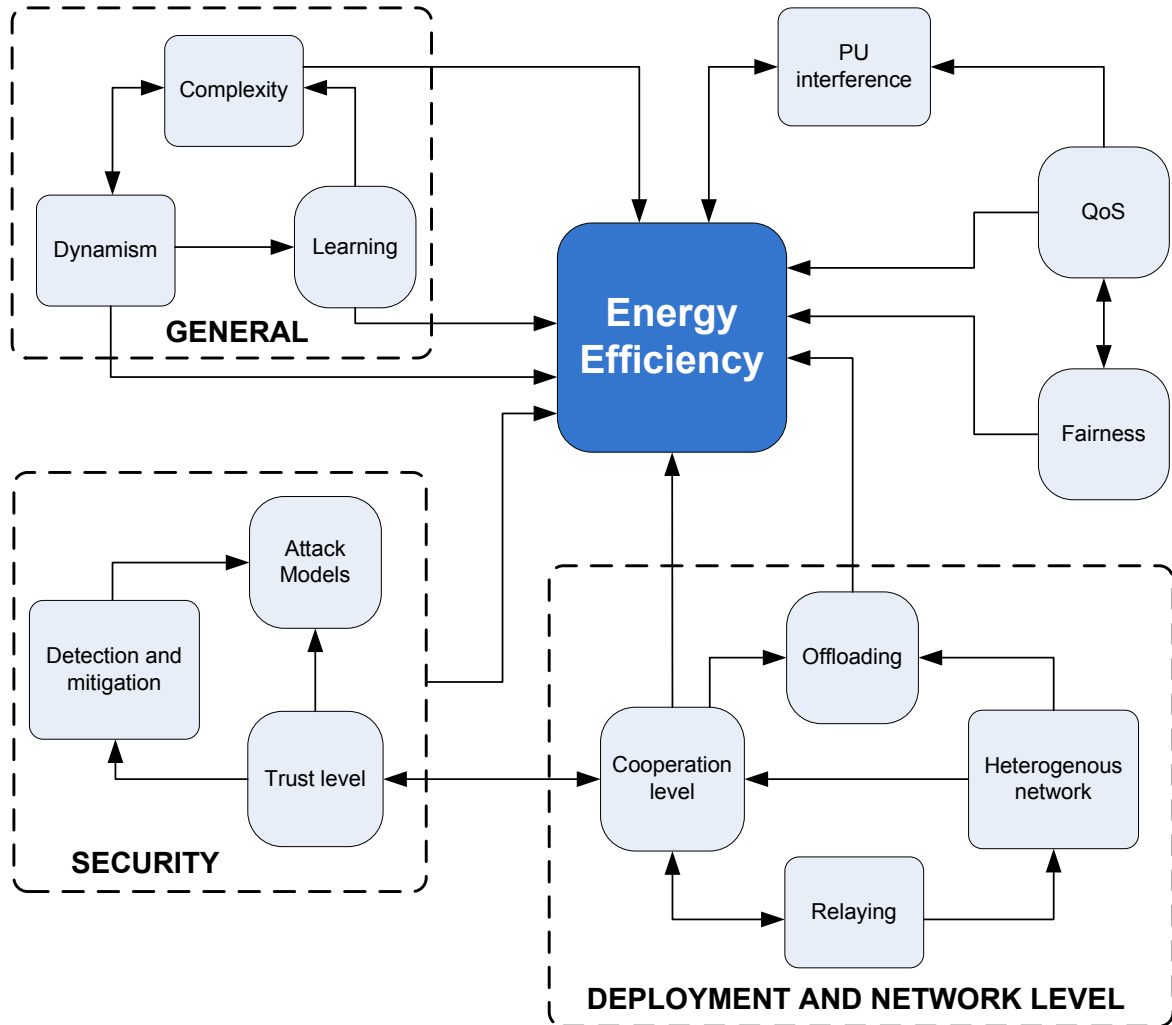


Figure 4.1. Interaction between EE related concepts for CR.

4.1.1. Energy Efficiency vs. QoS

The explosive growth in the use of real-time applications on mobile devices and proliferation of multimedia traffic have resulted in stricter QoS guarantees in terms of sustainable data-rates, packet drop limits, and delay bounds. CRNs have to address the relevant operational environment under these circumstances. This situation complicates the EE concerns since QoS requirements become harder to satisfy when the EE requirements are also applied. The interaction between QoS and EE is depicted in Figure 4.2. It is apparent that the QoS improvement mechanisms may be contradic-

tory to the EE requirements. Moreover, there are also inherent complicating factors such as interference limitations, power budget of the CR system, and imperfect channel sensing. Hence, this problem is typically reflected in resource allocation works for CRNs [53].

QoS for CRNs or CR embedded networks have been examined typically from the DSA perspective. Disruptions from fundamental operations involved in DSA protocols render the deployment of QoS mechanisms challenging. In that regard, QoS can be considered in three directions, the first being the *PU-centric approach* where the primary focus is to protect the QoS of PUs while facilitating DSA. For this purpose, the probability of misdetection is important. The sensing and medium access mechanisms should be highly conservative and SU-insensitive. Thus, the main constraint is not to disturb the incumbent users while maintaining QoS and EE. The EE dimension is not substantially critical for this case. The second approach is to have an *SU-centric* QoS environment by prioritizing the SUs without harming the PUs. For this setting, the interference limitations are relaxed and the solution space of the problem becomes larger. In this case, the aim is to reduce the probability of false alarm as much as possible. For both of these approaches, the specific probability criterion can be reduced by either increasing SNR and/or by increasing sensing time and sampling frequency. As the PU's SNR is beyond the control of the CRN and the sampling frequency is device dependent, increasing sensing time is the only viable solution. However, this increase also results in more energy consumption for the network, especially considering the periodic nature of sensing. Another alternative is to differentiate among SUs when their QoS requirements cannot be met. It is desirable to have the spectrum access opportunity related to the user priority if they belong to different priority classes [54]. The final approach, a natural extension of these two former approaches, is to have a *hybrid* setting where the QoS of the PUs and the SUs are not differentiated categorically but evaluated in a more flexible manner.

In centralized CRNs, once the list of available spectrum opportunities is determined, the CBS assigns these opportunities using one of the above-mentioned approaches. The CBS can exploit various diversities to attain the optimal trade-off

among EE and QoS goals. Conceptually, these diversity techniques can be categorized into four main groups: link diversity, spatial diversity, channel diversity, and CR diversity [55]. Each diversity technique can help improving EE via exploiting different dimensions in a CRN (e.g., CR diversity for throughput potential, channel diversity for lower transmission energy). The CBS can consider the time-varying channel conditions and CR diversity for assigning the favorable channels. However, the CRs operate in a wide range of frequencies, which may be spectrally distant from each other. Overhead of channel switching has to be taken into account, especially for fragmented spectrum (i.e., non-contiguous) together with each channel's throughput promise and energy demand. Since a CR spends non-negligible time in radio reconfiguration for tuning to the new channel, the time spent during channel switching reflects as throughput loss. Moreover, the CR also consumes power in channel reconfiguration, which translates into energy expenditure. Therefore, channel switching should be performed only if the new channel can provide net gains in EE of this CR [56]. To the best of our knowledge, the literature is not mature enough regarding the experimental results from the CRN testbeds on the cost of channel switching.

In multi-hop CRNs, ensuring QoS becomes more challenging due to routing as the paths among network nodes are highly dependent on channel availability [57]. A typical case is cognitive ad hoc networks where a routing algorithm can establish QoS paths with reserved bandwidth on a per flow basis in a multi-hop transmission. For routing, the fundamental QoS mechanism is to establish bandwidth guaranteed routes while considering EE. However, dynamism of CRNs complicates this class of solutions. For CRs, as the number of hops increases, finding a stable/reliable path between the sender and the receiver becomes a significant issue since the channel occupancy may change frequently between hops.

4.1.2. Energy Efficiency vs. Fairness

Fairness for a communication system refers to the degree at which the users utilize a fair share of the system resources [58]. Since CRs allow SUs to share the spectrum

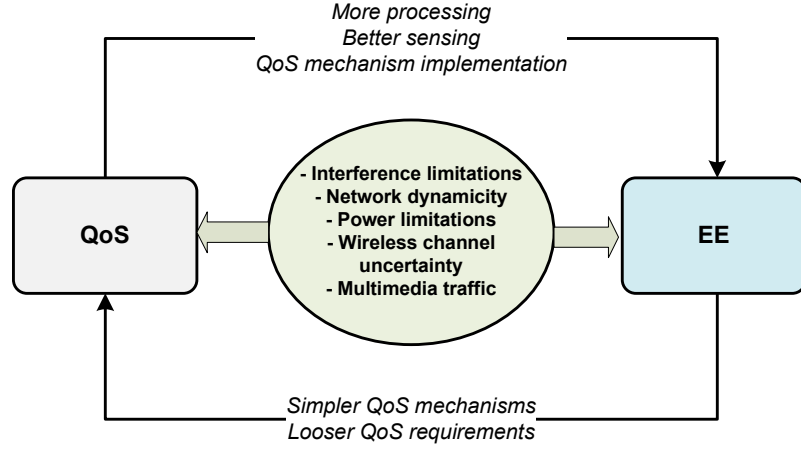


Figure 4.2. EE and QoS interaction.

with the PUs in a dynamic manner, providing fairness among SUs is challenging. Spectrum access and allocation methods should let each user get certain amount of spectrum regardless of its spectral environment, location, or neighbor distribution. The typical trade-off in EE setting is that being unfair in certain cases can be beneficial for EE. The basic underlying requirement is to allocate spectrum as fairly as possible while maximizing the spectrum resource usage and maintaining EE [59].

For fairness on the downlink of centralized systems, EE is usually not mandatory but desired in order to adopt less complex end-user hardware and decrease the operational costs of the operator. On the other hand, EE is required for the uplink due to the mobility and battery-powered operation of user devices. The fairness lends itself to a multiobjective optimization problem since it is not usually considered as the sole objective for CRN design and operation. Thus, the fairness trade-off is typically embedded in QoS and resource optimization problems. For instance, [56] introduces a *satisfaction ratio* for each SU in order to make the scheduler fairness-aware and incorporates this term as a multiplicative term in the resource allocation problem. However, the trade-off between the EE and fairness is yet to be explored adequately. The infrastructure sharing, which corresponds to common exploitation of spectrum and network infrastructure by independent service provider entities, is also an interesting concept to explore this trade-off. It introduces another layer of complexity where a fair allocation is desired among different CRNs while satisfying the inherent “PU-biased unfairness”, i.e. PU priority overriding any fairness requirements towards SUs.

4.1.3. Energy Efficiency vs. Primary User Interference

The fundamental restriction on the CR operation is that the CRs must not harm the PU communications. In other words, the resulting interference due to the CR transmission at the nearby PUs must be below the *tolerable interference limits* for underlay CRNs, and the simultaneous transmission time with the PUs must be considerably short for overlay CRNs. The interference arises under two cases: PU misdetection and PU reappearance. To cope with the first case, the CRs must sense with high detection accuracy, i.e. P^D , so that the probability of collision with a PU is very low. This calls for high P^D , which might be achieved by various techniques: cooperative sensing, longer sensing duration, and higher sampling frequency to name a few. On the other hand, these high P^D promising solutions may be costly in terms of energy consumption compared with a solution demanding less reliability (lower P^D which is still higher than the threshold reliability $_{th}P^d$ required by the PU regulations). For the case of a reappearing PU, no matter how high the achieved P^D is, the PU interference may be experienced due to the nature of *periodic sensing*.

CRNs typically operate on a frame basis where a certain portion of the frame is dedicated for sensing and the rest for transmission. The duration between two consecutive sensing periods determines the performance of spectrum opportunity discovery (thus the throughput) and the resulting PU interference. In periodic sensing, a CR does not notice a reappearing PU until the next sensing period. Frequent sensing leads to increased energy consumption and higher overhead while improving the sensing performance, which directly affects throughput. Hence, deciding on the sensing and transmission durations as well as the period [26] is of major concern for tuning the EE vs. PU interference trade-off.

To account for these two cases, a CR may select to be conservative at the sensing step and/or at the transmission step of the cognitive cycle. Solutions at the sensing step include period adaptation (considering PU traffic pattern [26]) and adjusting the sensing accuracy. At the transmission step, a CR can meet the $_{th}P^d$ restriction and

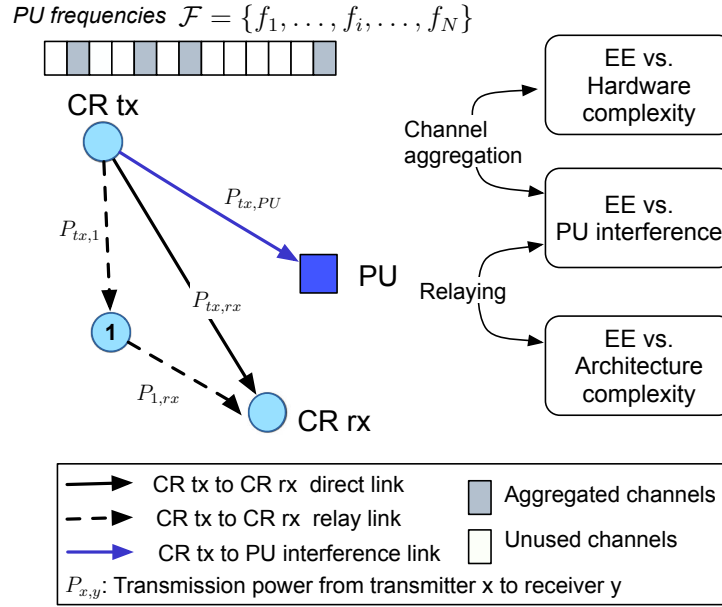


Figure 4.3. A CR can control its interference on a PU by adjusting its sensing accuracy and power adaptation along with relaying and channel aggregation.

$$P^{tx,rx} > P^{tx,1} \text{ and } P^{tx,rx} > P^{1,rx}.$$

can control the interference via regulating its transmission power (P^{tx}). Given that perceived interference at the victim node is a function of P^{tx} , a CR can decrease the PU interference by decreasing P^{tx} . However, as the Shannon's formula shows, the channel capacity also (logarithmically) decreases with P^{tx} . Consequently, both methods result in a trade-off between the EE and the PU interference. Avoiding PU collision is essential not only to protect the PUs, but also to avoid any retransmissions of the CR traffic and to achieve the maximum capacity of the channel. Hence, from the EE viewpoint, simultaneous transmission with the PU must be kept at minimum.

In order to change the EE-PU interference trade-off in favor of EE, the CRs can benefit from relaying [60] and channel aggregation [55]. As depicted in Figure 4.3, relaying lets the CR transmit with lower power but via multiple hops. In case some intermediate nodes relay the CR traffic, capacity improvement due to shorter transmission distance may compensate the channel capacity loss due to the lower P^{tx} . Regarding the cost, relaying may require a change in the network architecture if relays are supposed to be dedicated devices for assisting CRs. These devices evidently add

to the energy consumption of the network. We should recall that providing EE while satisfying the PU interference restrictions, requires us to tune the EE vs. network architecture trade-off. Alternatively, each CR may serve as a relay for the others at the expense of increased energy consumption.

On the other hand, channel aggregation facilitates the CRs to transmit simultaneously via multiple channels. This time, the channel capacity loss due to lower P^{tx} is compensated by higher bandwidth of the aggregated channels. However, channel aggregation demands more capable hardware at the CRs. Both schemes lead to new challenges that deserve further analysis, such as the selection of a relay, placement of the relays, and power allocation at each channel for the optimal EE.

4.1.4. Energy Efficiency vs. Network Architecture

Different types of network architectures may be considered for achieving higher EE in CRNs. Almost all of these architectures benefit from adding additional hops or an infrastructure layer between the CR and the core network to decrease the required transmission energy of CR by decreasing the transmission distance. These architectures can be listed as small cells, relays, ad hoc networks, and clustering.

The goal of deploying cognitive small cells is to offload user traffic from the CBS to small cell access point (SAP), be it a femtocell or a microcell, etc. Interpreting the usage statistics that the majority of traffic originates from indoors, small cells deployed either by the users or the operators can provide high capacity at small localities, e.g. home for femtocells or shopping malls/airports for pico/micro cells. Small cells benefit from spatial diversity to achieve better frequency reuse that leads to higher spectral/throughput efficiency. However, they induce an additional sensing energy component to the network if there is no centralized control (which is a fundamental motive for small cells) as they should not interfere with the surrounding small cells. When cooperative sensing is employed, the energy burden for spectrum sensing may be on the CRs served by the SAP. Furthermore, the number of handoffs a CR performs during operation increases drastically, especially for high mobility cases. We should

also mention that the handoff procedure is more complicated and more energy consuming in a heterogeneous CRN compared to a classical CRN architecture. On the upside, cognitive small cells can cope with the interference issue arising from the unplanned deployment of small cells to some extent by utilizing the unused PU spectrum opportunities.

Another alternative is to use relays together with amplify-and-forward or decode-and-forward type of cooperative communications to save transmission energy by both decreasing the distance and the number of retransmissions. If the CRs are used for relaying packets (which requires the nodes volunteer to spend their energy for the benefit of other CRs), they will suffer additional energy consumption. Moreover, some CRs may become bottlenecks due to their location, and their battery may drain rapidly. Even if dedicated relays are used, relaying may not be as energy-efficient as it seems if the traffic load is low, or the channel conditions are good, or the transmitter is close to the receiver [61]. Hence, it would be better to decide whether to relay or not on a case by case basis. In a highly dynamic radio environment or with highly mobile CRs, this decision induces extra overhead on the network. Another problem with relaying is that the time it takes for successful transmission is multiplied, which may not be feasible for delay-sensitive applications.

Both of the discussed approaches bring an additional layer to the system. The monetary and energy costs of operating additional hardware, like relays or SAPs, are usually neglected in the literature. However, it is known that idling (waiting idle for possible packet reception) consumes almost as much energy as reception [62]. Therefore, clever mechanisms are needed for reducing the operating costs such as sleep scheduling, which induces additional overhead together with decreased throughput. This approach should then be considered from the EE vs. QoS trade-off viewpoint. Moreover, the locations and the number of these additional network components should be selected carefully to be effective. In a dynamic cellular network, the solutions for these problems are not trivial.

Another concern about the choice of a specific network architecture is to decide

whether to utilize internal sensing or external sensing (i.e., spectrum sensing vs. geolocation databases). For the supporters of the latter, sensing and intelligence can be located at the network (i.e., Radio Environment Maps, a.k.a. REM) instead of individual CRs. This choice changes *sensing-throughput trade-off* for the benefit of throughput, and potentially improves EE assuming that REM provides reliable spectrum information. Although this approach contradicts with the essence of the CR, throughput and EE requirements may render it favorable. However, REMs have to be deployed at various scales (e.g., country-wide or campus-coverage) to enable such capabilities. Subsequently, each device contributes to the energy consumption required for processing, cooling, and synchronization. Besides, deploying such machines everywhere violates green networking. On the other hand, REM can ease the learning process by processing the gathered temporal data by the sensors (e.g., CRs or other external entities) and deriving the characteristics of the radio environment from more complete data. In this way, a CR can improve its environment awareness compared to the case where it just uses its own incomplete local observations. Hence, we have to consider the trade-off between deployment and operating costs introduced by these entities and the performance improvement in terms of EE.

Figure 4.4 presents a rough comparison of various network architectures in terms of the PU interference, network architecture complexity, and CR throughput. This analysis may change based on specific equipment, communication protocols and technology. All issues related to traditional ad hoc networks and clustering apply to the cognitive counterparts with the additional challenge of establishing a reliable common control channel. These architectures are simple but their uncontrolled/distributed operation may degrade the CR performance and can have difficulty in efficiently managing the PU interference. REMs provide high throughput with their efficient learning mechanisms and up-to-date information at the expense of high complexity. Conventional cellular networks with high power transmitters create more PU interference whereas small cells achieve high throughput and low interference owing to offloading and close proximity to the SAP.

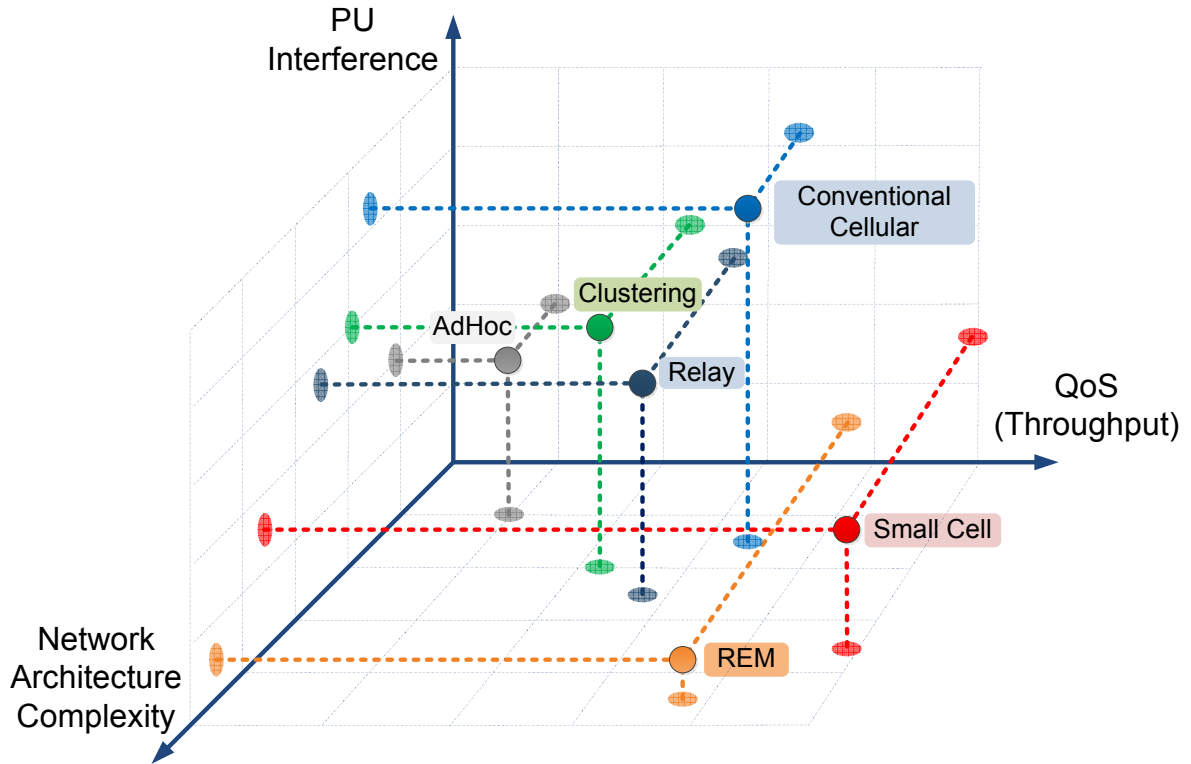


Figure 4.4. Three dimensions of CRN protocol design.

4.1.5. Energy Efficiency vs. Security

Equipping the CRs with security protocols results in additional processing both at the transmitter and the receiver. In secure environments, these protocols may decrease the EE of the network as each entity spends processing power/time and some of the channel capacity for transmitting these authentication and integrity messages. On the other hand, in environments with malicious or misbehaving nodes, additional security mechanisms may improve EE by avoiding interactions with malicious users and detecting the misbehaving nodes. For example, a CR with security protocols may detect PU emulation attacks, and can use the idle spectrum that would be wasted otherwise. Hence, the effect of security precautions on EE is intricate and highly dependent on the operating environment.

All widely-recognized attacks aim to collapse the CRN's sensing capability. These attacks make the CRN fail at the very early stage of cognitive cycle (i.e., sensing) because of the shortage of transmission opportunities. Authentication/authorization and

trust-based approaches via reward and punishment schemes are typically utilized to prevent attacks. These attacks can be generated either by an insider as in *spectrum sensing data falsification* (known as SSDF attack) in cooperative spectrum sensing, or by an external entity as in *PU emulation attacks*. In the latter case, the attacker emulates the PU signal to block the CR transmission in order to utilize the idle spectrum band selfishly. Althunibat *et al.* determine the optimal number of security bits in a message for attaining the highest trade-off between the obtained security level and EE for a CRN subject to SSDF attacks [63]. This optimal number depends on the fusion rule at the fusion center, the number of SSDF attackers, and the number of legitimate users.

To cope with the security threats while achieving EE, CRNs can define cooperative protocols that encourage cooperation among trusted CRs and keep track of the trustworthiness of each other. We discuss this issue further in Section 4.2 from a social network viewpoint.

4.2. Future Research Directions

The future research directions for the EE of CR can be broadly divided into two groups:

- CR Native – *endogenous* such as more energy-efficient sensing schemes, learning frameworks, and sensory data gathering,
- Integration with other networking paradigms – *exogenous* such as social networks, user behavior, and energy harvesting.

In this chapter, we focus on the latter which provides new degrees of freedom and opens new directions for the CR research. The trade-offs on which these directions have an impact are shown in Table 4.1. Broadly speaking, as a set of tools social network analysis (SNA) techniques can affect all the trade-offs; for example as shown in [47] social-awareness improves sensing performance or SNA may suggest an appropriate network architecture via choosing the most central nodes as the fusion centers/relays.

Energy harvesting has relatively narrower impact concentrating on QoS and network architecture trade-offs. For instance, energy harvesting can benefit energy-constrained nodes, enabling higher QoS via more sophisticated sensing and transmission schemes. However, user behavior is similar to SNA in terms of implications on a wide range of dimensions, the most critical being QoS.

Table 4.1. Future directions and their interactions with the trade-offs.

	QoS	Fairness	PU Interference	Network Architecture	Security
SNA	✓	✓	✓	✓	✓
User behavior	✓	✓	✓		✓
Energy harvesting	✓			✓	

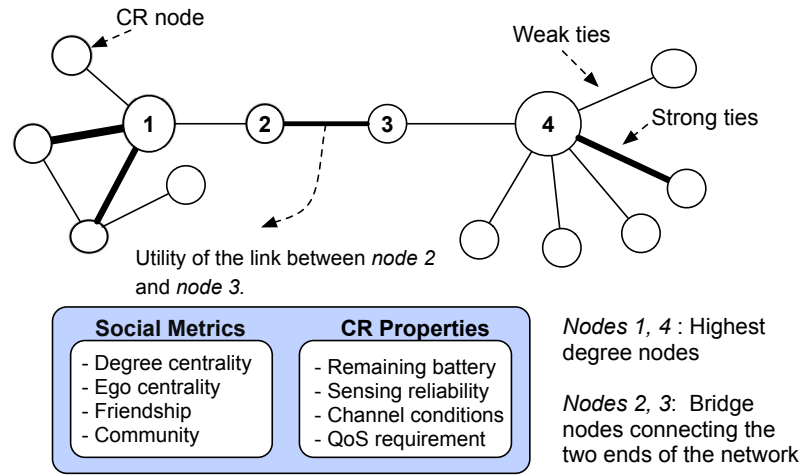


Figure 4.5. A CRN as a social network with different social ties.

4.2.1. Social Network Analysis (SNA)

A social network views a network as a group of nodes with their inter-relations (e.g., physical distance, contact frequencies) to benefit from these structural and social ties for higher efficiency. A CRN is unquestionably a social network in which the CRs may have various ties with each other depending on their spatial and social properties. Hence, uncovering the interconnections among CRs and designing protocols accordingly, can substantially improve the CRN performance. Figure 4.5 illustrates a social network of CRs in which nodes have different characteristics and diverse view of the same network according to their social ties. Social graphs are key to keeping track of

both interactions and social ties among the users. Interactions are beneficial for estimating the structure of the network such as connectivity and proximity of two users, whereas social ties may inform us about the trust among the nodes and the influential nodes in the network. This information can be exploited in designing energy-efficient cooperative protocols.

Previous works on cooperative sensing usually put the burden of cooperation onto the individual CRs (especially in terms of energy consumption) and implicitly assume that each CR is cooperative. However, such a cooperative behavior may not be applicable in practical CRNs. For instance, a user that does not have any active communication runs out of battery only because it receives sensing requests frequently from other CRs and consumes much of its battery on sensing. Instead, we envision a more realistic operation scheme in which the cooperation willingness of CRs' depends on the social ties among the users of these CR devices. Initial works show that the CRs benefit from such a social-aware cooperative sensing scheme where each CR selects a cooperation set based on its friendship ties together with the historical sensing performance of the cooperating nodes [47]. Moreover, the CRs can also make use of other CR's recommendations on the PU channels [64]. Thus, the CRs are expected to spend less effort for sensing and learning that leads to higher EE. Mukherjee *et al.* discuss a similar topic from the perspective of cooperative behavior diffusion in a game theoretical framework by analyzing under which conditions cooperation diffuses in the network, even though the CRs are selfish [65].

Environmental awareness improves the CR performance by letting the CR proactively take the best action at the expense of increased energy consumption due to constant environment monitoring. On the other hand, the CRs can share their experiences in order to reduce this burden. However, this solution raises the following question: To which extent a CR can *trust* to the other CRs' reports, and what if the recommendations are inaccurate? Although trust can be rather sophisticated in different contexts, we can model trust among the CRs based on their social ties (e.g. friendship and community) and can dynamically adapt the trust between the CRs based on their interactions and feedbacks. We expect such a cooperative learning scheme to improve

EE.

All of these discussed CR tasks can benefit from social-awareness to achieve higher performance (e.g., spectral efficiency) at lower energy cost, and thereby provide energy-efficient operation. However, these techniques require the CRs to share their social information (e.g., community), which people are hesitant to disclose for privacy concerns. Thus, social-aware schemes need to be enhanced with privacy preserving mechanisms.

4.2.2. User Behavior

The most important actor of any communication network is the user. CR is a learning entity that senses and decides based on the environment it operates. However, user-device interaction is usually ignored. We discuss an example from state-of-the-art cellular devices about how the user-device interaction can save energy, but the arguments also apply to CR devices.

Almost all of the modern cellular devices or smart phones come together Bluetooth, Wi-Fi, and GPS units in addition to 3G/4G. Moreover, these devices have both of these circuits switched *on* in their factory setting. On the other hand, an average user does not frequently use these protocols, especially Bluetooth and GPS. The critical point is that the user does not care about the energy consumption of these circuits unless the device has low battery. In addition, some users do not know how to turn them off to save energy. Thus, these protocols periodically seek some pairing/association all the time. A CR device can learn and analyze the user behavior such that when and/or where the user utilizes these types of additional communication units, and turn them off when it predicts that they are not needed.

In addition to the end user side, user behavior modeling can also let the operator and the network designer make their short and long term plans with EE in mind. These plans include elements such as frequency allocation, radio access network design, and operational timetable for the network equipment. For instance, the operator may switch the backbone equipment to low-power mode if its prediction based on the users'

behavior indicates that the network traffic will be minimal for a specific location and time period.

4.2.3. Energy Harvesting

Energy harvesting or scavenging is basically the process by which the energy is extracted from external ambient sources such as RF environment, thermal variations, or kinetic energy for improving EE or enabling energy-source free operation. It requires two main functionalities for being practical in wireless systems: energy generation and storage. However, the bursty nature of wireless traffic results in large spatio-temporal variances in system load. Additionally, the inherent randomness in energy harvesting, and thus energy flow prediction leads to the problem of consumption-generation matching and storage planning.

Environment-awareness is a key enabler for the optimization of energy harvesting functionality. Considering the fact that the CRs are expected to operate in a manner that is aware of their environment, they lend themselves to energy harvesting paradigm with their intrinsic capabilities. For instance, Park *et al.* explore how a CR with energy harvesting capability can adapt in both spectrum-limited and energy-limited regimes [66]. Moreover, the adaptation and learning capabilities of CRs can be augmented with energy harvesting. The assumed capabilities of advanced *sense-decide-act-learn* cycle of the CRs require fundamental changes in RF, baseband, and power management in wireless devices. These enhancements can also be utilized for energy harvesting. At the single node level, CRs may schedule their delay-tolerant traffic lazily according to the location and mobility pattern of the user in order to utilize upcoming energy harvesting opportunities efficiently. They can also be more aggressive if they predict a sluggish user behavior and an increasing energy harvesting potential in time and location dimensions. At the network level, CRs are envisioned to be self-aware agents communicating and cooperating with each other. In that regard, cooperation for network-level EE may rely on the altruistic load redistribution to make energy harvesting sufficient for the energy-source operation of underprivileged network nodes.

4.3. Chapter Summary

In this chapter, we have highlighted the challenges of designing energy-efficient CRNs with a focus on five major trade-offs: QoS, fairness, PU interference, network architecture, and security. We have also presented our perspective on future directions for improving EE of CRNs. In that regard, the social network approach is crucial due to central role of the interaction and cooperation among CRs. The CR device can also benefit in terms of energy by learning the user behavior and act accordingly. Moreover, the emerging CR capabilities can be utilized for energy generation where efficiency can be augmented with energy harvesting. We believe that these research directions can enable new solutions that will facilitate higher EE with a good strike of the listed trade-offs.

5. ENERGY-EFFICIENT MULTI-CHANNEL COOPERATIVE SENSING SCHEDULING WITH HETEROGENEOUS CHANNEL CONDITIONS FOR COGNITIVE RADIO NETWORKS

After discussing the trade-offs regarding EE in the previous chapter, we now turn our focus on the EE of CSS in a multi-channel CRN.

Previous works show the increase in sensing accuracy with the increase in sensing time [38]. On the other hand, SUs which are mostly mobile devices should be energy-efficient as they use their battery power. Therefore, from the energy (throughput) efficiency perspective, the more time is spent on sensing the more energy is consumed for overhead and less time remains for transmission. On the other hand, the throughput of the network is a function of the detection accuracy (i.e., probability of detection, P^D , and probability of false alarm, P^F). Hence, there is a trade-off between sensing and transmission durations for both throughput and EE.

In addition, it is shown that cooperation among the SUs increases the detection reliability of spectrum sensing at the expense of additional communication overhead, which increases with the number of cooperating SUs [67]. Different from cooperative sensing in a single channel, CSS has to balance the trade-off between the detection accuracy of a single channel and the number of channels being sensed in a multi-channel CRN. That is to say, *the more SUs are assigned to sense a single channel, the higher is the probability of detection for that channel at the expense of leaving some channels being unexplored*. While cooperative sensing has been well-investigated, CSS still remains unexplored. It is shown in previous works that CSS is NP-hard [9]. Taking the EE concerns into account makes this problem even more complicated.

The rest of the chapter is organized as follows: In Section 5.1, we state our contributions to the literature. In Section 5.2, we define the cooperative sensing system

model and introduce the basic theorems used in the formulated energy-efficient CSS scheme. Section 5.3 first formulates the problem and presents the methodology for finding the optimal solution. Proposed heuristic schemes are described in Section 5.4 and their performances are evaluated in Section 5.5. Finally, Section 5.6 concludes the chapter.

5.1. Contributions

The main contributions of this chapter can be summarized as follows [68]:

- We consider a scenario in which the number of SUs is larger than the number of primary channels. Therefore, our main concern is to select the SUs to sense all channels while the works in [35, 36] and [37] select a subset of primary channels to be sensed by all SUs. In addition, in the previous works an SU can sense at most one channel whereas in this work, SUs can sense multiple channels as long as they finish sensing in the dedicated time.
- Unlike these works, we account for the heterogeneity of the SU link conditions (i.e., received SNR of the PU signal at the SU). Therefore, our CSS solution additionally determines which SUs should sense a channel. Our work diverges from the previous works, which only determine the number of SUs to sense a specific primary channel.
- Moreover, sensing duration associated with an SU is adjusted according to the link SNR as opposed to the prior works, which consider identical sensing duration for all SUs. Simply, our approach bases on the fact that channels with high SNR values require shorter sensing time for a required detection probability and false alarm probability. Hence, an SU can save energy by sensing one of the channels with higher SNR as opposed to the fixed sensing duration scheme.

5.2. System Model

We assume an infrastructure-based CRN with N SUs, M channels, and a CBS. Our consideration is a specific case where the number of channels is less than the

number of SUs, i.e. $N \gg M$. We believe that in a cellular network this assumption generally holds as there are lots of users within the coverage area of the base station. If that is not the case, the CBS may select a subset of the channels based on their past data like availability, capacity, etc. such that there are enough SUs to sense all selected channels. This selection procedure has the potential to reduce energy consumption by eliminating the less favorable channels. SUs operate in a time synchronized manner within a frame based communication protocol. Each frame starts with a fixed length quiet sensing period of duration T^s during which SUs sense the channel(s) assigned to them. An SU may sense multiple channels during the quiet period as long as the total time dedicated to sensing by the SU does not exceed T^s . Then, all SUs that sense at least one channel report their hard decisions about these channels (0 or 1, indicating the absence or presence of primary user) to the CBS. We assume that the secondary network has a dedicated common control channel that is used for this reporting task and other control messages. The CBS combines the decisions using OR rule. The remaining time is used for transmission. We also assume that the SUs and the channels are heterogeneous. That is to say, the SNR of each SU over each channel is different due to different proximities from the PUs and different channel conditions (shadowing, fading, etc.). We assume the existence of a receiver block at each SU to estimate the SNR level and feedback it to the CBS through the error-free feedback channel [69]. With the help of the receiver block, we assume that the instantaneous SNR values are known. However, if that is not the case, long term SNR values can also be used. This time, the techniques discussed in this chapter can also be applied. However, the main objective becomes the minimization of expected energy, instead of the actual one. The frame structure is shown in Figure 5.1 where T , T^{rep} , and $\tau_{m,n}$ are the total frame length, the time dedicated for reporting sensing results, and the time that SU_n senses channel m , respectively.

Our main goal is to sense all M channels with minimum energy and sufficient accuracy such that cooperative detection probability of each channel is greater than some predefined threshold value (denoted by $_{th}P^{D,coop}$) and cooperative false alarm probability is smaller than another threshold (denoted by $_{th}P^{F,coop}$). Since channel

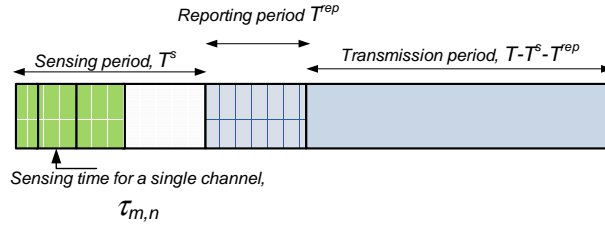


Figure 5.1. A frame starts with a sensing period followed by reporting and transmission periods.

sensing consumes energy, an SU may not utilize all of the quiet period duration for sensing if not necessary. On the other hand, it is desirable to sense a channel with a couple of SUs instead of a single SU (even though, it may satisfy the thresholds) in order to increase robustness. Hence, there is a trade-off between energy consumption and sensing reliability. The problem includes the assignment of SUs to channel(s) for the sensing task together with the decision of the sensing time for the channel(s) to be sensed by each SU.

Let $P_{m,n}^F$, $P_{m,n}^D$, $\gamma_{m,n}$ denote the probability of false alarm, probability of detection, SNR for SU_n over channel m , respectively. If we assume that $P_{m,n}^F$ is fixed, then for a complex-valued PSK channel with circularly symmetric complex Gaussian noise, $P_{m,n}^D$ is given by [38]

$$P_{m,n}^D = \mathcal{Q} \left(\frac{\mathcal{Q}^{-1}(P_{m,n}^F) - \sqrt{\tau_{m,n} f_s \gamma_{m,n}}}{\sqrt{2\gamma_{m,n} + 1}} \right) \quad (5.1)$$

where f_s is the sampling frequency and \mathcal{Q} is the complementary cumulative distribution of a standard Gaussian.

Theorem 5.1. $P_{m,n}^D$ is an increasing function of $\tau_{m,n}$. Furthermore, it is also concave if

$$-\frac{1}{\sqrt{\tau_{m,n}}} + \frac{\gamma_{m,n} \sqrt{f_s}}{(2\gamma_{m,n} + 1)} (\mathcal{Q}^{-1}(P_{m,n}^F) - \sqrt{\tau_{m,n} f_s \gamma_{m,n}}) < 0. \quad (5.2)$$

This theorem is well known, and its proof is given in Appendix A.

Lemma 5.1. $P_{m,n}^D$ is a concave function of $\tau_{m,n}$ if $P_{m,n}^D > 0.5$.

Lemma 5.1. is a straightforward application of Theorem 5.1. The proof can be found in Appendix A.1.

Lemma 5.2.: $1 - P_{m,n}^D$ is a non-negative decreasing function of $\tau_{m,n}$. It is also convex if the condition in (5.2) is satisfied.

Let \mathcal{S}_m and $P_m^{D,coop}$ denote the set of SUs sensing channel m , and cooperative detection probability for channel m , respectively. Using OR rule for decision combining gives

$$\begin{aligned} P_m^{D,coop} &= 1 - \prod_{n \in \mathcal{S}_m} (1 - P_{m,n}^D) \\ &= 1 - \prod_{n \in \mathcal{S}_m} \left(1 - \mathcal{Q} \left(\frac{\mathcal{Q}^{-1}(P_{m,n}^D) - \sqrt{\tau_{m,n} f_s \gamma_{m,n}}}{\sqrt{2\gamma_{m,n} + 1}} \right) \right). \end{aligned}$$

Theorem 5.2. $P_m^{D,coop}$ is an increasing function of $\tau_{m,n}$. Moreover, it is also concave if the condition in (5.2) is satisfied $\forall n \in \mathcal{S}_m$.

The proof of this theorem is given in Appendix B.

5.3. Optimization Model and Solution Methodology

5.3.1. Energy Consumption Model

Let P^s and $E_{m,n}^s$ be the power consumed during channel sensing and energy dissipated by SU_n for sensing channel m , respectively. $E_{m,n}^s$ is equal to $P^s \tau_{m,n}$. Then,

energy consumption for channel sensing (denoted by E^s) can be written as

$$E^s = \sum_{m=1}^M \sum_{n=1}^N P^s \tau_{m,n}.$$

Besides channel sensing, SUs also consume energy by transmitting their local results to the CBS. We assume that SU transmits its sensing report as a single packet regardless of the number of channels sensed, and the reporting period is long enough such that all SUs can send their packets. Let E_n^{rep} denote the energy consumed for reporting the sensing result to CBS, which depends on the location of SU_n relative to the CBS. In addition, let \mathcal{S}^{rep} denote the set of SUs that perform sensing in this frame that are required to report their local decisions to the CBS. Then, the total energy consumption for reporting is given by

$$E^{rep} = \sum_{n \in \mathcal{S}^{rep}} E_n^{rep}.$$

This model assumes that all reporting packets are transmitted successfully. If that is not the case, the model can be modified as follows: Let p denote the probability of successful packet transmission that is geometrically distributed, then the expected number of transmission attempts for an SU is given by $1/p$, and E^{rep} is given by $E^{rep} = 1/p \sum_{n \in \mathcal{S}^{rep}} E_n^{rep}$.

5.3.2. Optimization Model for Energy-Efficient Sensing

We first define the decision variables that are used in the optimization model.

Let

$$\begin{aligned} \tau_{m,n} &= \text{time spent by } SU_n \text{ for sensing channel } m, \\ x_{m,n} &= \begin{cases} 1, & \text{if channel } m \text{ is sensed by } SU_n \\ 0, & \text{o/w.} \end{cases}, \\ y_n &= \begin{cases} 1, & \text{if } SU_n \text{ transmits sensing result to CBS} \\ 0, & \text{o/w.} \end{cases}. \end{aligned}$$

From (5.1), for a given $P_{m,n}^d$ value the required $\tau_{m,n}$ can be written as

$$\tau_{m,n} = \left(\frac{\mathcal{Q}^{-1}(P_{m,n}^F) - \mathcal{Q}^{-1}(P_{m,n}^D) \sqrt{2\gamma_{m,n} + 1}}{\gamma_{m,n} \sqrt{f_s}} \right)^2. \quad (5.3)$$

In addition, let $\tau_{m,n}^{min}$ denote the sensing time required for SU_n in order to achieve a $P_{m,n}^D$ value of 0.5. It can be calculated from (5.3) as

$$\tau_{m,n}^{min} = \left(\frac{\mathcal{Q}^{-1}(P_{m,n}^F)}{\gamma_{m,n} \sqrt{f_s}} \right)^2.$$

We assume that a channel should be sensed by at least δ^{min} SUs. δ^{min} defines the minimum number of cooperating SUs for a channel. The selection of δ^{min} value is a design criterion. In order to encourage cooperation and improve robustness, a δ^{min} value greater than one is preferred. On the other hand, regarding EE concern, δ^{min} should not be high as each additional SU used for sensing incurs sensing and reporting energy consumption.

If we assume that $P_{m,n}^F = P^F \forall m, n$, then $P_m^{F,coop}$ is given by

$$P_m^{F,coop} = 1 - \prod_{n \in \mathcal{S}_m} (1 - P^F).$$

Since $P_m^{F,coop} \leq_{th} P^{F,coop}$, then the maximum number of cooperating SUs, denoted by δ^{max} , can be calculated as

$$\delta^{max} = \lfloor \frac{\log(1 -_{th} P^{F,coop})}{\log(1 - P^F)} \rfloor. \quad (5.4)$$

In other words, δ^{max} is the maximum number of cooperating SUs that satisfy the cooperative false alarm constraint. The solution methodology we apply can also be used for the case where $P_{m,n}^F$ values differ. We discuss this case in detail at the end of the following section. The optimization model can be written as

$$\mathbf{P1:} \quad \min w = \sum_{m=1}^M \sum_{n=1}^N P^s \tau_{m,n} + \sum_{n=1}^N E_n^{rep} y_n \quad (5.5)$$

subject to:

$$\tau_{m,n} \geq \tau_{m,n}^{min} x_{m,n} \quad \forall m \in M, \forall n \in N \quad (5.6)$$

$$\sum_{m=1}^M \tau_{m,n} \leq T^s y_n \quad \forall n \in N \quad (5.7)$$

$$\sum_{n=1}^N x_{m,n} \geq \delta^{min} \quad \forall m \in M \quad (5.8)$$

$$\sum_{n=1}^N x_{m,n} \leq \delta^{max} \quad \forall m \in M \quad (5.9)$$

$$\sum_{m=1}^M x_{m,n} \leq M y_n \quad \forall n \in N \quad (5.10)$$

$$_{th} P^{D,coop} - P_m^{D,coop} \leq 0 \quad \forall m \in M \quad (5.11)$$

$$x_{m,n}, y_n \in \{0, 1\} \quad \forall m \in M, \forall n \in N \quad (5.12)$$

$$\tau_{m,n} \geq 0 \quad \forall m \in M, \forall n \in N, \quad (5.13)$$

where this time $P_m^{D,coop}$ is defined as

$$P_m^{D,coop} = 1 - \prod_{n=1}^N \left(1 - \mathcal{Q} \left(\frac{\mathcal{Q}^{-1}(P^F) - \sqrt{\tau_{m,n} f_s \gamma_{m,n}}}{\sqrt{2\gamma_{m,n} + 1}} \right) x_{m,n} \right).$$

Hence, SUs with $x_{m,n}$ value of 0 contribute 1 to the above multiplication, whereas those with $x_{m,n}$ value of 1 contribute $(1 - P_{m,n}^D)$.

The objective in (5.5) minimizes the total energy consumption associated with sensing for a frame. Constraint (5.6) specifies that if SU_n senses channel m , the sensing duration should be at least $\tau_{m,n}^{min}$. In this way, we guarantee that the concavity condition always holds. Constraint (5.7) denotes that total time spent by an SU for sensing should be less than or equal to the sensing duration of a frame. It also forces all $\tau_{m,n}$ values associated with SU_n to zero, if $y_n = 0$. Constraint (5.8) requires that each channel should be sensed by at least δ^{min} SUs. Similarly, constraint (5.9) limits the number of cooperating SUs for a channel in order to satisfy the false alarm probability threshold. Constraint (5.10) forces y_n value for an SU to 1, if that SU senses any channels. The requirement for cooperative detection probability being greater than the threshold for each channel is expressed by constraint (5.11). Finally, constraints (5.12) and (5.13) specify the types of variables.

The above problem is a Mixed Integer Non-linear Programming problem because of constraint (5.11), even though its objective is linear. We resort to the outer linearization (OL) algorithm to solve the above problem.

5.3.3. Outer Linearization

As proven before, once the $x_{m,n}$ values are fixed, $P_m^{D,coop}$ value is concave in terms of $\tau_{m,n}$. Thus, constraint (5.11) is convex, and the outer linearization procedure can be used to find the optimal solution [70]. Outer linearization works by first ignoring the mixed integer non-linear constraints to obtain an initial solution. If the solution

satisfies all previously ignored constraints, then it is optimal. On the other hand, if it does not, then the most violated constraint is linearized using the current solution, and added to the current problem as a new constraint to obtain another solution. The linearization process goes on until all constraints are satisfied with an ϵ tolerance. Since the constraints are convex, the procedure is guaranteed to terminate in finite number of steps [71]. The steps of the procedure are as follows:

- Step 1: Initialize the iteration counter, $k = 1$. Solve the initial Mixed Integer Linear Programming problem (**P2**) formed by ignoring constraint (5.11), and obtain the initial solution $\tau_{m,n}^1, x_{m,n}^1, y_n^1$.
- Step 2: Identify the most violated constraint, g_m , among the M constraints of (5.11) with the current solution $(\tau_{m,n}^k, x_{m,n}^k, \text{ and } y_n^k)$. That is to say, g_m is the cooperative detection probability constraint corresponding to the channel that deviates from the threshold value most. Let v_m denote the corresponding deviation.
- Step 3: If the maximum violation is smaller than ϵ , stop; the current solution is optimal with ϵ feasibility tolerance. Otherwise, proceed with Step 4.
- Step 4: Linearize the most violated constraint by adding the following linear constraint to **P2**:

$$\nabla g_m(\dots x_{m,i}^k, \dots \tau_{m,i}^k, \dots)^T \begin{pmatrix} \vdots \\ x_{m,i} - x_{m,i}^k \\ \vdots \\ \tau_{m,i} - \tau_{m,i}^k \\ \vdots \end{pmatrix} + v_m \leq 0$$

where $\nabla g_m(\dots x_{m,i}^k, \dots \tau_{m,i}^k, \dots)$ is the gradient of g_m evaluated at the current solution. Its individual entries are given by

$$\begin{aligned} \frac{\partial g_m}{\partial x_{m,i}} &= -Q \left(\frac{Q^{-1}(P^F) - \sqrt{\tau_{m,i} f_s} \gamma_{m,i}}{\sqrt{2\gamma_{m,i} + 1}} \right) B_{m,i} \\ \frac{\partial g_m}{\partial \tau_{m,i}} &= -\frac{x_{m,i} \gamma_{m,i} \sqrt{f_s}}{2\sqrt{\tau_{m,i}} \sqrt{2\pi} \sqrt{2\gamma_{m,i} + 1}} A_{m,i} B_{m,i} \end{aligned}$$

where $A_{m,i}$ is given in Appendix B and $B_{m,i}$ is equal to

$$\prod_{n=1, n \neq i}^N \left[1 - \mathcal{Q} \left(\frac{\mathcal{Q}^{-1}(P^F) - \sqrt{\tau_{m,n} f_s \gamma_{m,n}}}{\sqrt{2\gamma_{m,n} + 1}} x_{m,n} \right) \right].$$

Set $k = k + 1$, solve the current problem to obtain $\tau_{m,n}^k$, $x_{m,n}^k$, and y_n^k values. Proceed with Step 2.

In the remainder of this chapter, we refer to the application of outer linearization to Problem P1 as OL.

For the case where $P_{m,n}^f$ values differ, false alarm constraint assumes the following form

$$1 - \prod_{n=1}^N (1 - P_{m,n}^F x_{m,n}) - th P^{F,coop} \leq 0.$$

The outer linearization procedure can still be applied in this case, but this time $2M$ constraints (cooperative false alarm probability constraint in addition to cooperative detection probability constraint for each channel) need to be checked for feasibility. The other steps of the procedure are the same.

5.3.4. Transmission Time Maximization (TXT)

The aforementioned model optimizes the total energy dedicated to the sensing task while achieving satisfactory sensing performance in terms of detection and false alarm probabilities. However, in this approach, sensing duration of a frame (denoted by T^s) is constant. Hence, if we denote the frame duration by T and reporting time of the sensing outcomes by T^{rep} , which are also constant, then the transmission time for data packets is given by $T - T^s - T^{rep}$. Another approach is to maximize the data transmission duration of a frame. This time, we treat T^s as a decision variable. Assuming a quiet sensing period, T^s is given by $\max_n \left\{ \sum_{m=1}^M \tau_{m,n} \right\}$. In other words, T^s is the maximum of total sensing times for all SUs as the network should wait for the

SU with the longest total sensing time before moving on the next phase of a frame. Then, the objective becomes $\max_n z_1 = T - T^{rep} - \max_n \left\{ \sum_{m=1}^M \tau_{m,n} \right\}$. Since T and T^{rep} are constants, this objective is equivalent to $\min_n z_2 = \max_n \left\{ \sum_{m=1}^M \tau_{m,n} \right\}$ subject to constraints (5.6), (5.8), (5.9), (5.10), (5.11), (5.12), and (5.13). To solve this problem, we resort to the outer linearization procedure again as the constraints are almost the same.

5.4. Heuristic Approaches

In this section, we propose two suboptimal but fast heuristic approaches for the energy-efficient sensing problem. The first one focuses on greedily minimizing the sensing energy while disregarding the reporting energy. On the other hand, the second heuristic initially considers the reporting energy, then it regards the sensing energy.

Unlike the previous two approaches that support different detection probabilities for different channel and user pairs, these heuristics require a fixed detection probability, P^D , for all channels and users for the sake of simplicity and quick execution time. This approach is frequently applied in the literature [23, 31, 33]. For both heuristics, we sense each channel with δ^{min} SUs. Thus, the required P^D value can be calculated as

$$P^D = \max\{1 - (1 - {}_{th}P^{D,coop})^{1/\delta^{min}}, P_{min}^D\},$$

which guarantees a minimum detection probability of P_{min}^D . As the $P_{m,n}^F$ values are assumed to be the same for all SU-channel pairs as before, the goal of the heuristics is to find the best SU/channel assignment.

5.4.1. Sensing Energy Minimization Heuristic (SEM)

This heuristic minimizes the sensing energy by selecting SUs with high SNR values for a channel while disregarding reporting energy. Initially, remaining sensing time of all SUs are equal to T^s . The heuristic starts with the first channel, sorts the

SUs in descending order based on their $\gamma_{m,n}$ values, and selects the first SU in the list. Then, it calculates the required $\tau_{m,n}$ value for the selected SU to obtain a detection probability of P^D . If the remaining sensing time of the selected SU is greater than $\tau_{m,n}$, the selected SU is assigned to sense channel m . Otherwise, we move on to the next SU. The algorithm runs until δ^{min} SUs are assigned to all channels. The pseudo code for this heuristic is given in Figure 5.2.

<p>Require: $P^D, \delta^{min}, M, N, \gamma_{m,n}, T^s$</p> <p>1: $remainingTime[n] = T^s \quad \forall n$</p> <p>2: for $m = 1$ to M do</p> <p>3: Sort SUs in descending order of $\gamma_{m,n}$ and let $index$ be the list of indices of the sorted entries such that $index[1]$ corresponds to the index of SU with the highest $\gamma_{m,n}$ and $index[N]$ corresponds to the index of SU with the lowest $\gamma_{m,n}$.</p> <p>4: $assignmentNo = 0, k = 1$</p> <p>5: while $assignmentNo < \delta^{min}$ do</p> <p>6: $n = index[k]$</p> <p>7: Select SU_n as a candidate and calculate $\tau_{m,n}$ value to achieve P^D using (5.3).</p> <p>8: if $\tau_{m,n} \leq remainingTime[n]$ then</p> <p>9: $remainingTime[n] = remainingTime[n] - \tau_{m,n}$</p> <p>10: $assignmentNo = assignmentNo + 1$</p> <p>11: end if</p> <p>12: $k = k + 1$</p> <p>13: end while</p> <p>14: end for</p>

Figure 5.2. Sensing Energy Minimization Heuristic.

Starting with the first channel, the heuristic selects δ^{min} SUs with the best $\gamma_{m,n}$ values and enough remaining sensing time for the sensing task. The outer loop takes $O(M)$ steps. Sorting SUs based on their $\gamma_{m,n}$ values is $O(N \log N)$, whereas the inner loop is $O(N)$. Hence, the total running time is $O(MN \log N)$.

5.4.2. Reporting Energy Minimization Heuristic (RPEM)

The main difference between the Reporting Energy Minimization (RPEM) heuristic and SEM is that RPEM first considers SUs that are already assigned to sense a channel. Let \mathcal{S}^{rep} be the set of SUs that are going to perform sensing and transmit their reports for this frame. Similarly, \mathcal{S}^{nrep} is the set of SUs that are not assigned to sense a channel yet. Initially, $\mathcal{S}^{rep} = \emptyset$, $\mathcal{S}^{nrep} = \{SU_1, SU_2, \dots, SU_N\}$. The heuristic first looks for SUs among the ones in \mathcal{S}^{rep} in order to save reporting energy. If enough SUs are not found, then it moves on to \mathcal{S}^{nrep} . As in the previous case, SUs in \mathcal{S}^{rep} and \mathcal{S}^{nrep} are processed in decreasing order of $\gamma_{m,n}$ values for the considered channel. The pseudo code of RPEM is given in Figure 5.3.

This time both inner while loops (line 6 and line 18) take $O(N)$, and the sorting operations are still $O(N \log N)$. As in the previous case, the total running time is $O(MN \log N)$.

5.5. Results

We assume that received SNR at an SU ($\gamma_{m,n}$) follows an exponential distribution with mean μ^{SNR} . In order to be consistent, we use the same $\gamma_{m,n}$ values for a given μ^{SNR} across different runs. For a given parameter set, we first run the TXT method to obtain the ideal sensing time denoted by T_{opt}^s . For the other methods, we scale this value with an α value ($\alpha > 1$), and use αT_{opt}^s as the sensing time for the other methods. The values for the other parameters are given in Table 5.1.

By using (5.4), we obtain $\delta^{max}=10$ for the given P^F and $thP^{F,coop}$ values. The reader should note that the presented results are for a single frame. Hence, the cumulative effect will be much higher if multiple frames are considered. Furthermore, the processing order of the channels is important for the given heuristics as they converge to local optimal solutions. Even though the channels are ordered naturally in the given pseudo-code, we also run both heuristics with randomly ordered channels 20

```

Require:  $P^D, \delta^{min}, M, N, \gamma_{m,n}, T^s$ 
1:  $remainingTime[n] = T^s \quad \forall n$ 
2:  $\mathcal{S}^{rep} = \emptyset, \mathcal{S}^{nrep} = \{SU_1, SU_2, \dots, SU_N\}$ 
3: for  $m = 1$  to  $M$  do
4:   Sort SUs in  $\mathcal{S}^{rep}$  in descending order of  $\gamma_{m,n}$  and let  $indexRep$  be the list of indices
   of the sorted entries.
5:    $assignmentNo = 0, k = 1$ 
6:   while ( $assignmentNo < \delta^{min}$ ) && ( $k \leq |\mathcal{S}^{rep}|$ ) do
7:      $n = indexRep[k]$ 
8:     Select  $SU_n \in \mathcal{S}^{rep}$  as a candidate and calculate  $\tau_{m,n}$  value to achieve  $P^d$  using (5.3).
9:     if  $\tau_{m,n} \leq remainingTime[n]$  then
10:        $remainingTime[n] = remainingTime[n] - \tau_{m,n}$ 
11:        $assignmentNo = assignmentNo + 1$ 
12:     end if
13:      $k = k + 1$ 
14:   end while
15:   if  $assignmentNo < \delta^{min}$  then
16:     Sort SUs in  $\mathcal{S}^{nrep}$  in descending order of  $\gamma_{m,n}$  and let  $indexNrep$  be the list of
     indices of the sorted entries.
17:      $k = 1$ 
18:     while  $assignmentNo < \delta^{min}$  do
19:        $n = indexNrep[k]$ 
20:       Select  $SU_n \in \mathcal{S}^{nrep}$  as a candidate and calculate  $\tau_{m,n}$  value to achieve  $P^d$  using
       (5.3).
21:       if  $\tau_{m,n} \leq remainingTime[n]$  then
22:          $remainingTime[n] = remainingTime[n] - \tau_{m,n}$ 
23:          $assignmentNo = assignmentNo + 1, \mathcal{S}^{rep} = \mathcal{S}^{rep} \cup \{SU_n\}, \mathcal{S}^{nrep} = \mathcal{S}^{nrep} \setminus$ 
            $\{SU_n\}$ 
24:       end if
25:        $k = k + 1$ 
26:     end while
27:   end if
28: end for

```

Figure 5.3. Reporting Energy Minimization Heuristic.

Table 5.1. Parameter values.

M	40
N	{160, 180, 200, 220, 240}
f_s	{1 kHz, 10 kHz}
μ^{SNR}	[-10 dB, 5 dB] with 1 dB increments
δ^{min}	3
P^F	0.01
α	[1.1, 3] with 0.1 increments
T^s	αT_{opt}^s
ϵ	10^{-6}
P^s	1000 mW
E_n^{rep}	1 mJ $\forall n$
P_{min}^D	0.5
$th P^{D,coop}$	0.9
$th P^{F,coop}$	0.1

times. The results given below for the heuristics are the best of the 21 runs in terms of energy consumption.

We first observe the total energy consumption and its individual components in Figures 5.4a and 5.4b for μ^{SNR} values of -5 dB and 2 dB, respectively. For low μ^{SNR} , the sensing component of the energy consumption is more dominant. On the other hand, reporting energy consumption becomes the major component when μ^{SNR} is higher. As we can see, the reporting energy consumption is similar in both cases. Hence, the difference stems from the sensing energy consumption. With high μ^{SNR} , the time required to achieve a particular detection probability decreases, which in turn decreases the required sensing time. In both cases, TXT achieves the worst performance since its objective does not consider the energy consumption at all. On the other hand, the performance of OL is always superior compared to other methods. Furthermore, SEM is slightly superior compared to RPEM for low SNR because it prioritizes the sensing energy. Contrariwise, RPEM achieves lower total energy for high SNR value since it

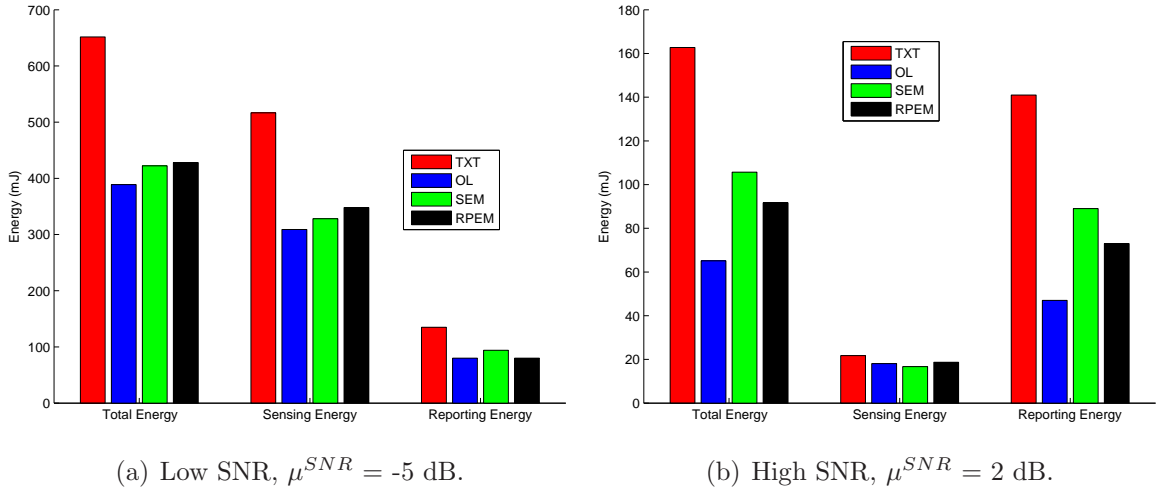


Figure 5.4. Energy consumption profiles with $N = 200$, $\delta^{min} = 3$, $\alpha = 2$.

first considers the reporting energy component.

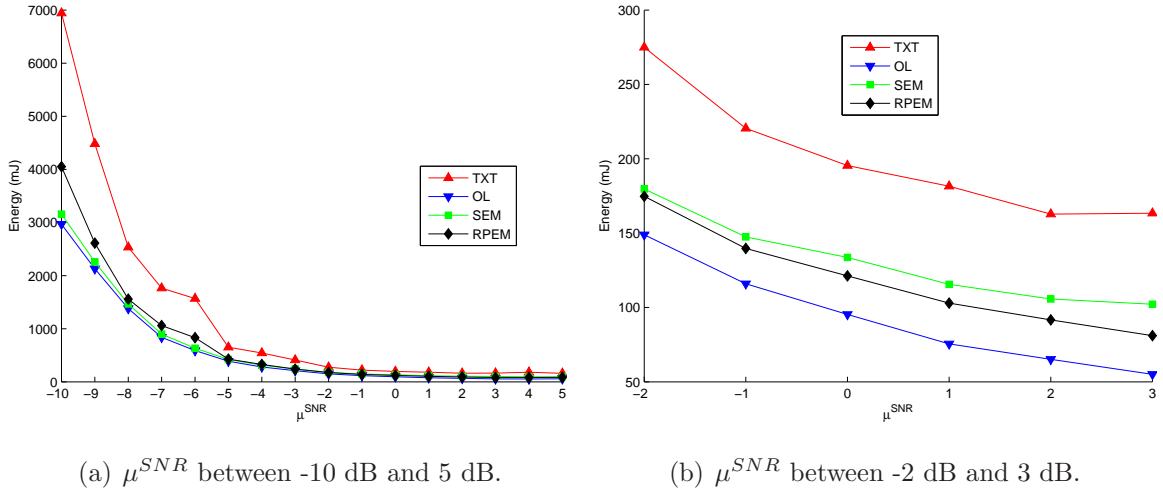


Figure 5.5. Effect of μ^{SNR} on total sensing energy consumption with $N = 200$, $\delta^{min} = 3$, $\alpha = 2$.

The effect of changing μ^{SNR} on the total sensing energy consumption can be seen in Figure 5.5. Figure 5.5a shows a broader range whereas Figure 5.5b shows the high SNR regime. Initially, increasing μ^{SNR} values have a significant impact on the total energy consumption for all methods whereas beyond a certain point the benefits are minimal. In this case, OL provides 7 percent improvement over the next best method, namely SEM heuristic, when μ^{SNR} is -10 dB. Moreover, the improvement over other methods is much better when μ^{SNR} assumes higher values which can be seen in Figure 5.5b. As an example, using OL results in 22 percent reduction in the total energy consumption compared to the next best method, RPEM this time, when

μ^{SNR} is 0 dB. In addition, both figures support our previous claim that SEM achieves better performance than RPEM for low SNR values, while the reverse is true for high SNR values.

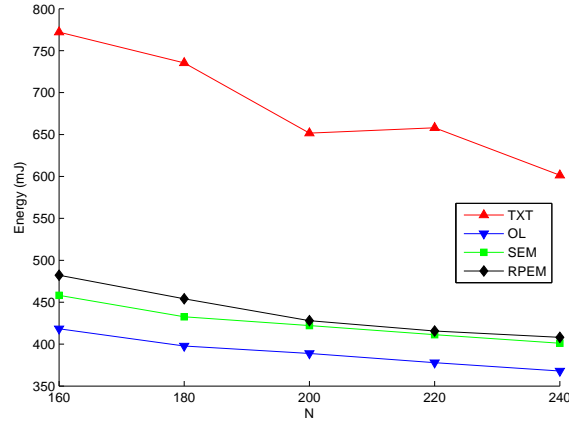


Figure 5.6. Effect of number of SUs on total sensing energy consumption with $\mu^{SNR} = -5$ dB, $\delta^{min} = 3$, $\alpha = 2$.

Figure 5.6 illustrates the change in the total energy consumption with respect to the increase in the number of SUs. Apart from TXT method, all schemes yield better results as N increases. The main reason for this performance improvement is the diversity brought by the added SUs. That is to say, with more SUs, the probability of finding an SU with a high $\gamma_{m,n}$ value increases for a given channel m . On the other hand, TXT method shows slight variations since its goal is not related to the energy consumption.

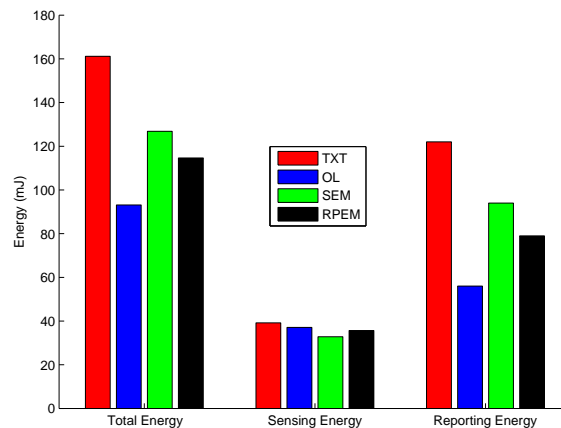


Figure 5.7. Energy consumption profiles with $N = 200$, $\delta^{min} = 3$, $\alpha = 2$, $f_s = 10$ kHz, $\mu^{SNR} = -5$ dB.

The total energy consumption and its individual components for $f_s = 10$ kHz case are presented in Figure 5.7. In comparison to Figure 5.4, increasing f_s has a similar effect as increasing SNR value. However, the effect of SNR is more prominent. For instance, with all other factors constant, increasing μ^{SNR} from -5 dB to 2 dB (almost a fivefold increase) results in nearly 83 percent reduction in the energy consumption for OL. On the other hand, increasing f_s tenfold from 1 kHz to 10 kHz gives 76 percent decrease for OL. These observations are in accordance with (5.3). In addition, similar to the case in Figure 5.5b, with a higher sampling rate, RPEM heuristic provides lower energy consumption than SEM.

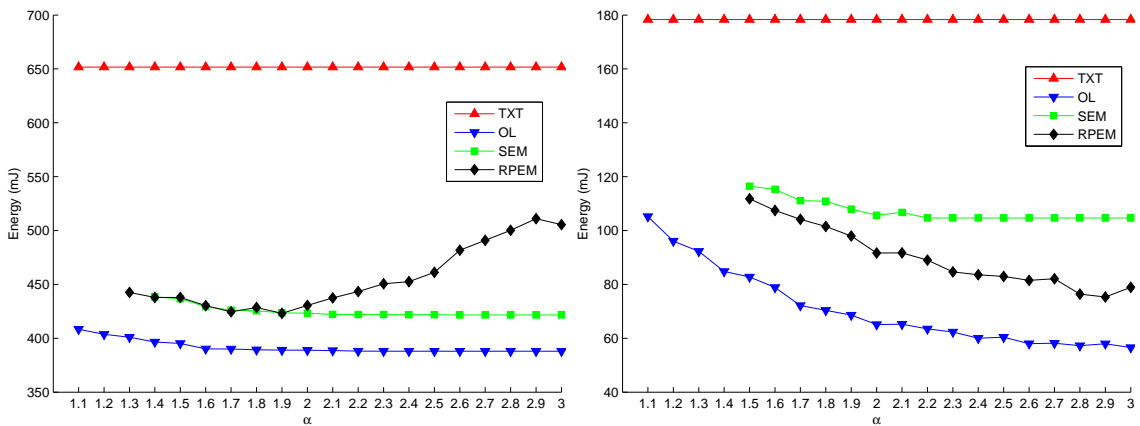
(a) Low SNR, $\mu^{SNR} = -5$ dB.(b) High SNR, $\mu^{SNR} = 2$ dB.

Figure 5.8. Effect of sensing duration (T_s) under low and high SNR values with $N = 200$, $\delta^{min} = 3$.

The energy consumption values for various values of α are given in Figures 5.8a and 5.8b for μ^{SNR} values -5 dB and 2 dB, respectively. As α is not a parameter for TXT, it is not affected by the change in α . For low α values, the results for SEM and RPEM are not shown because both heuristics fail to provide a feasible solution. For the low SNR regime, both OL and SEM produce lower energy consumption with increasing α but the decrease is marginal. Unlike SEM and OL, the results for RPEM first decrease and then start to increase. The rationale behind this pattern can be explained as follows: since RPEM prefers SUs that are already assigned a channel for sensing when selecting SUs for channel m , a long sensing duration causes SUs with low $\gamma_{m,n}$ to be assigned to channel m . We observe that sensing energy component dominates in low SNR regime, so this causes an increase in the total energy consumption for RPEM. On

the contrary, for high SNR regime RPEM produces lower energy consumption values as reporting energy component is the dominating factor. Both figures show that with only a small amount of additional sensing time, great energy savings are possible.

To sum up, all three energy minimization methods (OL, SEM, and RPEM) provide significant energy savings compared to a pure transmission time maximization technique. In all cases, OL achieves the best energy values whereas the performance of SEM and RPEM depend on the parameter values. On the one hand, a low μ^{SNR} or a high α favors SEM. On the other hand, a high μ^{SNR} or a high f_s supports RPEM. As both heuristics have very low complexities, both can be executed in a short amount of time, and one can select the method with the better energy consumption.

5.6. Chapter Summary

In this chapter, we have formulated the energy-efficient cooperative sensing scheduling problem for a CRN and presented various approaches for this problem. Each scheme ensures the minimum detection probability constraint as a PU protection criteria and the maximum false alarm probability constraint as CRN operability criteria in each channel. OL, SEM, and RPEM aim to minimize energy expenditure for sensing while TXT minimizes time spent for the sensing task in order to leave more time for data transmission. We have investigated the performance of our proposals with various parameters. To find the optimal solution we have employed the outer linearization method. Numerical evaluations have shown that by sacrificing very little data transmission time, significant amount of energy can be saved. Furthermore, reporting energy is an important factor in the energy consumption, especially, when the SNR or sampling frequency is high.

As future work, we plan to incorporate different fusion rules, e.g. AND, MAJORITY into our model. Another point to pursue is to treat false alarm probabilities as decision variables, and jointly optimize them together with sensing times.

6. CHANNEL SWITCHING AWARE AND ENERGY-EFFICIENT COOPERATIVE SENSING SCHEDULING FOR COGNITIVE RADIO NETWORKS

Our work in this chapter follows the footsteps of the previous chapter. The main difference is that in this chapter, we also take the time and energy cost of channel switching into account [72].

The remainder of this chapter is organized as follows: Section 6.1 defines the system under consideration while Section 6.2 provides a formal definition of the problem using network flows. Next, Section 6.3 first presents the outer linearization based solution methodology and then introduces Energy Aware Sensing scheduler (EASE), the heuristic solution with lower complexity for the considered problem. Section 6.4 evaluates the performance of the presented schemes. Finally, Section 6.5 summarizes this chapter.

6.1. System Model

Similar to Chapter 5, we assume an infrastructure-based CRN where the CBS coordinates the SUs. The system operates in a frame based fashion, and there is a quiet sensing period with length T^s at the beginning of each frame. During this *sensing period*, SUs sense the channels assigned to them. In a sensing period, an SU may sense multiple channels one after another by tuning its antenna to the corresponding channel. However, channel switching is not immediate and comes with a time and an energy overhead so deciding on the order of sensing is of paramount importance. For the sake of energy saving, an SU that completes all its sensing tasks switches to low energy consuming *idling mode* till the end of sensing period. The sensing period is followed by a *reporting period* during which SUs report their local sensing results to CBS for fusion. Fusion operations are performed using OR rule. After the reporting period, *data transmission* begins and continues until the end of the frame. Figure 6.1 depicts

the organization of a frame.

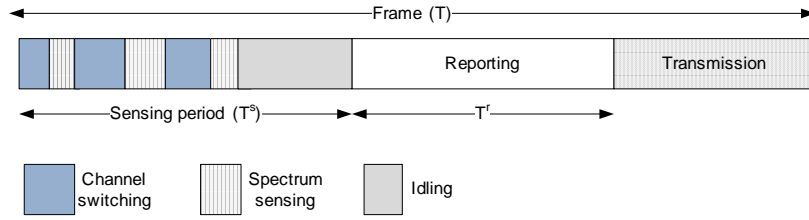


Figure 6.1. Frame organization.

Let M and N denote the number of primary channels and the number of SUs, respectively. We assume that $M \ll N$, and the SNR value of the received PU signal is assumed to differ for each SU over each channel, which is denoted by $\gamma_{m,n}$. We require that each channel is sensed by at least δ^{min} SUs to ensure diversity. We have the same goal of sensing all M channels with minimum energy consumption while providing adequate accuracy such that cooperative detection and false alarm probabilities are in accordance with their respective thresholds.

Energy Consumption Model: In a typical CRN, the total energy spent for sensing (E^{total}) has three components:

Sensing Energy (E^s): This component is the same as the previous chapter, and it is given by $\sum_{m=1}^M \sum_{n=1}^N P^s \tau_{m,n}$ where P^s and $\tau_{m,n}$ denote the sensing power and sensing duration for channel m for SU_n , respectively.

Channel Switching Energy (E^{cs}): This component is the new energy component that we include in the total energy calculation. It is the energy consumed when SUs switch channels during the sensing period. Frequency switching is performed via changing the input voltage of the voltage-controlled oscillator (VCO) operating in a phase locked loop (PLL) to generate the desired output frequency. The power required to complete this operation is referred to as channel switching power (P^{cs}) and the related energy consumption is given as $P^{cs}T^{cs}$ where T^{cs} is the total time required for completing the channel switch. T^{cs} is given by $t^{cs}|f - f'|$ where t^{cs} is the time required to

switch to the adjacent channel and $|f - f'|$ is the absolute value of separation between the two frequencies [73]. Let f_n^0 denote the frequency of the channel to which the antenna of the SU_n is tuned at the beginning of the quiet period, and \mathcal{C}_n be the ordered set of frequencies that are going to be sensed by SU_n , i.e., $\mathcal{C}_n = \{f_n^1, f_n^2, \dots\}$. Then $E^{cs} = P^{cs} t^{cs} \sum_{n=1}^N (|f_n^0 - f_n^1| + \sum_{k=1}^{|\mathcal{C}_n|-1} |f_n^k - f_n^{k+1}|)$ where $|\mathcal{C}_n|$ is the cardinality of \mathcal{C}_n .

Reporting Energy (E^{rep}): The reporting energy is the energy spent by the SUs for transmitting their local sensing results to CBS through the common control channel. We assume that the reporting period is long enough such that all SUs can transmit their local results and regardless of the number of channels sensed, an SU transmits a single packet if it participates in sensing. Furthermore, we also assume that the channel is error free so all transmitted packets are successfully received. Let E_n^{rep} denote the energy required by SU_n to transmit a single packet, and let \mathcal{S} denote the set of SUs participating in sensing. Then, E^{rep} is given by $\sum_{n \in \mathcal{S}} E_n^{rep}$.

6.2. Problem Formulation

We assume that all SUs have the same false alarm probability for all channels, denoted by P^F . The relationship between probability of detection for SU_n over channel m ($P_{m,n}^D$) is again given by

$$P_{m,n}^D = \mathcal{Q} \left(\frac{\mathcal{Q}^{-1}(P^F) - \sqrt{\tau_{m,n} f_s \gamma_{m,n}}}{\sqrt{2\gamma_{m,n} + 1}} \right) \quad (6.1)$$

where f_s is the sampling frequency and \mathcal{Q} is the complementary cumulative distribution of a standard Gaussian [38]. The cooperative probability of detection using OR rule for channel m , $P_m^{D,coop}$, is given as

$$P_m^{D,coop} = 1 - \prod_{n \in \mathcal{S}_m} (1 - P_{m,n}^D) \quad (6.2)$$

where \mathcal{S}_m is the set of SUs sensing channel m . In our previous work [68], we showed that the cooperative detection probability for channel m is a concave function of $\tau_{m,n}$ if

all the individual detection probabilities of SUs participating in the sensing of channel m are greater than 0.5. Let $\tau_{m,n}^{min}$ denote the minimum time required to achieve a $P_{m,n}^D$ value of 0.5, that is given by

$$\tau_{m,n}^{min} = \left(\frac{Q^{-1}(P^F)}{\gamma_{m,n}\sqrt{f_s}} \right)^2. \quad (6.3)$$

In addition, to ensure a cooperative false alarm threshold of $th P^{F,coop}$, a channel should be sensed by at most $\lfloor \frac{\log(1-th Q^F)}{\log(1-P^F)} \rfloor$ number of SUs.

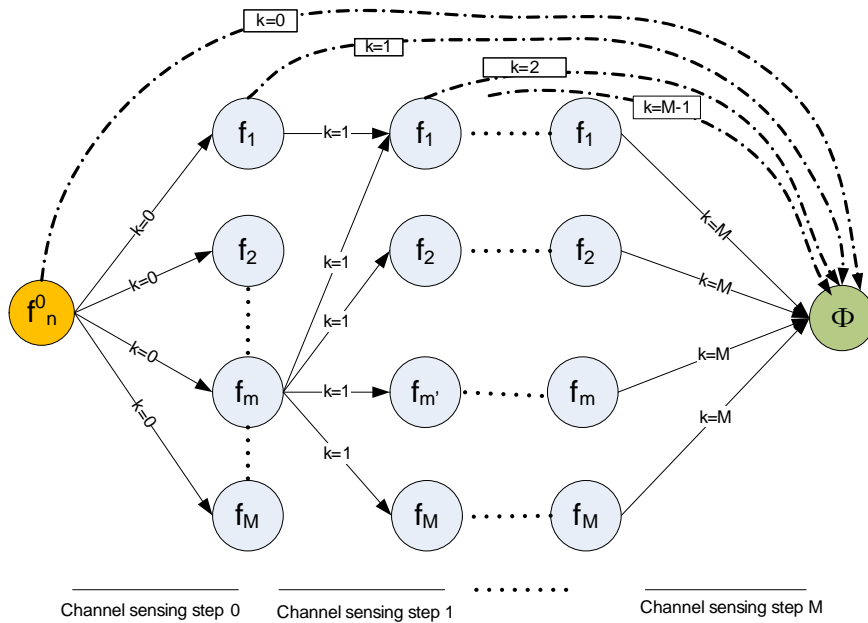


Figure 6.2. Channel sensing sequence.

In the following parts, we present our model which makes use of network flows in order to represent the set of frequencies sensed by an SU and the sensing sequence of these channels. Let ϕ denote a virtual terminal channel that indicates the end of sensing, and f_m be the frequency of channel m . Figure 6.2 illustrates the network flow representation for the sensing actions for an SU. At the beginning of a frame, SU_n 's antenna is tuned to f_n^0 . Likewise, each SU tunes to a virtual channel ϕ after performing all sensing tasks. Since there are M frequencies in the system, an SU may sense all these M channels one after another. However, it can also sense less channels resulting in SU to have an outgoing arrow directly after k th sensing. For instance, in Figure 6.2 the arrow from f_n^0 to ϕ marked with $k = 0$ shows a case in which SU senses no channels

whereas the arrow from f_1 to ϕ marked with $k = 1$ shows a case in which SU senses f_1 and ends sensing. This can be generalized to k step sensing similarly.

We now present the optimization model that minimizes the energy consumption related to sensing corresponding to the given system model. Let $\tau_{m,n}$ be a non-negative continuous variable (i.e., $\tau_{m,n} \geq 0$) denoting the time SU_n spends for sensing channel m , $x_{m,m',n}^k$ be a binary variable (i.e., $x_{m,m',n}^k \in (0, 1)$) with value 1 if SU_n switches from f_m to $f_{m'}$ at step k , and y_n be a binary variable (i.e., $y_n \in (0, 1)$) with value 1 if SU_n transmits its sensing outcomes to the base station. Our decision variables are $\tau_{m,n}$, $x_{m',m,n}^k$, and y_n . Then the optimization model can be written as:

$$\begin{aligned}
P1: \min w = & \sum_{m=1}^M \sum_{n=1}^N P^s \tau_{m,n} + \sum_{n=1}^N E_n^{rep} y_n \\
& + P^{cs} t^{cs} \sum_{n=1}^N \left(\sum_{m=1}^M |f_n^0 - f_m| x_{f_n^0, m, n}^0 + \sum_{m=1}^M \sum_{\substack{m'=1 \\ m' \neq m}}^M \sum_{k=1}^{M-1} |f_m - f_{m'}| x_{m, m', n}^k \right) \quad (6.4)
\end{aligned}$$

subject to:

Flow related constraints:

$$x_{f_n^0, \phi, n}^0 + \sum_{m=1}^M \sum_{k=1}^M x_{m, \phi, n}^k = 1, \quad \forall n \quad (6.5)$$

$$x_{f_n^0, \phi, n}^0 + \sum_{m=1}^M x_{f_n^0, m, n}^0 = 1, \quad \forall n \quad (6.6)$$

$$x_{f_n^0, m, n}^0 - \left(x_{m, \phi, n}^1 + \sum_{\substack{m'=1 \\ m' \neq m}}^M x_{m, m', n}^1 \right) = 0, \quad \forall m, \forall n \quad (6.7)$$

$$\sum_{\substack{m'=1 \\ m' \neq m}}^M x_{m', m, n}^{M-1} - x_{m, \phi, n}^M = 0, \quad \forall m, \forall n \quad (6.8)$$

$$\sum_{\substack{m'=1 \\ m' \neq m}}^M x_{m', m, n}^k - \sum_{\substack{m'=1 \\ m' \neq m}}^M x_{m, m', n}^{k+1} = 0, \quad \forall m, \forall n, k = 1, \dots, M-2 \quad (6.9)$$

$$x_{f_n^0, m, n}^0 + \sum_{\substack{m'=1 \\ m' \neq m}}^M \sum_{k=1}^{M-1} x_{m', m, n}^k \leq 1, \quad \forall m, \forall n \quad (6.10)$$

Sensing time related constraints:

$$\tau_{m,n} - \tau_{m,n}^{\min}(x_{f_n^0,m,n}^0 + \sum_{\substack{m'=1 \\ m' \neq m}}^M \sum_{k=1}^{M-1} x_{m',m,n}^k) \geq 0, \quad \forall m, \forall n \quad (6.11)$$

$$t^{\text{cs}} \sum_{m=1}^M (|f_n^0 - f_m| x_{f_n^0,m,n}^0 + \sum_{\substack{m'=1 \\ m' \neq m}}^M \sum_{k=1}^{M-1} |f_m - f_{m'}| x_{m',m,n}^k) + \sum_{m=1}^M \tau_{m,n} \leq T^s y_n, \quad \forall n \quad (6.12)$$

Sensing quality related constraints:

$$\sum_{n=1}^N (x_{f_n^0,m,n}^0 + \sum_{\substack{m'=1 \\ m' \neq m}}^M \sum_{k=1}^{M-1} x_{m',m,n}^k) \geq \delta^{\min}, \quad \forall m \quad (6.13)$$

$$\sum_{n=1}^N (x_{f_n^0,m,n}^0 + \sum_{\substack{m'=1 \\ m' \neq m}}^M \sum_{k=1}^{M-1} x_{m',m,n}^k) \leq \lfloor \frac{\log(1 - th P^{F,coop})}{\log(1 - P^F)} \rfloor, \quad \forall m \quad (6.14)$$

$$th P^{D,coop} - P_m^{D,coop} \leq 0, \quad \forall m \quad (6.15)$$

where $P_m^{D,coop}$ is calculated as follows:

$$P_m^{D,coop} = 1 - \prod_{n=1}^N \left(1 - P_{m,n}^D(x_{f_n^0,m,n}^0 + \sum_{\substack{m'=1 \\ m' \neq m}}^M \sum_{k=1}^{M-1} x_{m',m,n}^k) \right). \quad (6.16)$$

Hence, SUs that switch to channel m contribute to the multiplication with $1 - P_{m,n}^D$ corresponding to their $\tau_{m,n}$, whereas other SUs contribute with 1, not effecting the result of the multiplication.

The objective in (6.4) minimizes the total energy expenditure due to sensing for a frame. The first part of the third term is the energy consumption due to the initial channel switch from f_n^0 whereas the second part is for the succeeding channel switches. Constraint (6.5) indicates that the sensing of all SUs should end at some step k . Constraint (6.6) ensures that sensing operation of all SUs should start with

step 0. In this equation, having $x_{f_n^0, \phi, n} = 1$ implies that SU_n does not sense a channel. Constraints (6.7), (6.8) and (6.9) are flow conservation equations for step 0, step M , and intermediate steps, respectively. They imply that if SU_n switches from channel m' to channel m , then it should switch from channel m to some other channel where switching to ϕ denotes the end of sensing for SU_n . As switching consumes energy, an SU performs a channel switch to channel m only for sensing channel m . Constraint (6.10) states that an SU can sense a given channel at most once for a frame. Constraint (6.11) enforces $\tau_{m,n}$ to be greater than or equal to $\tau_{m,n}^{min}$ if SU_n switches to channel m , which in turn enforces the concavity condition for $P_m^{D,coop}$ to hold. The requirement that total time spent on sensing be smaller than quiet sensing period for each SU is expressed in constraint (6.12). The first two terms on the left hand side constitute the total time spent for channel switching, and the third term is the total of actual time spent for sensing by SU_n . Constraint (6.13) forces each channel to be sensed by at least δ^{min} SUs. On the other hand, constraint (6.14) forces the cooperative false alarm probability be smaller than the respective threshold for each channel. Constraint (6.15) is the cooperative detection probability constraint.

6.3. Outer Linearization (OL)

The given model is a mixed integer non-linear problem with a linear objective in which the non-linearity comes from constraint set (6.15). However, it is convex once $x_{m',m,n}^k$ are fixed since $P_m^{D,coop}$ is concave in terms of $\tau_{m,n}$. Thus, we apply the outer linearization algorithm that was given in the previous chapter, which first ignores all the non-linear constraints, then iteratively linearizes the violated ones by using the gradient until all of them are satisfied [70].

6.3.1. A Low Complexity Heuristic Algorithm: Energy Aware Sensing scheduling (EASE)

EASE is a fast heuristic that assigns δ^{min} SUs to sense a channel such that all assigned SUs have the same detection probability, P^D , that is calculated as $1 - (1 - P^{D,coop})^{1/\delta^{min}}$ for OR rule. The aim of our heuristic, given in Figure 6.3, is to choose

the set of SUs that will consume the least energy for sensing each channel. At each iteration (i.e., assignment for f_m), SUs are sorted in increasing order according to their additional energy consumption required to sense this channel (ΔE_n) which includes channel switching, spectrum sensing and reporting costs. Our algorithm assigns SUs to channels sequentially and updates the channel sensing sequence to obtain the least channel switching energy. For finding the best sequence, an SU first tunes to the channel with the minimum or maximum frequency depending on which one is the closest to its initial frequency. If the minimum one is visited first, then the other ones are visited in ascending order of their frequencies whereas if the maximum one is the first, then the others are visited in descending order. As an example, suppose an SU is initially tuned to f_{10} and it is assigned to sense f_{11}, f_{13} . Suppose f_9 is added to the sequence. Then the ideal sequence will be f_9, f_{11}, f_{13} . If f_2 is added to the sequence at a subsequent step, then the ideal sequence becomes f_{13}, f_{11}, f_9, f_2 .

Considering the reporting energy, an SU that is not assigned a channel for sensing incurs a reporting energy cost. On the contrary, an SU that is already assigned a channel has no reporting cost for this channel. Among all sorted SUs, first δ^{min} SUs that have sufficient remaining sensing time are added to \mathcal{S}_m , the set of SUs sensing channel m . Remaining sensing time for these selected SUs are reduced accordingly. The complexity of our algorithm is $O(MN \log N)$ due to the sorting of SUs based on ΔE_n being in the order of $O(N \log N)$ and repeating this for all M frequencies.

6.4. Performance Evaluation

We analyze the performance of both methods in a network with 20 contiguous channels with 100kHz bandwidth each and 100 SUs. We assign f_n^0 randomly. Furthermore, we assume $\gamma_{m,n}$ values are exponentially distributed with mean μ^{SNR} . For both f_n^0 and $\gamma_{m,n}$, we use the same randomly assigned values for fair comparison. The other parameters are given in Table 6.1. The results given below are for a single frame. Hence, cumulative energy savings in the long run will be noticeably higher. As the results of EASE depend on the order of the channels for assignment, we run EASE

```

Require:  $P^D, \delta^{min}, M, N, \gamma_{m,n}, T^s, f_n^0$ .

for all  $SU_n$  do
    Set remaining sensing time for  $SU_n$  ( $T_n^{rem}$ ) to  $T^s$ 
    Set reporting energy cost for  $SU_n$  to ( $E_n^{rep}$ ) to  $E_n^{rep}$ 
    Set  $\mathcal{C}_n$ , set of channels to be sensed by  $SU_n$ , to  $\emptyset$ 
end for

while there is an unsensed channel do
    Select a channel  $f_m$  randomly among unselected frequencies and set  $\mathcal{S}_m = \emptyset$ 

    for all  $SU_n$  do
        Compute the best sensing sequence for minimum switching energy for  $f_m$  with additional switching time  $\Delta T_n^{cs}$ 
        Calculate  $\tau_{m,n}$  required for achieving  $P^D$ 
        Calculate additional energy consumption ( $\Delta E_n$ ) for  $SU_n$  to sense  $f_m$ 
    end for

    Sort SUs according to  $\Delta E_n$  in ascending order
    Select the first  $\delta^{min}$  SUs in the list that also satisfies  $\tau_{m,n} + \Delta T_n^{cs} \leq T_n^{rem}$ 

    for all  $SU_n$  do
        if  $SU_n$  is selected then
             $\mathcal{S}_m = \mathcal{S}_m \cup SU_n$ 
             $E_n^{rep} = 0$ 
             $T_n^{rem} = T_n^{rem} - \tau_{m,n} - \Delta T_n^{cs}$ 
        end if
    end for
end while

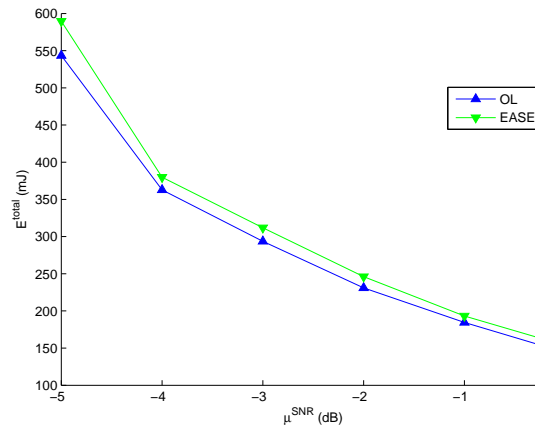
```

Figure 6.3. EASE algorithm.

Table 6.1. Model parameters.

δ^{min}	3
T^s	20ms
P^F	0.01
f_s	1kHz
P^s	1000mW
P^{cs}	1000mW
E_n^{rep}	1mJ, $\forall n$
μ^{SNR}	Between -5 and 0 dB
t^{cs}	Between 0.5ms and 1.5ms per 100kHz
$th P^{D,coop}$	0.9
$th P^{F,coop}$	0.1
ϵ	10^{-4}

with 20 random orderings and give the results for the ordering with the minimum total energy consumption.

Figure 6.4. Energy vs μ^{SNR} with $t^{cs}=1\text{ms}/100\text{kHz}$.

We first give the impact of μ^{SNR} value on total energy (E^{total}) in Figure 6.4. Increasing μ^{SNR} improves total energy as less sensing time is required to achieve a particular detection probability. Moreover, the improvement in total energy for 1 dB increase in μ^{SNR} is diminishing. For instance, going from -5 dB to -4 dB provides 181 mJ savings whereas the savings for going from -1 dB to 0 dB is 40 mJ. Another point

to note is that EASE performs well, always within 10 percent of OL.

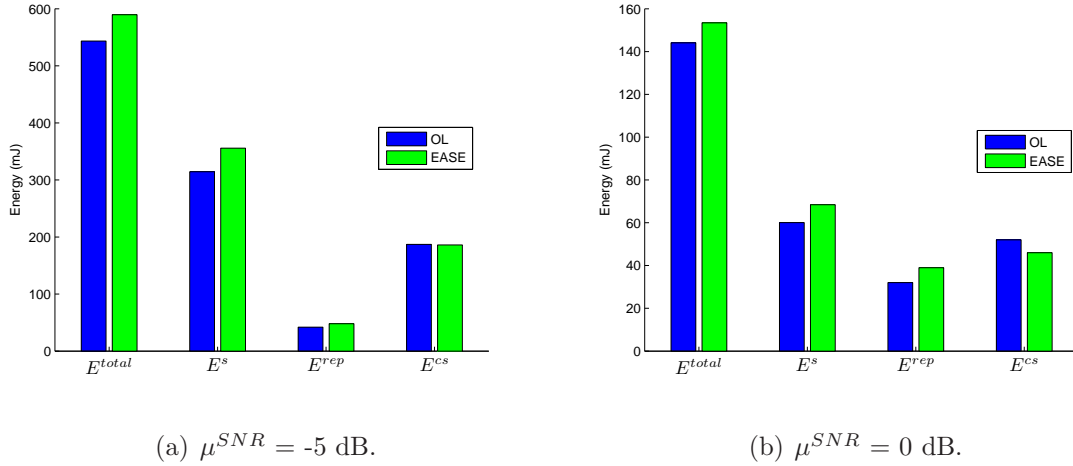


Figure 6.5. Energy consumption profiles with $t^{cs} = 1\text{ms}/100\text{kHz}$.

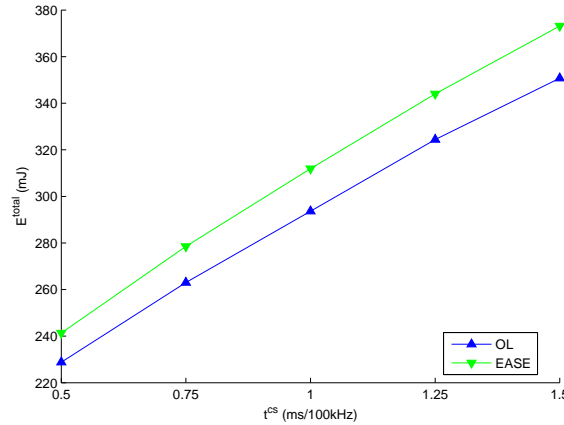
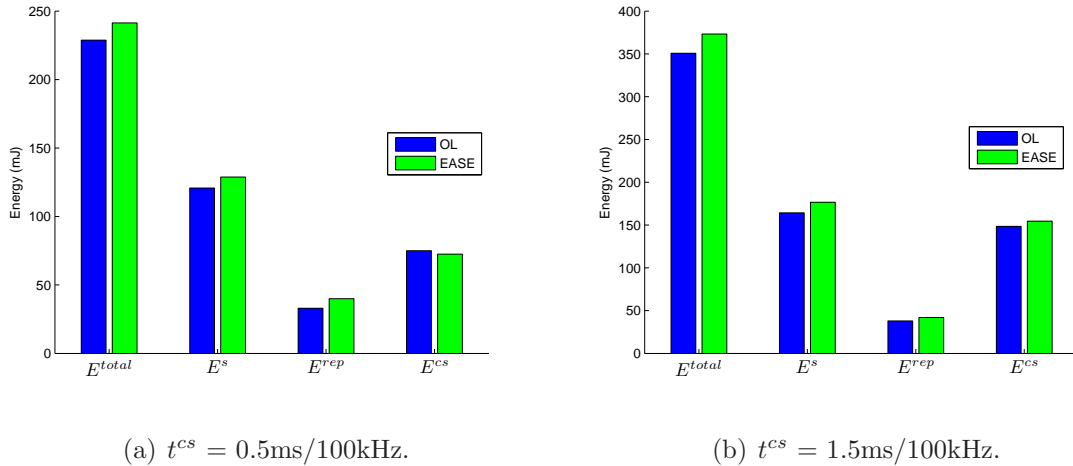


Figure 6.6. Energy vs t^{cs} .

The breakdown of the total energy into individual components for high and low values of μ^{SNR} is given in Figure 6.5. We observe that reporting energy (E^{rep}) is almost the same for both cases. Sensing energy (E^s) is the most dominating factor for low μ^{SNR} , accounting about 60 percent of total energy followed by channel switching energy (E^{cs}) with 35 percent. On the other hand, with high μ^{SNR} , the percentage of sensing energy drops to 40 percent. The share of channel switching energy remains almost the same whereas the share of reporting energy increases from 8 percent to 22 percent. One last thing to note is that, even though the channel switching energy is not directly related to μ^{SNR} , increasing μ^{SNR} also decreases the channel switching energy, as more SUs become candidates for sensing a particular channel within the sensing period, which in turn helps the algorithms to find better sensing sequences.

The effect of t^{cs} on the total energy is shown in Figure 6.6. For both methods, increasing t^{cs} causes an almost linear increase in the total energy. Again, EASE performs close to OL (within 7 percent). As t^{cs} depends on the hardware, we emphasize that fast switching mobile hardware is essential for energy savings.

(a) $t^{cs} = 0.5\text{ms}/100\text{kHz}$.(b) $t^{cs} = 1.5\text{ms}/100\text{kHz}$.Figure 6.7. Energy consumption profiles with $\mu^{SNR} = -3\text{dB}$.

The individual components of the total energy for high and low values of t^{cs} are shown in Figure 6.7. Increasing t^{cs} increases both channel switching energy and sensing energy. Channel switching energy is directly proportional to t^{cs} so the increase is expected. On the other hand, a high t^{cs} implies less time for sensing, which in turn decreases the number of candidate SUs that can sense a particular channel. Furthermore, an SU with a high SNR for a channel may refrain from sensing that channel as switching cost becomes significant and some other SU with smaller SNR can be assigned to that channel if its switching cost is smaller. Hence, the sensing energy also increases with increasing t^{cs} .

6.5. Chapter Summary

In this chapter, a cooperative sensing scheduling scheme that minimizes energy consumption of spectrum sensing while ensuring satisfactory sensing quality for each channel is proposed. SUs with better SNR are favored to sense a channel due to the inverse relationship between the sensing time and the channel SNR. Additionally, cost of channel switching between frequencies is taken into account. The optimal solution

and a low complexity heuristic that achieves close to the optimum are presented.

7. OPTIMAL COOPERATOR SET SELECTION IN SOCIAL COGNITIVE RADIO NETWORKS

In cooperative sensing, an SU senses for other SUs in the hope that others will sense in return when it needs the spectrum. Due to the diverse channel conditions (i.e. SNR values) and SU properties, cooperator selection has to consider this diversity and favor SUs with short sensing durations [68]. However, SUs may exhibit various sensing reliability: some may act maliciously, or some may unintentionally have low sensing accuracy, etc. Cooperative sensing schemes should combat these challenges while ensuring low communication and computation overhead. These two key points are considered in the literature, but the incentives for cooperation have mostly been overlooked. In other words, SUs may lack incentives to cooperate in such a model that does not account for the dynamism of cooperation, e.g., *under which conditions nodes are likely to cooperate*. Besides, a CR is generally an energy-limited mobile device that should use its energy budget cautiously, i.e., deciding on not to cooperate if the incentives are not sufficient. Referring to real cognitive agents, e.g. human beings, cooperation depends on the social ties between the two ends of the cooperation [52]. Having said this, we attempt to provide an abstraction of SU cooperation behavior that depends on the social ties between SUs.

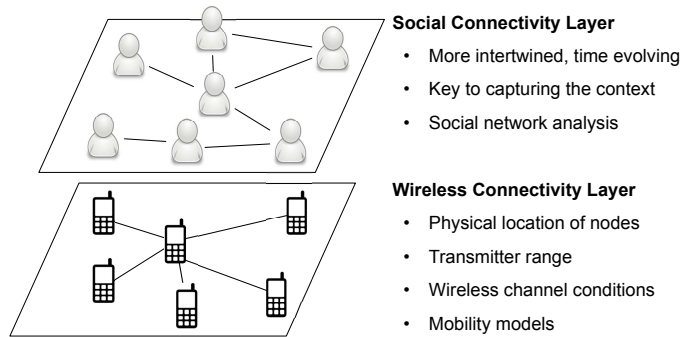


Figure 7.1. Two layered view of a network.

We can abstract a network in two layers as in Figure 7.1: the first layer being the *wireless connectivity layer* and the second being the *social connectivity layer* [49, 74].

Although not depicted in Figure 7.1, wireless connectivity layer is also affected by the social behavior of the nodes as, e.g. for human networks, node mobility is not random but a function of social behavior [75]. Hence, these layers are not independent. The majority of the CRN literature considers only the wireless connectivity layer. However, for a better grasp of the information in and about the network, CR protocols should also take the social connectivity layer into account. We call a CRN as *social CRN* if CRs operate based on the ties in the social connectivity layer. Additionally, we define a protocol as *social-aware protocol* if it exploits the knowledge in the social connectivity layer.

In this chapter, we consider a cooperative spectrum sensing scenario in which each CR decides on its possible cooperators for sensing based on the information about both the social connectivity layer and wireless connectivity layer. For the former, it takes the willingness to cooperate and sensing reliability of other CRs into account, whereas for the latter the channel conditions are considered. In a traditional CRN architecture, when the dedicated transmitter CR_i requests the cooperation of CR_j for sensing, CR_j responds with probability 1. However, this is not the case in a social CRN as the CRs may not be willing to sacrifice their energy for the benefit of others. Let $w_{i,j}^{soc}$ be the strength of the social tie between CR_i and CR_j . Moreover, let $p_{i,j}$ denote the probability that CR_j complies with the sensing request of CR_i , which we call the *cooperation probability*. $p_{i,j}$ is a function of $w_{i,j}^{soc}$, but it may also depend on some other parameters based on the context of the network and/or choice of the network designer. Throughout the chapter, we discuss several formulations for $p_{i,j}$. For instance, $p_{i,j}$ may be related to the sensing burden that is put on CR_j by other CRs. Furthermore, we also consider scenarios with a malicious CR in the network.

The contributions of this chapter can be listed as follows:

- We develop a simple trust mechanism for a CR that estimates the sensing accuracy of CRs who performed sensing for this CR (Section 7.1). Using the introduced trust metric as well as the cooperation probability of CRs, a CR can select its cooperator set more efficiently, e.g., avoiding malicious CRs.

- We formulate and solve the optimal cooperator selection problem as a probabilistic multi-objective optimization model that aims to strike a balance between throughput and sensing accuracy (Sections 7.2 and 7.3). When all the CRs have good intentions, our solution method lies within 90 percent of the expected throughput-optimal solution. On the other hand, in case of a malicious CR, it outperforms the expected throughput-optimal solution by 16 percent.
- We analyze the effect of social ties and try different cooperation probability ($p_{i,j}$) formulations by simulating various scenarios for the same network in Section 7.4. We design a flexible cooperation scheme such that it facilitates the CRs to operate also in *foreign* environments (e.g., different than home network) where they do not have any socially-connected nodes in the neighborhood. In addition, our scheme should avoid the CRs being exploited by excessive sensing. Motivated by these two points, we introduce *system willingness* and *peer willingness* concepts in Section 7.4. Moreover, we assess the impact of certain factors that are specific to each CR such as location and number of social ties.

With these contributions, we assess the performance of a realistic CRN in which cooperation may be limited due to several factors such as friendship, battery restrictions and security concerns.

7.1. System Model

7.1.1. Notations and Assumptions

In this chapter, we consider an ad hoc CRN as in Figure 7.2. There exist a single mobile primary user and N stationary CRs, all of which are within each other's communication range.² As shown in Figure 7.2, the link between CR_i and CR_j is marked by three values:

²Even though CRs are assumed to be stationary, our proposal also works with mobile CRs. This assumption is just for decreasing the degree of freedom for the problem in order to simplify the analysis.

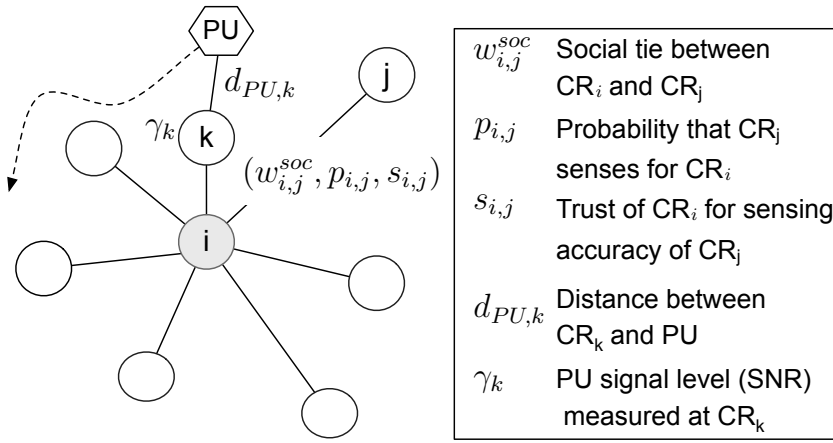


Figure 7.2. System model: A CR and $N - 1$ CRs in its transmission range. Only some representative links are depicted. The link between CR_i and CR_j is marked with the social tie, cooperation probability, and trust information $(w_{i,j}^{soc}, p_{i,j}, s_{i,j})$ from CR_i's viewpoint.

- *Social tie* ($w_{i,j}^{soc}$): CRs are connected to other CRs with social ties. Let $w_{i,j}^{soc}$ be the strength of the social tie between CR_i and CR_j, e.g., closely connected or a far friend. We assume that $w_{i,j}^{soc} = w_{j,i}^{soc}$ and they are known by CR_i and CR_j.
- *Cooperation probability* ($p_{i,j}$): It is the probability that CR_j senses for CR_i if asked for cooperation by CR_i. We assume $p_{i,j}$ is a function of $w_{i,j}^{soc}$ and consider various models for $p_{i,j}$ in Section 7.4.
- *Trust* ($s_{i,j}$): Additionally, CR_i maintains the degree of *trust* (Section 7.1.3) it has for CR_j's sensing accuracy ($s_{i,j}$). Different than $w_{i,j}^{soc}$, $s_{i,j}$ is computed at CR_i, may not be known by CR_j, and is not necessarily equal to $s_{j,i}$.

The CRN operates in a frame based manner. At the beginning of a frame, one of the CRs is assigned as the candidate transmitter and has the right to initiate cooperative sensing. As the access control is beyond the scope of this work and we target to see the effect of social ties, we employ a simple round robin scheduling to select the candidate transmitter. We assume that the PU is active with probability P^{on} during a frame, and its state does not change within the duration of the frame. CRN employs cooperative sensing with hard decisions (0 for the outcome “channel is idle”, and 1 for the outcome “channel is busy”) for detecting transmission opportunities at

the beginning of each frame. Let γ_j denote the PU's SNR at CR_{*j*} that is given by [76]:

$$\gamma_j = \frac{P_{PU}^{tx} L_j G_{PU} G_j}{N_{th}} \quad (7.1)$$

where P_{PU}^{tx} is the transmission power of the PU, L_j is the path loss between the PU and CR_{*j*}, G_{PU} and G_j are the antenna gains for the PU and CR_{*j*}, and N_{th} is the noise floor. We use the following path loss model:

$$L_j = \left(\frac{c}{4\pi f} \right)^2 \left(\frac{1}{d_{PU,j}} \right)^l \quad (7.2)$$

where c is the speed of light, f is the channel frequency, $d_{PU,j}$ is the distance between the PU and CR_{*j*}, and l is the path loss exponent.

For a complex valued Phase Shift Keying (PSK) channel with circularly symmetric complex Gaussian noise, the required sensing time by CR_{*j*} (τ_j) in order to achieve a specified probability of detection (P^D) and probability of false alarm (P^F) is given by [38]:

$$\tau_j = \frac{(\mathcal{Q}^{-1}(P^F) - \mathcal{Q}^{-1}(P^D) \sqrt{2\gamma_j + 1})^2}{f_s \gamma_j^2} \quad (7.3)$$

in which \mathcal{Q} is the complementary cumulative distribution of standard Gaussian and f_s is the sampling frequency.

7.1.2. Frame Structure

We propose a cooperation scheme that follows the steps in Figure 7.3 where each frame is divided into time intervals. At the beginning of the frame (T^{req}), the candidate transmitter CR (CR_{*i*}) sends a packet and asks for cooperation of the selected CRs, that is denoted by \mathcal{N}^{req} . These requested CRs (CR_{*j*}s) may perform sensing for CR_{*i*} based on the $p_{i,j}$ values. The second part of the frame (T^s) is dedicated to CRs that decide to cooperate with CR_{*i*}, denoted by \mathcal{N}_k^{req} . After all cooperating CRs complete sensing,

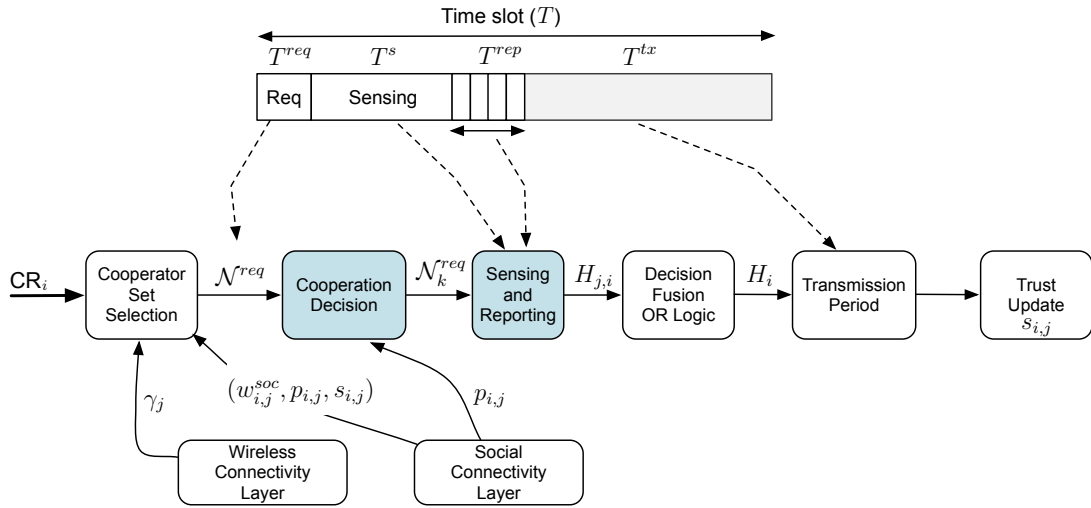


Figure 7.3. Steps of the proposed sensing scheme and the time period corresponding to each step in the frame structure. Steps in shaded boxes (cooperation decision and sensing/reporting) are performed by the requested CR, CR_j .

each CR sends its hard decision to CR_i in a time-sharing manner in the reporting period (T^{rep}). CR_i fuses reported sensing outcomes using OR rule. Depending on the final decision, CR_i transmits its data during the transmission period (T^{tx}) if the channel is decided to be vacant. If the fusion decision declares that the PU channel is busy, CR_i stays silent till the beginning of the next frame. Figure 7.4 illustrates these steps of cooperative sensing. The first and the third step occur on the common control channel whereas the other steps occur on the sensed PU channel.

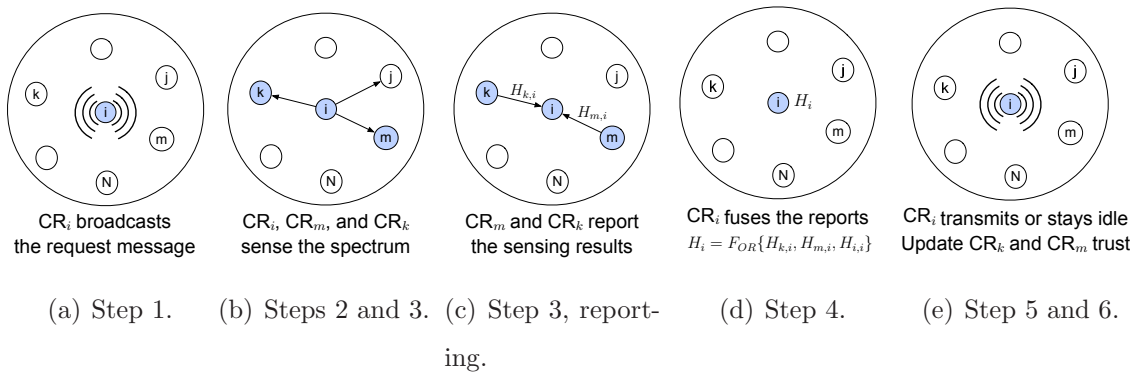


Figure 7.4. Steps of social-aware cooperative sensing. Steps in the figure correspond to the steps depicted in Figure 7.3.

Below, we discuss the length and further details of each period.

- T^{req} : The requesting period is of fixed length as it is a single packet transmission that specifies which CRs are asked to cooperate. \mathcal{N}^{req} may not include CR_i itself (i.e. the required sensing time for CR_i may be too long to be feasible).
- T^s : For the sake of simplicity, we assume that the required sensing reliability (i.e., P^D and P^F values) for each cooperating CR is identical and fixed. Given these constant P^D and P^F values, T^s can be formulated as:

$$T^s = \max_{\text{CR}_j \in \mathcal{N}^{req}} \{\tau_j\} \quad (7.4)$$

where τ_j values are calculated as in (7.3). T^s equals to the maximum sensing time of the CRs in the requested set. However, that maximum may not be realized as $\text{CR}_j \in \mathcal{N}^{req}$ with the largest τ_j may not sense, i.e., $\text{CR}_j \notin \mathcal{N}_k^{req}$.

- T^{rep} : If we assume that a single time slot for reporting takes t^{rep} , the total required duration for reporting is:

$$T^{rep} = |\mathcal{N}^{req} \setminus \text{CR}_i| t^{rep}. \quad (7.5)$$

In (7.5), we exclude CR_i from the reporting set as it does not send a report packet to itself. The size of this modified set is the maximum number of CRs that may send a report packet. Furthermore, during the slots assigned to non-cooperating CRs, CR_i listens idly as it cannot know the set of sensing CRs in advance. The TDMA scheme that we employ is a simple ID based one, where the slots are allocated to CRs in ascending order of their IDs.

- T^{tx} : If CR_i decides that the channel is vacant, this time period is used for transmission. Otherwise, CR_i switches to a low power mode to save energy until the next frame. Let T be the length of the whole frame, then T^{tx} is given by:

$$T^{tx} = T - (T^{req} + T^s + T^{rep}). \quad (7.6)$$

In this work, as the cooperative detection and false alarm probabilities are not known in advance due to the probabilistic nature of cooperation, their realizations may not satisfy the threshold values. Among these two criteria, we believe the

detection probability is more crucial as it is for PU protection whereas false alarm probability only affects the secondary network performance. To reflect this into the system, we forbid a CR to access the channel if the detection probability constraint is not satisfied, even if the channel is considered to be vacant.

7.1.3. Trust

In our model, each CR tracks the performance of other CRs who have sensed for it. Let us define $s_{i,j}$ as the trust of CR_{*i*} for CR_{*j*}, which measures how accurately CR_{*j*} performs spectrum sensing when requested by CR_{*i*}. Thus, it is a sensing reliability metric. In order to measure the trust, we employ a window based approach where CR_{*i*} stores the result of the last K interactions with CR_{*j*}. Let $o_{i,j,k}$ denote the k th interaction between CR_{*i*} and CR_{*j*}. Furthermore, let $H_{j,i}$, H_i , and H be the CR_{*j*}'s sensing outcome, the final decision of CR_{*i*} after fusing the sensing outcomes, and the PU channel's actual occupancy state, respectively. If $H_{j,i}$ is believed to be true (false), $o_{i,j,k}$ gets the value 1 (-1).

Let us focus on a single interaction between these two CRs. If we apply OR rule for decision fusion, there are six cases to consider depending on $H_{j,i}$, H_i , and H that are listed in Table 7.1.

Table 7.1. Possible cases for sensing accuracy evaluation.

	$H_{j,i}$	H_i	H	Action
Case 1	0	0	0	Channel access, success
Case 2	0	1	0	No access
Case 3	1	1	0	No access
Case 4	0	0	1	Channel access, collision
Case 5	0	1	1	No access
Case 6	1	1	1	No access

Cases 1 and 4 are easy to evaluate as in both cases CR_{*i*} accesses the channel and can directly observe the ground truth. In Case 1, the transmission of CR_{*i*} is going

to be successful. Therefore, CR_i concludes that $H_{j,i}$ is correct resulting in $o_{i,j,k} = 1$. On the other hand, CR_i is going to collide with the incumbent PU in Case 4. Hence, CR_i concludes that $H_{j,i}$ is erroneous and sets $o_{i,j,k} = -1$. For the remaining cases, the evaluation is not straightforward since CR_i does not access the channel. For these cases, we compare the decision of CR_j with the majority decision of the cooperating CRs. If CR_j 's decision complies with the majority, it is assumed to be true. Otherwise, it is considered as false. However, in the case of a tie where the number of cooperators is even (equal number of 0s and 1s), we break the tie by favoring the set with the higher total trust. If there is still a tie and CR_i itself was one of the cooperators, we assume CR_i 's decision to be true. Otherwise, we skip the evaluation for this interaction.

As the interactions are evaluated, CR_i gets a sense of the reliability of other CRs. We calculate $s_{i,j}$ by using these observations. In order to account for a possible trend, we emphasize the recent observations. Let us assume the observations from $o_{i,j,1}$ to $o_{i,j, \lfloor \theta K \rfloor}$ are the most recent ones where $0 \leq \theta \leq 1$ is a system parameter that shows up to what percentage of the observations are recent. We calculate the trust value of CR_i for CR_j as:

$$s_{i,j} = \lambda \frac{\sum_{k=1}^{\lfloor \theta K \rfloor} o_{i,j,k}}{\lfloor \theta K \rfloor} + (1 - \lambda) \frac{\sum_{k=\lfloor \theta K \rfloor + 1}^K o_{i,j,k}}{K - \lfloor \theta K \rfloor} \quad (7.7)$$

where $0 \leq \lambda \leq 1$ is the weight of recent observations. Hence, $s_{i,j}$ is a value between -1 and 1, that measures the sensing accuracy of CR_j from CR_i 's point of view.

7.1.4. Sensing Accuracy of Social-aware Cooperative Sensing

Let $P_{N^{req}}^{D,soc}$ denote the *social-aware probability of detection* and $P_{N^{req}}^{F,soc}$ denote the *social-aware probability of false alarm* of our social-aware cooperative sensing scheme. Since a requested CR cooperates with the requester probabilistically (i.e., $p_{i,j}$), these probabilities are difficult to compute compared to traditional cooperative sensing. In the following, we present how we calculate the expected values of $P_{N^{req}}^{D,soc}$ and $P_{N^{req}}^{F,soc}$.

Let $\mathcal{P}(\mathcal{N}^{req})$ be the power set of \mathcal{N}^{req} . If we consider a subset of \mathcal{N}^{req} , say $\mathcal{N}_k^{req} \in \mathcal{P}(\mathcal{N}^{req})$, the probability that the realized sensing set be \mathcal{N}_k^{req} (i.e. only the CRs in \mathcal{N}_k^{req} sense the channel) is:

$$P(\mathcal{N}_k^{req}) = \prod_{\text{CR}_j \in \mathcal{N}_k^{req}} p_{i,j} \prod_{\text{CR}_m \in \mathcal{N}^{req} \setminus \mathcal{N}_k^{req}} (1-p_{i,m}). \quad (7.8)$$

Considering the OR rule, the probability of detection and false alarm for \mathcal{N}_k^{req} are calculated as:

$$P^{D,coop}(\mathcal{N}_k^{req}) = 1 - (1 - P^D)^{|\mathcal{N}_k^{req}|}. \quad (7.9)$$

$$P^{F,coop}(\mathcal{N}_k^{req}) = 1 - (1 - P^F)^{|\mathcal{N}_k^{req}|}. \quad (7.10)$$

Then, the expected probability of detection for \mathcal{N}^{req} is:

$$P_{\mathcal{N}^{req}}^{D,soc} = E[P_{\mathcal{N}^{req}}^{D,coop}] = \sum_{\mathcal{N}_k^{req} \in \mathcal{P}(\mathcal{N}^{req})} P(\mathcal{N}_k^{req}) P^D(\mathcal{N}_k^{req}). \quad (7.11)$$

Similarly, we calculate $P_{\mathcal{N}^{req}}^{F,soc}$ as follows:

$$P_{\mathcal{N}^{req}}^{F,soc} = E[P_{\mathcal{N}^{req}}^{F,coop}] = \sum_{\mathcal{N}_k^{req} \in \mathcal{P}(\mathcal{N}^{req})} P(\mathcal{N}_k^{req}) P^F(\mathcal{N}_k^{req}). \quad (7.12)$$

For a legitimate operation, PU detection probability is crucial and has to be kept equal or above a recommended level, e.g., 0.9 according to IEEE 802.22. CR_i determines its cooperation set \mathcal{N}^{req} such that the expected detection probability meets the threshold. However, as some of the CRs may not participate in sensing, the realized detection probability achieved by \mathcal{N}_k^{req} may be lower than the required PU detection

accuracy. If that is the case, we forbid a CR to access the channel whatever the final sensing decision is.

There are also several practical issues to be discussed regarding the calculation of $P_{\mathcal{N}^{req}}^{D,soc}$ and $P_{\mathcal{N}^{req}}^{F,soc}$.

- *Unknown $p_{i,j}$ values:* The exact values of $p_{i,j}$ may not always be available to CR_i . For such a setting, CR_i can estimate $p_{i,j}$, say $\tilde{p}_{i,j}$, based on its interactions with CR_j . Consequently, CR_i calculates $P_{\mathcal{N}^{req}}^{D,soc}$ and $P_{\mathcal{N}^{req}}^{F,soc}$ with $\tilde{p}_{i,j}$ instead of $p_{i,j}$.
- *Too large neighborhood:* The number of one hop neighbors of CR_i may be large. Hence, selecting \mathcal{N}^{req} takes considerable time with the exponential growth of number of subsets. If that is the case, then CR_i first eliminates some candidate CRs. The criteria for this elimination may be γ_j , $p_{i,j}$ or a combination, e.g., CRs with the largest $\gamma_j p_{i,j}$ values can be selected as candidates for \mathcal{N}^{req} .

7.2. Cooperator Set Selection

7.2.1. Objectives

In our model, a CR desires to attain high throughput and cooperate with the CRs that it trusts. In the following parts, we present these two objectives.

Throughput (C): We assume a backlogged traffic model for each CR, i.e., each node always has packets to transmit. Hence, a CR transmits for T^{tx} time units whenever it detects an idle channel successfully. In case of a false alarm or a detected active PU, CR keeps silent during the transmission period.

Let x_j be the binary optimization variable that is defined as:

$$x_j = \begin{cases} 1, & \text{if } \text{CR}_i \text{ asks the cooperation of } \text{CR}_j \\ 0, & \text{otherwise.} \end{cases}$$

For a particular assignment vector $\mathbf{x} = [x_j]$, we calculate $P^{F,soc}$ as follows:

$$P^{F,soc} = \sum_{\substack{\mathcal{N}^{req} \\ \in \mathcal{P}(N)}} P^{F,soc}(\mathcal{N}^{req}) \left[\prod_{j \in \mathcal{N}^{req}} x_j \prod_{k \notin \mathcal{N}^{req}} (1-x_k) \right]. \quad (7.13)$$

The multiplicative term takes the value 1 only for the set of CRs such that $x_j = 1$.

For \mathbf{x} , the expected throughput over the channel with Shannon capacity R bits/sec is:

$$C = (1 - P^{on})(1 - P^{F,soc})RT^{tx}. \quad (7.14)$$

where $P^{F,soc}$ and T^{tx} are the corresponding false alarm probability and transmission time, respectively.

Trust (S): CR_{*i*} desires to cooperate with the CRs towards which it has high trust values (i.e. more accurate sensing results). Hence, our second objective maximizes the minimum expected trust value of the cooperators which is expressed as:

$$S = \min\{(x_j p_{i,j} s_{i,j}) + (1 - x_j)\}. \quad (7.15)$$

In (7.15), $p_{i,j} s_{i,j}$ is the expected trust obtained from CR_{*j*} if it is selected for cooperation ($x_j = 1$). The second term covers the case of unselected CRs ($x_j = 0$) to have the minimum value only occur in the set of selected CRs.

7.2.2. Problem Formulation

Given (7.14) and (7.15), we model the cooperator set selection problem as a Multi-objective Optimization Problem (MOP) [77]. In a MOP with conflicting objectives, the system has a trade-off point, i.e., after some point one objective can only be improved at the expense of the other. A solution is said to dominate another solution if and only if it is strictly better in at least one objective, and not worse in the remaining objectives.

The set of non-dominated solutions is called the *Pareto front* and the best operating point can be determined by the decision maker according to the weight/importance of the objectives from the decision maker's perspective. We can identify \mathcal{N}^{req} in terms of $\mathbf{x} = [x_j]$ as follows:

$$\mathcal{N}^{req} = \{CR_j, x_j = 1\}.$$

Then, our MOP formulation for determining $\mathbf{x} = [x_j]$ is:

$$Pareto-max: \begin{cases} C = (1 - P^{on})(1 - P^{F,soc})RT^{tx} \\ S = \min\{(x_j p_{i,j} s_{i,j}) + (1 - x_j)\} \end{cases} \quad (7.16)$$

s.t.

$$T^{tx} = T - \left(T^{req} + T^s + t^{rep} \sum_{j=1, j \neq i}^N x_j \right) \quad (7.17)$$

$$T^{tx} \geq 0 \quad (7.18)$$

$$T^s \geq \tau_j x_j \quad \forall j \quad (7.19)$$

$$P^{D,soc} \geq 0.9 \quad (7.20)$$

$$P^{F,soc} \leq 0.1 \quad (7.21)$$

$$P^{D,soc} = \sum_{\substack{\mathcal{N}^{req} \\ \in \mathcal{P}(N)}} P^{D,soc}(\mathcal{N}^{req}) \left[\prod_{j \in \mathcal{N}^{req}} x_j \prod_{k \notin \mathcal{N}^{req}} (1 - x_k) \right] \quad (7.22)$$

$$P^{F,soc} = \sum_{\substack{\mathcal{N}^{req} \\ \in \mathcal{P}(N)}} P^{F,soc}(\mathcal{N}^{req}) \left[\prod_{j \in \mathcal{N}^{req}} x_j \prod_{k \notin \mathcal{N}^{req}} (1 - x_k) \right] \quad (7.23)$$

$$x_j \in \{0, 1\} \quad \forall j. \quad (7.24)$$

Constraint (7.17) mathematically defines the value of T^{tx} . In this constraint, $\sum_{j=1, j \neq i}^N x_j$ gives us the maximum number of sensing results CR_i may get from other users, which is equal to the number of TDMA slots that needs to be allocated by

CR_i . Constraint (7.18) states that the time remaining for transmission cannot be negative. Constraint (7.19) sets T^s to the maximum τ_j value of the requested CRs. Constraints (7.20) and (7.21) ensure that the selected set's expected detection and false alarm values meet the sensing requirements. In this work, we set a minimum detection probability of 0.9, and a maximum false alarm probability of 0.1, which are in accordance with IEEE 802.22 standard. Constraints (7.22) and (7.23) mathematically define the social-aware detection and false alarm probabilities, respectively. Finally, constraint (7.24) states that the variables are binary.

In the next section, we present our solution for the above formulated problem, which finds T^{tx} , T^s , and \mathcal{N}^{req} .

7.3. Evolutionary Multi-objective Optimization

As our model is a binary integer nonlinear problem (BINLP) that is neither convex nor concave and difficult to solve in general, we resort to evolutionary multi-objective optimization algorithm (EMOA) [77, 78] for its solution. In EMOA, a set of solutions called *population* is stored. Each solution represents an individual of the population. The individuals in one generation mate to produce offspring. Then, each offspring is mutated with some probability, p_m . Furthermore, only a subset of the current population in addition to the generated offspring is included in the next generation based on their *fitness* values. Figure 7.5 shows the steps of EMOA, which is explained in detail below.

Encoding scheme: We use bit strings of length N to represent a solution. Having a value 1 in the n th bit denotes the fact that CR_i requests sensing from CR_n (i.e. $x_n = 1$), and vice versa. We should emphasize that this request does not necessarily imply that CR_n actually senses the channel.

Fitness function: Fitness function represents the goodness of a solution. Before discussing the fitness function, let us introduce the concept of *constrained domination*.

```

1:  $iterNo = 0$ 
2: Generate the initial population,  $\mathcal{B}_0 = \text{INITIALIZE}(\mathcal{B}_0)$ 
3: while  $iterNo < maxIter$  do
4:   Initialize the current offspring population,  $\mathcal{C}_t = \emptyset$ 
5:   while  $|\mathcal{C}_t| < C_{size}$  do
6:     Select first parent,  $b_1 = \text{BINARYTOUR}(\mathcal{B}_t)$ 
7:     Select second parent,  $b_2 = \text{BINARYTOUR}(\mathcal{B}_t)$ 
8:     Generate two children,  $c_1, c_2 = \text{CROSSOVER}(b_1, b_2)$ 
9:     Mutate first child with probability  $p_m$ ,  $c_1 = \text{MUTATION}(c_1)$ 
10:    Mutate second child with probability  $p_m$ ,  $c_2 = \text{MUTATION}(c_2)$ 
11:     $\mathcal{C}_t = \mathcal{C}_t \cup c_1 \cup c_2$ 
12:   end while
13:   Select next generation,  $\mathcal{B}_{t+1} = \text{SELECTION}(\mathcal{B}_t \cup \mathcal{C}_t)$ 
14:    $iterNo = iterNo + 1$ 
15: end while
16: Select final solution,  $b_{final} = \text{FINALSELECTION}(\mathcal{B}_t)$ 

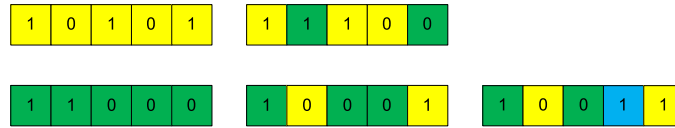
```

Figure 7.5. Evolutionary multi-objective optimization algorithm (EMOA).

In a constrained MOP, a solution u is said to constrained dominate another solution v if and only if:

- both solutions are feasible and u dominates v in both objective values, or
- u is feasible whereas v is not, or
- both solutions are infeasible and total constraint violation of u is smaller than v .

In our model, Constrains (7.18), (7.20), and (7.21) are the critical ones. Constraint (7.18) is the most important one as having a negative transmission time is not tolerable. Therefore, if a solution violates this constraint, we set its fitness value to $-\infty$ in order to eliminate this solution. Otherwise, we calculate both of the objective values and the total violation regarding constraints (7.20) and (7.21) related to a solution. Then, each solution's rank is calculated by simply counting the number of other solutions that constrained dominate this solution. Finally, the fitness of the individual is calculated as the difference between the number of individuals in the population and the rank of the current individual. As non-dominated solutions have rank 0, their fitness values are equal to the size of the population.



(a) Solution representation. (b) Crossover. (c) Mutation.

Figure 7.6. Example solutions for EMOA.

INITIALIZE: We generate the initial population of size B_{size} randomly. That is to say, each bit of the solution string is randomly assigned to 0 or 1. Figure 7.6a depicts two example solutions.

BINARYTOUR: In order to select a parent, we choose two candidate solutions using *roulette wheel selection*. Although roulette wheel selection picks the candidate solutions randomly, individuals with better fitness values are more likely to be selected. After two candidate solutions are selected, we choose the one with the better fitness

value as the first parent (binary tournament strategy). The ties are broken arbitrarily. The other parent is also selected using the same approach.

CROSSOVER: Crossover operation is the mating of two solutions to produce children. In our implementation, two parents mate to generate two offspring. In order to mate the selected parents, we employ uniform crossover strategy, which selects the i th bit from a parent randomly. Since we generate two children from the parents, the i th bit of the first children is obtained from a randomly selected parent and the second children gets the i th bit of the other parent. As an example, Figure 7.6b shows the possible children that are generated from the two solutions in Figure 7.6a.

MUTATION: Each generated child is mutated with probability p_m . Mutation operation is defined as flipping the value of a randomly selected position in the bit string of the individual. For instance, mutation operation applied to the second solution in Figure 7.6b may produce the solution shown in Figure 7.6c.

SELECTION: After generating the offspring population, we add them to the current population and select the best of them to constitute the next generation. To achieve this task, we utilize two criteria: *non-domination level* of a solution and its *crowding distance*. Non-domination level of a solution represents which front the solution belongs to. Non-dominated solutions with rank 0 constitute the first Pareto front, \mathcal{I}^1 . Solutions that are only dominated by the solutions in \mathcal{I}^1 constitute the second Pareto front, \mathcal{I}^2 , so on. We employ fast non-dominating sorting for finding the Pareto fronts [79]. After all the Pareto fronts are found, we assign crowding distances to all solutions grouped by their Pareto front. The crowding distance, denoted by d , is a measure of diversity that shows how far a given solution is from its closest (i.e., two neighboring) solutions in the same Pareto front in the objective space. Figure 7.7 shows the pseudo-code for crowding distance assignment for solutions in a Pareto front [80]. In Figure 7.7, z_{min}^k and z_{max}^k denote the minimum and maximum values in the population for objective k . A solution u is considered to be better than another solution v if $u.rank < v.rank$ or $(u.rank = v.rank \wedge u.d > v.d)$. By using this partial ordering, we

```

1: for each Pareto front  $\mathcal{I}_h$  do
2:    $l = |\mathcal{I}_h|$ 
3:   for each solution  $u \in \mathcal{I}_h$  do
4:      $u.d = 0$  {d is the crowding distance}
5:   end for
6:   for each objective  $k$  do
7:     Sort  $\mathcal{I}_h$  in ascending order based on objective  $k$ 
8:      $\mathcal{I}_h[1].d = \mathcal{I}_h[l].d = \infty$ 
9:     for  $m = 2$  to  $l - 1$  do
10:       $\mathcal{I}_h[m].d = \mathcal{I}_h[m].d + \frac{(\mathcal{I}_h[m+1].z^k - \mathcal{I}_h[m-1].z^k)}{(z_{max}^k - z_{min}^k)}$ 
11:    end for
12:  end for
13: end for

```

Figure 7.7. Crowding distance assignment algorithm.

select the best B_{size} solutions to populate the next generation, \mathcal{B}_{t+1} .

FINALSELECTION: After *maxIter* iterations, EMOA generates the first Pareto front (the set of non-dominated solutions). However, only one solution should be selected among this front to be used as the final solution. The best way of selecting the final solution in real life scenarios is to leave the selection to the decision maker. Since we want to automatize the process, we choose the solution with the largest hypervolume [81] as the final solution among the non-extremal (inner) solutions in the Pareto front. With this choice, we aim to select the best solution that maintains a desirable trade-off between the two objectives. An example Pareto front together with the hypervolumes corresponding to each inner solution is shown in Figure 7.8.

7.4. Numerical Analysis

In this section, we analyze the performance of the proposed social-aware sensing scheme under different scenarios where we change the social ties between CRs. We aim to cover a wide range of realistic scenarios by considering various models for $p_{i,j}$. For

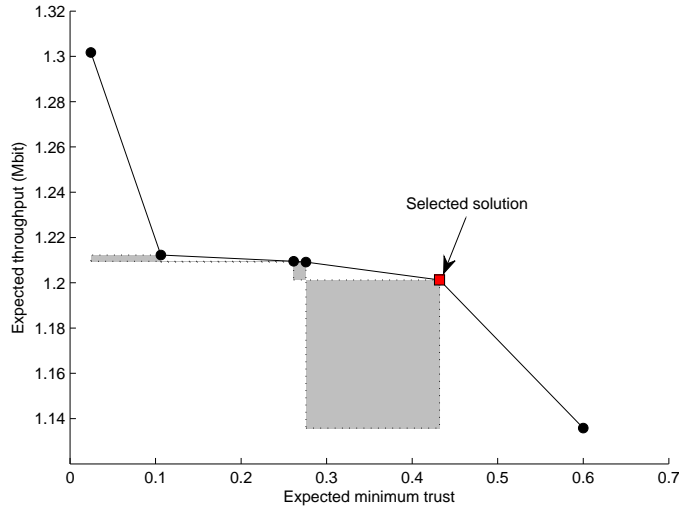


Figure 7.8. An example Pareto front found by EMOA. The marked solution is the selected final solution with the highest hypervolume.

each scenario, we compare our EMOA approach with the expected throughput-optimal (EXP-THR-OPT) scheme that only maximizes the expected throughput without considering trust objective. EXP-THR-OPT solution is found by implicit enumeration of all possible solutions. However, it becomes impossible to find even for moderate values of N due to the combinatorial nature of the problem.

Figure 7.9a illustrates the considered network. For the sake of analysis, we keep the network size small: there are eight CRs within the cell (outer circle in the figure) where a single PU is active with probability P^{on} . At the beginning of each frame, one of the CRs is assigned as the dedicated transmitter in a round robin manner. We should emphasize that since the sensing schemes operate based on some expected values (e.g., expected cooperation probability), the resulting performance may deviate from the expected performance. As the realization of these estimated values is more important from the designer's viewpoint, we only report these realized values. As performance criteria, we concentrate on the following three metrics:

- realized throughput,
- *missed opportunity ratio*: the ratio of *lost* vacant frames (i.e., CR does not access the channel although there is no PU traffic) to the total number of vacant frames, and

- *collision probability*: the probability that a CR accessing the channel collides with an active PU.

The presented results are the average of ten different runs. Table 7.2 lists the parameters of our experiments while Table 7.3 lists EMOA-related parameters. Although the discussions we present are for the considered small network, our observations are still valid in general since a computationally efficient algorithm should work on a small set of nodes by first applying an elimination procedure to reduce the number of candidates, and then, making the cooperator selection decision on this smaller set.

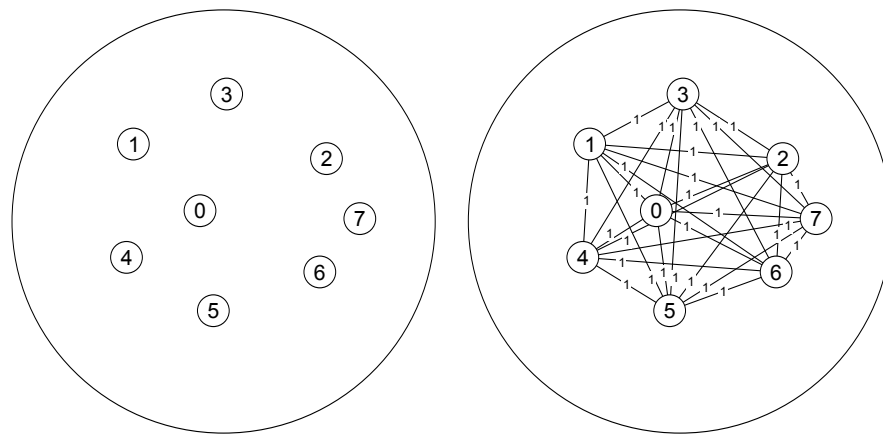
Table 7.2. Simulation parameters.

Parameter	Value
Cell radius	400 m
P^{on} (Probability of PU being active)	0.2
N (Number of CRs)	8
f_s (Sampling rate)	1 kHz
P_{PU}^{tx} (PU transmission power)	1000 mW
N_{th} (Noise floor)	-105 dB
l (Path loss exponent)	3
f (Channel frequency)	800 MHz
T (Frame length)	200 ms
T^{req} (Length of the requesting period)	5 ms
t^{rep} (Length of a single reporting slot)	5 ms
R (Channel bit rate)	10 Mbps
G_{PU} (Antenna gain of PU)	0 dB
$G_j \forall j$ (Antenna gain of CR _{<i>j</i>})	0 dB
P^D (Required individual detection prob.)	0.7
P^F (Required individual false alarm prob.)	0.02
K (Window size for trust observations)	10
θ (Fraction of recent observations)	0.5
λ (Weight of recent observations)	0.7
Simulation length/warmup period	16000/4000 frames

In Figure 7.9, we present the social graphs corresponding to the scenarios. An

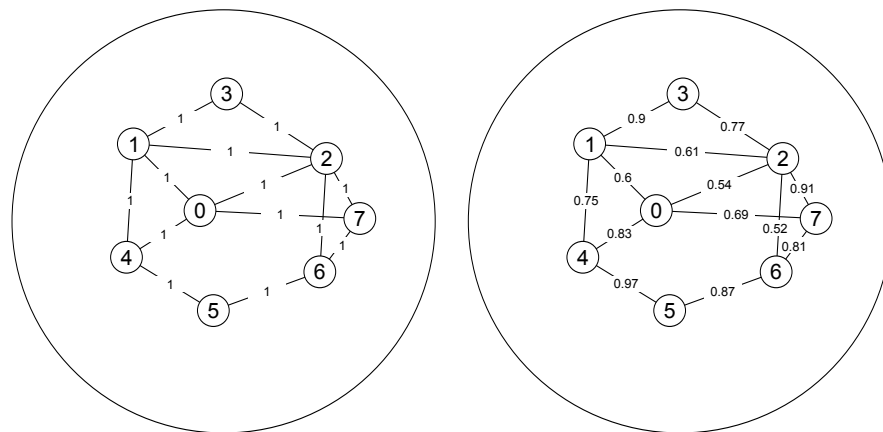
Table 7.3. EMOA parameters.

B_{size} (Population size)	100
C_{size} (Offspring pop. size)	20
p_m (Mutation probability)	0.05
t_{max} (Number of iterations)	100



(a) Simulated network topology.

(b) Scenario A.



(c) Scenario B.

(d) Scenarios C, F, G, H, I.

Figure 7.9. Physical location of CRs and social graphs

(a) Physical location of CRs (b,c,d) Social graphs used for scenarios where each edge

has $w_{i,j}^{soc}$ as its label.

edge connecting two CRs implies that the corresponding CRs are socially tied to each other where the strength of the social tie ($w_{i,j}^{soc}$) is shown on the connecting edge. We assume that the $w_{i,j}^{soc}$ values are between 0 and 1. If that is not the case (e.g. social tie is equal to the number of mutual friends), they can still be mapped onto $[0,1]$ interval by using some appropriate normalization (e.g. the ratio of mutual friends to total number of friends). In our network, the social ties are symmetrical but the model can also handle asymmetric values. For all scenarios, we indicate the used $p_{i,j}$ values.

- *Scenario A*: In this scenario, depicted in Figure 7.9b, the social graph is complete, and all the social ties are equal to 1. Hence, this scenario corresponds to the traditional sensing where CR_j always senses for CR_i . We set $p_{i,j} = w_{i,j}^{soc} = 1 \quad \forall i, j$.
- *Scenario B*: This scenario depicted in Figure 7.9c represents the case of binary social ties which implies that not all CRs are socially connected. Furthermore, the number of connected nodes for each CR differs. For instance, CR_0 has a large number of neighbors, whereas CR_3 does not. We set $p_{i,j} = w_{i,j}^{soc}$ and $w_{i,j}^{soc} \in \{0, 1\} \quad \forall i, j$.
- *Scenario C*: This scenario is shown in Figure 7.9d and it is based on the previous one with a slight difference on $w_{i,j}^{soc}$ values. In this scenario, $p_{i,j}$ is set as $p_{i,j} = w_{i,j}^{soc}$ and $w_{i,j}^{soc} \in [0, 1] \quad \forall i, j$.
- *Scenario D*: In this scenario, CR_j determines its cooperation probability based on how much it has already contributed to the whole CRN, rather than deciding based on its social ties. Let us define *system willingness* (w_j^{sys}) for CR_j as:

$$w_j^{sys} = 1 - \frac{\# \text{ of accepted requests for other CRs}}{\# \text{ of received requests from other CRs}}.$$

The second term of this equation is the ratio of accepted requests from other CRs, which can be interpreted as the system burden on CR_j . Thus, w_j^{sys} is inversely related to the burden put on CR_j . This setting may cover operating environments which are new to a CR (e.g., different than home network) and the CR does not

have any social tie. Hence, cooperation is still possible among the CRs but it is restricted by w_j^{sys} parameter. That is, w_j^{sys} enables cooperation among CRs when there is no social tie while at the same time it prevents exploitation of each CR by excessive sensing. In our setting, w_j^{sys} is a function of ratio of satisfied requests but it may also depend on internal state of a CR such as battery level. In this scenario, $p_{i,j} = w_j^{sys}$.

- *Scenario E*: Similar to the system willingness, let us define *peer willingness* as:

$$w_{i,j}^{peer} = 1 - \frac{\# \text{ of accepted requests by CR}_j \text{ for CR}_i}{\# \text{ of received requests by CR}_j \text{ from CR}_i}.$$

In other words, $w_{i,j}^{peer}$ is inversely proportional to the burden put on CR_j by CR_i. Similar to the social tie concept, peer willingness takes one to one relations between CRs into account. However, contrary to the social tie, peer willingness dynamically evolves with time. This scenario may cover cases where CRs do not restrict total number of cooperations but want to avoid exploitation by a specific CR. In this scenario, $p_{i,j} = w_{i,j}^{peer}$.

- *Scenario F*: This case is a combination of system willingness concept with the social ties used in Scenario C. We set $p_{i,j}$ as $p_{i,j} = \max\{w_j^{sys}, w_{i,j}^{soc}\}$ for encouraging more cooperation.
- *Scenario G*: Similar to Scenario F, we define $p_{i,j}$ as the combination of system willingness, peer willingness, and social ties: $p_{i,j} = \max\{w_j^{sys}, w_{i,j}^{peer}, w_{i,j}^{soc}\}$.
- *Scenario H*: This scenario is based on Scenario F. However, this time CR₀ is a malicious node that performs spectrum sensing data falsification (SSDF) attack to the network [82]. In this type of attack, the malicious CR performs sensing, but reports the reverse of its sensing result in order to degrade the environmental awareness of CR_i. Hence, CR₀ always reports the inverse of its sensing result to other CRs. We select CR₀ as the malicious user to analyze as a worst case due to its central location and high number of social ties.
- *Scenario I*: This final scenario is very similar to Scenario H. The only difference is that CR₀ now always reports the existence of PU when it senses for other

CRs. Similar to PU emulation attack [83], this scenario may represent the case where a selfish CR desires to use the spectrum itself by making others believe that spectrum is occupied.

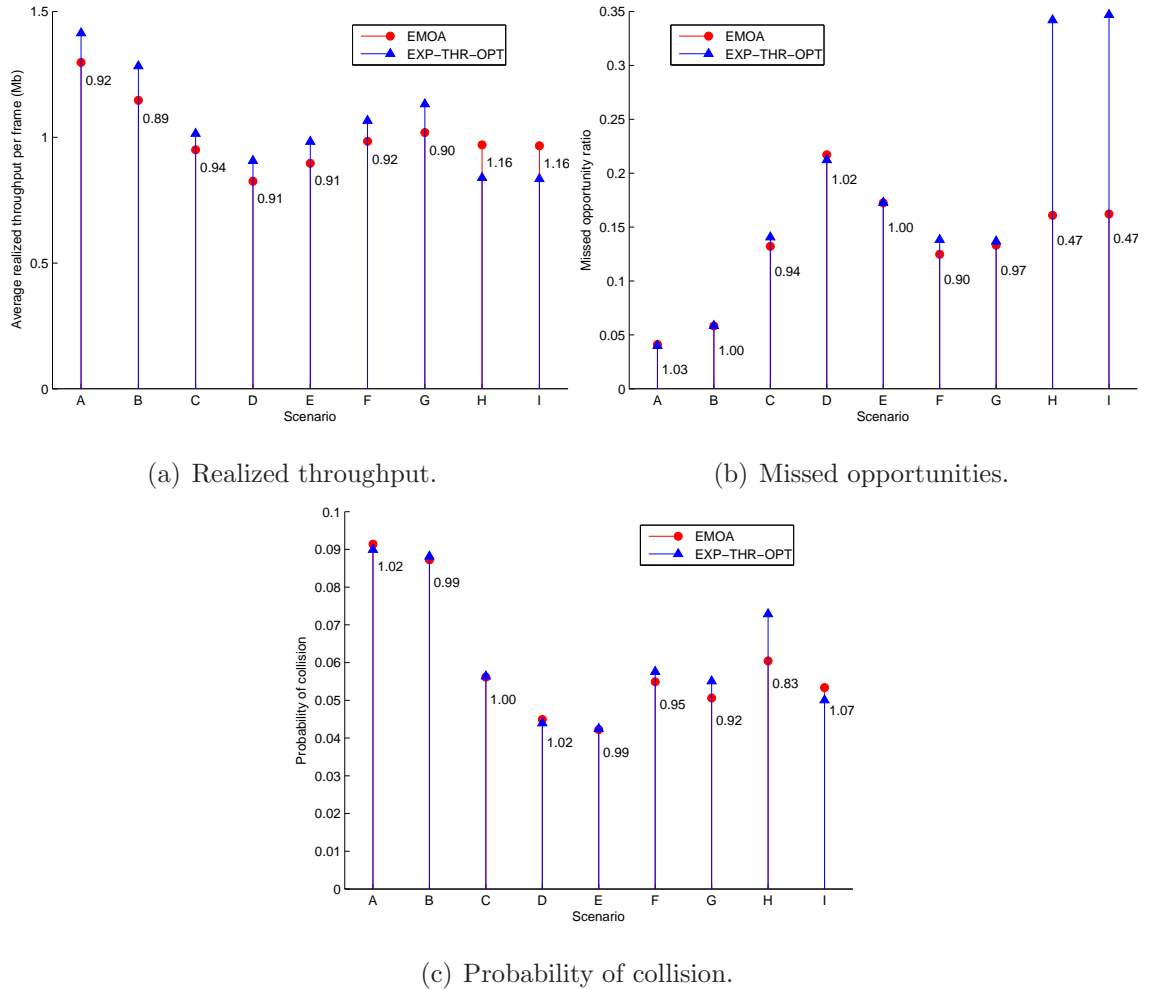


Figure 7.10. Performance evaluation for different scenarios.

Figure 7.10 depicts the performance of EMOA and EXP-THR-OPT for all scenarios. In each of these figures, numbers on the lines mark the ratio of the performance achieved by EMOA to the one achieved by EXP-THR-OPT.

Figure 7.10a illustrates the resulting throughput for all scenarios. We can see that EMOA maintains near-optimal performance. Specifically, EMOA achieves at least 89 percent of the throughput of EXP-THR-OPT. Furthermore, we observe that EMOA outperforms EXP-THR-OPT under malicious user cases (Scenarios H and I) and provides a relatively stable operation. The throughput reduction of EXP-THR-OPT be-

tween Scenarios F and H is 21 percent whereas it is 1.5 percent for EMOA. As the trust objective causes EMOA to select sub-optimal solutions in terms of throughput when there are no malicious users, being about 90 percent of the EXP-THR-OPT in terms of throughput is satisfying.

Comparing different scenarios with each other, we observe that the realized throughput decreases with decreasing $p_{i,j}$ values. For instance, the maximum throughput is achieved in Scenario A – the scenario where all $p_{i,j} = 1$ - and going from Scenario A to Scenario F causes a 25 percent decrease for both methods. We attribute this effect to the restriction on PU detection accuracy. That is, when expected $P^{D,soc}$ is below 0.9, CRs are forbidden to access the channel. In scenarios with low $p_{i,j}$ values, sensing is performed with a low number of cooperators which may lead to low $P^{D,soc}$. The implication of this behavior (i.e., high $p_{i,j}$ resulting in high throughput) is twofold. First, we can argue that the high performance of Scenario A compared with others, say Scenario C, may lead to over-estimation of the network throughput if social behavior of CRs are neglected. In other words, a CRN would be expected to provide throughput as in Scenario A although only about 72 percent of that value (Scenario C) would be achieved. Second, it may indicate that CRs benefit from being social hence they have the incentive to be social and cooperative.

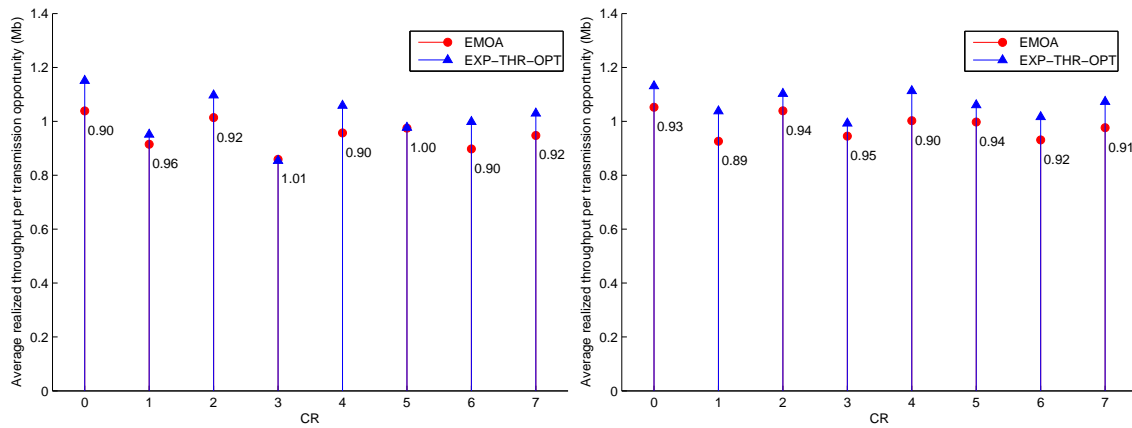
Figure 7.10b shows the missed opportunity ratio. We should recall that an opportunity is missed either due to a false alarm or due to low detection probability. Hence, it reflects the throughput loss more than just the false alarm. For the scenarios under legitimate operation (scenarios excluding the attack scenarios), we see that high $p_{i,j}$ values result in more aggressive channel usage thereby resulting in low missed opportunity ratio. On the other hand, EXP-THR-OPT wastes almost one third of the frames in case of an attack. As seen already in Figure 7.10a, EMOA provides robust operation also in terms of missed opportunity ratio. The increase in missed opportunities between Scenarios F and H is 29 percent and 147 percent for EMOA and EXP-THR-OPT, respectively.

We can observe similar behavior in terms of collision probability, as shown in

Figure 7.10c. Aggressive channel access (high $p_{i,j}$) causes more collisions. However, all of the values are within the tolerable limits (i.e., below 0.10 corresponding to tolerable misdetection probability) as our scheme prevents CRs from accessing the channel without a satisfactory detection probability. The increase for Scenario H (where CR_0 reports 0 when it senses and PU is active) compared to Scenario F is still within the limits due to the low P^{on} value. For a PU channel with higher PU traffic (i.e., higher P^{on}), this aggressive access may lead to harmful interference to the PU. However, as CRNs aim to operate on PU channels with low P^{on} , we do not provide additional interference avoidance mechanisms to our solution. Scenario I shows a decrease in collision probability as this time CR_0 always reports 1 regardless of the actual PU state, which results in less collisions at the expense of very high missed opportunity ratio as depicted in Figure 7.10b.

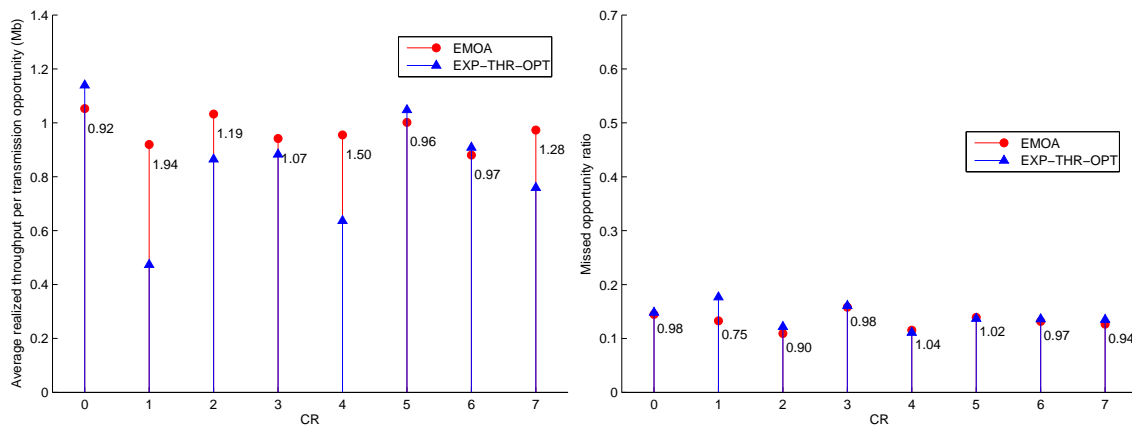
In Figure 7.11, we show the individual performances of CRs in terms of realized throughput and missed opportunities for selected scenarios: Scenario C, F, and H. With this analysis, we aim to gain insights to the following aspects: (i) how each CR's performance differs depending on its social ties, (ii) whether the performance gap between EMOA and EXP-THR-OPT for a specific CR depends on its social properties, and (iii) whether some CRs, e.g., CRs with low social connectivity, benefit from different $p_{i,j}$ models more than the others. For (i) and (ii), we focus on a single scenario whereas for (iii) we compare different scenarios.

Figure 7.12 summarizes the social ties associated with each CR. For CR_i , *node degree* denoted by n_i is the number of directly connected nodes; *aggregate social tie* denoted by δ_i is the sum of $w_{i,j}^{soc}$ across all links of CR_i ; and *average social tie* denoted by $\tilde{\delta}_i$ is the ratio of aggregate social tie to the node degree, i.e., $\tilde{\delta}_i = \delta_i/n_i$. For Scenario C in which only social ties are considered for cooperation, we observe that CRs with low δ_i and n_i , e.g., CR_3 and CR_5 , have the lowest realized throughput. However, we should note that the realized throughput depends on both the social ties in social connectivity layer, $P^{F,soc}$ in (7.14), and sensing time in wireless connectivity layer, T^{tx} in (7.14). Since we fix required sensing accuracy for each cooperating CR, $P^{F,soc}$ depends only on



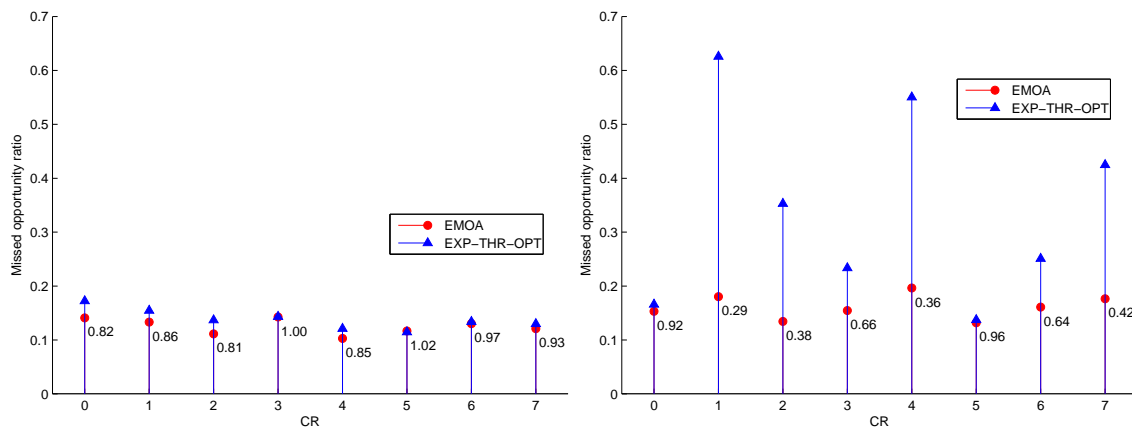
(a) Realized throughput per CR, Scenario C.

(b) Realized throughput per CR, Scenario F.



(c) Realized throughput per CR, Scenario H.

(d) Missed opportunities per CR, Scenario C.



(e) Missed opportunities per CR, Scenario F.

(f) Missed opportunities per CR, Scenario H.

Figure 7.11. Performance values per CR for selected scenarios.

number of cooperators (see (7.12)), whereas T^{tx} is also a function of the sensing time τ . Thus, the physical location of a CR as well as its neighbors determines the length of the sensing period and therefore T^{tx} .

We observe the effect of physical location in the diverging performance between CR_1 and CR_0 . Although both have high δ_i and n_i , CR_0 has significantly higher realized throughput compared to the former. Since CR_0 is very close to the center of the cell, it experiences high SNR values on the average as a result of short distance to the PU on average. This in turn facilitates it to have a short sensing time, τ . Therefore, when it is CR_0 's turn to transmit, it can usually be one of the sensing CRs. This results in savings in terms of reporting time, which implies longer transmission time and in turn higher realized throughput.

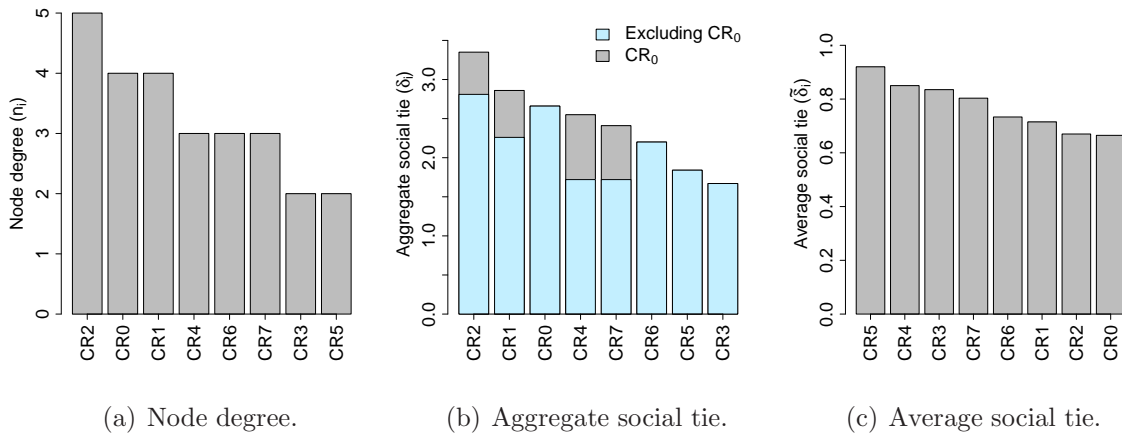


Figure 7.12. CR properties: node degree, aggregate social tie (with and excluding tie with CR_0), and average social tie. In the figures, CRs are sorted according to their property in decreasing order.

While we observe some correlation between δ_i and realized throughput of a CR, we do not observe that between $\tilde{\delta}_i$ and realized throughput for our setting. We should also mention that these assessments may not be applicable for all network topologies. As a counterexample, consider a CR, say CR_x , with 100 neighbors within the communication range and connected to each one of them with weak social ties, say $w_{x,j}^{soc} = 0.25$. On the other hand, consider another CR, say CR_y , again with 100 neighbors. This time let us assume that CR_y is strongly connected to only a few of its neighbors (assume $w_{y,j}^{soc} = 1$ for these neighbors) and very weakly connected to the remaining ones (assume

$w_{y,j}^{soc} = 0.05$). Even though $\delta_x > \delta_y$ and $\tilde{\delta}_x > \tilde{\delta}_y$, the performance of CR_y will be better as it can safely depend on its strongly tied neighbors for cooperation.

Regarding the performance gap between EMOA and EXP-THR-OPT, we observe that the performance gap approaches to 0 when n_i is low. This is expected as there are fewer options for both schemes and EMOA has higher likelihood of choosing cooperators as EXP-THR-OPT does. For example, in Scenario C, while EXP-THR-OPT achieves higher realized throughput for CRs with high n_i , both methods are almost the same for CRs with low n_i , CR_3 and CR_5 . That means EMOA is almost as good as EXP-THR-OPT for CRs with low social ties.

Comparing Figures 7.11a, 7.11b and 7.11c, we conclude that CR_1 , CR_3 and CR_5 benefit most if system willingness is activated on top of social willingness – going from Scenario C to F. The increases for these nodes are 9 percent, 16 percent and 8 percent for EXP-THR-OPT, respectively. On the other hand, the gains for other CRs are marginal (below 5 percent). Hence, the system willingness concept benefits CRs with low n and δ most.

Table 7.4. Realized throughput decrease (percent) in case of an SSDF attack (Scenarios F and H).

	CR_0	CR_1	CR_2	CR_3	CR_4	CR_5	CR_6	CR_7
EMOA	0	1	1	1	4	0	5	0
EXP-THR-OPT	1	54	22	11	43	1	11	29

For the SSDF attack case (Scenario H), Table 7.4 lists the decrease in realized throughput for each CR compared to Scenario F for both methods. The trust objective used in EMOA minimizes the effects of the attack whereas EXP-THR-OPT fails avoiding the attacker, which results in significant realized throughput decrease. All CRs connected to CR_0 are affected by the attack: CR_1 , CR_2 , CR_4 , and CR_7 . Additionally, the realized throughput decrease is larger for those CRs that have few social ties excluding the tie with CR_0 (see Figure 7.12b). For CR_2 , the decrease is lower as EMOA selects more trustworthy neighbors that can meet the required $P^{D,soc}$ and $P^{F,soc}$ values. We attribute the realized throughput decrease for CR_3 and CR_6 – the nodes

that are not connected to CR_0 directly— to the system willingness concept that encourages cooperation despite the lack of social ties between nodes. These CRs occasionally cooperate with CR_0 , which degrades the sensing accuracy and in return leading to lower realized throughput. However, this decrease is smaller compared to CRs having strong ties with CR_0 . This side effect of system willingness stems from encouraging cooperation among socially weakly connected or not connected nodes. This attitude is more vulnerable to attacks and may cause larger number of CRs to be effected compared to cooperation among only strongly connected CRs. Finally, we should mention that EMOA achieves at least 90 percent of EXP-THR-OPT under normal operation, and performs significantly better for the attack scenario.

Figures 7.11d, 7.11e, and 7.11f show the missed opportunity ratio for each CR. Regarding Scenario C, we observe that the missed opportunity ratios are very close to each other, within 0.05 range. Adding system willingness (Scenario F) decreases the missed opportunities in general as the number of possible cooperators increases. However, there is an increase for EXP-THR-OPT compared to Scenario C for CR_0 , CR_2 , and CR_4 . Hence, we can safely state that CRs with large and/or strong social ties are adversely affected with more uncertainty in cooperation behavior for EXP-THR-OPT. For Scenario H, EMOA limits the missed opportunities to at most 20 percent for all CRs. On the contrary, EXP-THR-OPT causes intolerable missed opportunity ratios for CR_0 's direct neighbors. Specifically, missed opportunity ratio is 0.35, 0.43, 0.55, and 0.63 for CR_2 , CR_7 , CR_4 , and CR_1 , respectively. That is to say, the CRs that are tied to the malicious CR starve without an attack avoidance mechanism. The trust objective in EMOA serves as an attack avoidance mechanism without bringing too much overhead.

7.5. Chapter Summary

In this chapter, we have studied a social CRN that employs cooperative sensing. A CR may not always sense the channel for the benefit of other CRs in a social CRN, and its cooperation probability depends on the social ties. We have proposed a CR trust metric that measures the reliability of other CRs' sensing results. Using this trust

metric, we have formulated a multi-objective optimization problem that maximizes the expected throughput and sensing accuracy. Compared to a scheme that only considers the expected throughput, our proposal is always 90 percent of the optimal solution when there are no malicious CRs, and performs significantly better in case of a malicious CR. Moreover, we have also suggested and analyzed various cooperation probability formulations that focus on social ties, peer interactions, and system interactions.

As future work, we plan to incorporate penalty and reward mechanisms to the network so that the social ties within the network evolve with time depending on the behavior of CRs in a realistic manner. Other topics we like to explore are the analysis of a multi-channel CRN in a social network setting and the effect of social ties in cooperative (e.g. relaying) CRNs.

8. CONCLUSIONS AND FUTURE RESEARCH DIRECTIONS

This chapter summarizes the thesis by listing our main findings and contributions and explores several future research directions related to CSS and EE.

8.1. Summary of Contributions

- (i) *Joint channel and user selection for transmission and sensing*: This thesis proposes a scheduling algorithm that maximizes the expected throughput of a CRN. In our setting, the number of channels is large, and all of them cannot be sensed. Our algorithm takes the varying SNR values, data rate requirements of SUs and channel bit rates into account, and decides on the channels to sense, SUs sensing those channels, and transmitting SUs over vacant channels. The resulting optimization model is a non-linear problem, which we solve with a clever use of the genetic algorithm and CPLEX software.
- (ii) *Fundamental trade-offs regarding EE in CRNs*: We also analyze the trade-offs involved in providing EE in CRNs. The main trade-offs are listed as: QoS, fairness, PU interference, network architecture and security. We discuss each trade-off separately together with their interactions with each other. Furthermore, we elaborate on the challenges involved in operating an energy-efficient CRN from the viewpoint of these factors.
- (iii) *Energy Efficient CSS*: This thesis contains a number of CSS schemes that are focused on the EE of CRNs. Different from the literature, all of our schemes support SUs to sense multiple channels in a single sensing period and also enables different sensing durations among SUs based on their SNR values. As channel sensing is performed periodically, even a small savings in terms of energy can accumulate to a large amount in the long run. We first focus on the case where we consider the energy cost of sensing and reporting. We design two optimal methods both of which provide adequate PU protection and false alarm probability. The

first method minimizes the total CSS energy consumption. On the other hand, the second method maximizes the remaining transmission time in order to increase throughput. Both methods account for the diversity in SNR conditions among SUs. Besides, these two methods, we also propose two suboptimal but time efficient greedy heuristics. All schemes take the energy cost of decision reporting into account, which is usually neglected in the literature. Moreover, we also take the time and energy cost of channel switching into account in the second part of our research since switching from one frequency to another is not immediate and requires antenna tuning. We provide the optimization model and solution methodology together with a heuristic method. We observe that even a small sacrifice in terms of transmission time results in large energy savings.

- (iv) *CSS for social CRNs*: Finally, we delve into the CSS problem in a social CRN where the sensing request of an SU is satisfied by other SUs probabilistically. This time, our aim is to find the cooperator set for an SU. We give the formulations for cooperative detection and false alarm probabilities in this setting. In addition, we develop a simple trust mechanism that enables SUs to track the sensing accuracy of other SUs. By using these formulations, we give the multi-objective optimization model that maximizes the expected throughput and sensing accuracy together. We solve the mentioned model using EMOA, and perform the analysis with various formulations for cooperation probability. Our solution is within 90 percent of the throughput optimal scheme when there are no misbehaving users. On the other, it significantly outperforms the throughput optimal scheme when there is a malicious user.

8.2. Future Research Directions

In Chapter 4, we explored the trade-offs involved in energy-efficient CRNs. Regarding these trade-offs, the future research can focus on endogenous topics such as sensing schemes, sensory data gathering, and learning frameworks or exogenous topics like social networks, user behavior, and energy harvesting. Analyzing social networks within the CRN context allows more realistic operation models. On the other hand, user behavior enables energy savings both in the mobile equipment and network equip-

ment domains. Finally, energy harvesting supports increased battery lifetime for CR devices. Among these topics, we explore energy-efficient sensing schemes in Chapters 5 and 6 and throughput-efficient social CRNs in Chapter 7.

For social CRNs that we study in Chapter 7, clever punishment and reward mechanisms that allow the SUs to strengthen/weaken the social ties based on the intention and performance of other SUs can support the CRN operation in a more realistic scenario. In addition, the probabilistic nature of social CRNs may further be explored in a multi-channel and/or heterogeneous setting such as the one in Chapters 5 and 6.

We consider various CSS schemes in this thesis, namely Chapters 3, 5, 6, and 7. In all of these methods, we assume hard decision combining together with a single fusion rule. As an extension, on the fly selection of fusion rules for different channels can be considered. This dynamic selection of fusion rule can improve the performance in terms of both energy and throughput compared to a static selection. Moreover, treating false alarm probabilities among SU as decision variables (instead of assuming constant and given) may result in a better performance at the expense of increased complexity.

APPENDIX A: PROOF OF THEOREM 5.1.

The first derivative of $P_{m,n}^d$ with respect to $\tau_{m,n}$ is

$$\frac{dP_{m,n}^D}{d\tau_{m,n}} = \frac{\gamma_{m,n}\sqrt{f_s}}{2\sqrt{\tau_{m,n}}\sqrt{2\pi}\sqrt{2\gamma_{m,n}+1}}A_{m,n}$$

where

$$A_{m,n} = \exp\left(-\frac{1}{2}\left(\frac{\mathcal{Q}^{-1}(P_{m,n}^F) - \sqrt{\tau_{m,n}f_s}\gamma_{m,n}}{\sqrt{2\gamma_{m,n}+1}}\right)^2\right).$$

The first derivative is always positive, hence, $P_{m,n}^D$ is an increasing function of $\tau_{m,n}$.

The second derivative of $P_{m,n}^D$ with respect to $\tau_{m,n}$ is given by

$$\frac{d^2P_{m,n}^D}{d\tau_{m,n}^2} = \frac{\gamma_{m,n}\sqrt{f_s}A_{m,n}}{4\sqrt{2\pi}\sqrt{2\gamma_{m,n}+1}}\left[-\frac{1}{\sqrt{\tau_{m,n}^3}} + \frac{\gamma_{m,n}\sqrt{f_s}}{\tau_{m,n}(2\gamma_{m,n}+1)}(\mathcal{Q}^{-1}(P_{m,n}^F) - \sqrt{\tau_{m,n}f_s}\gamma_{m,n})\right].$$

The second derivative is negative if

$$\frac{-1}{\sqrt{\tau_{m,n}^3}} + \frac{\gamma_{m,n}\sqrt{f_s}}{\tau_{m,n}(2\gamma_{m,n}+1)}(\mathcal{Q}^{-1}(P_{m,n}^F) - \sqrt{\tau_{m,n}f_s}\gamma_{m,n}) < 0.$$

Reducing the $\tau_{m,n}$ term leads to

$$-\frac{1}{\sqrt{\tau_{m,n}}} + \frac{\gamma_{m,n}\sqrt{f_s}}{(2\gamma_{m,n}+1)}(\mathcal{Q}^{-1}(P_{m,n}^F) - \sqrt{\tau_{m,n}f_s}\gamma_{m,n}) < 0.$$

Thus, $P_{m,n}^D$ is a concave function of $\tau_{m,n}$ if the condition in (5.2) is satisfied.

A.1. Proof of Lemma 5.1.

By combining (5.1) and (5.2), we get

$$-\frac{1}{\sqrt{\tau_{m,n}}} + \frac{\gamma_{m,n}\sqrt{f_s}\mathcal{Q}^{-1}(P_{m,n}^D)}{\sqrt{2\gamma_{m,n} + 1}} < 0.$$

The first term is always negative, whereas the second term is negative if $P_{m,n}^D > 0.5$. Since it is reasonable to assume a $P_{m,n}^D$ value greater than 0.5, we can safely say that $P_{m,n}^D$ is a concave function of $\tau_{m,n}$ most of the time.

APPENDIX B: PROOF OF THEOREM 5.2.

Let $\tau_{\mathbf{n}}$ denote the τ vector with n entries that consists of $\tau_{m,n}$ values for channel m . Moreover, let $f_{m,k}$ and $h_{m,k}$ denote $(1 - P_{m,k}^D)$, and $f_{m,1}f_{m,2} \dots f_{m,k}$, respectively. The proof is by induction on the number of elements in \mathcal{S}_m denoted by $|\mathcal{S}_m|$.

- $|\mathcal{S}_m| = 2$: Without loss of generality, assume SUs 1 and 2 are in \mathcal{S}_m . We can rewrite $P_m^{D,coop}$ as $1 - h_{m,2}$.

The gradient of $h_{m,2}$ is given by

$$\frac{\partial h_{m,2}}{\partial \tau_2} = \left[-\frac{\gamma_{m,1}\sqrt{f_s}A_{m,1}}{2\sqrt{\tau_{m,1}}\sqrt{2\pi}\sqrt{2\gamma_{m,1}+1}}f_{m,2}, \right. \\ \left. -\frac{\gamma_{m,2}\sqrt{f_s}A_{m,2}}{2\sqrt{\tau_{m,2}}\sqrt{2\pi}\sqrt{2\gamma_{m,2}+1}}f_{m,1} \right]$$

where

$$A_{m,n} = \exp \left(-\frac{1}{2} \left(\frac{\mathcal{Q}^{-1}(P_{m,n}^F) - \sqrt{\tau_{m,n}f_s\gamma_{m,n}}}{\sqrt{2\gamma_{m,n}+1}} \right)^2 \right).$$

Both terms are always negative, thus, $h_{m,2}$ is a decreasing function of τ_2 . Therefore, $coopPd_m$ is an increasing function of τ_2 since $\frac{\partial P_m^{D,coop}}{\partial \tau_2} = -\frac{\partial h_{m,2}}{\partial \tau_2}$. In addition, as shown in Lemma 5.2., both $f_{m,1}$ and $f_{m,2}$ are non-negative, decreasing, and convex functions so their multiplication, $h_{m,2}$, is also convex [84], which leads to the concavity of $P_m^{D,coop}$.

- Let us assume that the theorem holds for $|\mathcal{S}_m| = k$ and show that it also holds for $|\mathcal{S}_m| = k + 1$. This time $P_m^{D,coop}$ can be written as

$$P_m^{D,coop} = 1 - h_{m,k+1} = 1 - h_{m,k}f_{m,k+1}.$$

The gradient of $h_{m,k+1}$ is given by

$$\frac{\partial h_{m,k+1}}{\partial \tau_{\mathbf{k}+1}} = \left[\frac{\partial h_{m,k}}{\partial \tau_{\mathbf{k}+1}} f_{m,k+1}, h_{m,k} \frac{\partial f_{m,k+1}}{\partial \tau_{\mathbf{k}+1}} \right].$$

Let us focus on the first term. Since $\frac{\partial h_{m,k}}{\partial \tau_{\mathbf{k}+1}}$ is negative by induction, and $f_{m,k+1}$ is non-negative, then their multiplication is negative. For the second term, $h_{m,k}$ is a non-negative function, and $\frac{\partial f_{m(k+1)}}{\partial \tau_{\mathbf{k}+1}}$ is negative by Lemma 5.2. Thus, their multiplication is also negative. Since both terms are negative, $h_{m,k+1}$ is a decreasing function of $\tau_{\mathbf{k}+1}$.

We apply the same logic as in the previous step to prove the convexity of $h_{m,k+1}$. Both $h_{m,k}$ and $f_{m,k+1}$ are decreasing convex functions (convexity of $h_{m,k}$ comes from induction), then their multiplication, $h_{m,k+1}$, is also convex. Thus, $P_m^{D,coop}$ is a concave and increasing function of $\tau_{\mathbf{k}+1}$.

Proving both the base step and the induction step leads to the conclusion that $P_m^{D,coop}$ is an increasing concave function of $\tau_{m,n}$ if (5.2) is satisfied.

REFERENCES

1. Doyle, L., J. Kibilda, T. Forde, and L. DaSilva, “Spectrum Without Bounds, Networks Without Borders”, *Proceedings of the IEEE*, Vol. 102, No. 3, pp. 351–365, 2014.
2. Ganesan, G. and Y. Li, “Cooperative Spectrum Sensing in Cognitive Radio, Part I: Two User Networks”, *IEEE Transactions on Wireless Communications*, Vol. 6, No. 6, pp. 2204–2213, 2007.
3. Ganesan, G. and Y. Li, “Cooperative Spectrum Sensing in Cognitive Radio, Part II: Multiuser Networks”, *IEEE Transactions on Wireless Communications*, Vol. 6, No. 6, pp. 2214–2222, 2007.
4. Ashraf, I., F. Boccardi, and L. Ho, “Sleep Mode Techniques for Small Cell Deployments”, *IEEE Communications Magazine*, Vol. 49, No. 8, pp. 72–79, 2011.
5. Gür, G. and F. Alagöz, “Green Wireless Communications via Cognitive Dimension: An Overview”, *IEEE Network*, Vol. 25, No. 2, p. 50, 2011.
6. Gao, P., A. Curtis, B. Wong, and S. Keshav, “It’s not Easy Being Green”, *Proc. of the ACM SIGCOMM*, pp. 211–222, 2012.
7. “Cisco Visual Networking Index: Global Mobile Data Traffic Forecast Update, 2011-2016”, Technical report, Cisco, 2012.
8. Partridge, C., “Forty Data Communications Research Questions”, *SIGCOMM Comput. Commun. Rev.*, Vol. 41, No. 5, pp. 24–35, 2011.
9. Song, C. and Q. Zhang, “Cooperative Spectrum Sensing with Multi-Channel Coordination in Cognitive Radio Networks”, *2010 IEEE International Conference on Communications*, pp. 1–5, 2010.

10. Shen, J., S. Liu, L. Zeng, G. Xie, J. Gao, and Y. Liu, "Optimisation of Cooperative Spectrum Sensing in Cognitive Radio Network", *IET Communications*, Vol. 3, No. 7, pp. 1170–1178, 2009.
11. Shen, J., T. Jiang, S. Liu, and Z. Zhang, "Maximum Channel Throughput via Cooperative Spectrum Sensing in Cognitive Radio Networks", *IEEE Transactions on Wireless Communications*, Vol. 8, No. 10, pp. 5166–5175, 2009.
12. Jiang, H., L. Lai, R. Fan, and H. V. Poor, "Optimal Selection of Channel Sensing Order in Cognitive Radio", *IEEE Transactions on Wireless Communications*, Vol. 8, No. 1, pp. 297–307, 2009.
13. Fan, R. and H. Jiang, "Optimal Multi-Channel Cooperative Sensing in Cognitive Radio Networks", *IEEE Transactions on Wireless Communications*, Vol. 9, No. 3, pp. 1128–1138, 2010.
14. Zhang, T., Y. Wu, K. Lang, and D. H. K. Tsang, "Optimal Scheduling of Cooperative Spectrum Sensing in Cognitive Radio Networks", *IEEE Systems Journal*, Vol. 4, No. 4, pp. 535–549, 2010.
15. Zhang, T. and D. H. K. Tsang, "Cooperative Sensing Scheduling for Energy-Aware Cognitive Radio Networks", *IEEE International Conference on Communications (ICC)*, pp. 1–6, 2011.
16. Peh, E. C. Y., Y.-C. Liang, Y. L. Guan, and Y. Zeng, "Optimization of Cooperative Sensing in Cognitive Radio Networks: A Sensing-Throughput Tradeoff View", *IEEE Transactions on Vehicular Technology*, Vol. 58, No. 9, pp. 5294–5299, 2009.
17. Song, J., J. Xue, Z. Feng, P. Zhang, and Z. Liu, "Optimal Cooperative Spectrum Sensing Strategies in Cognitive Radio Networks", *IEEE 71st Vehicular Technology Conference*, pp. 1–6, 2010.
18. Qu, Q., L. Milstein, and D. Vaman, "Cognitive Radio Based Multi-User Resource

- Allocation in Mobile Ad Hoc Networks Using Multi-Carrier CDMA Modulation”, *IEEE Journal on Selected Areas in Communications*, Vol. 26, No. 1, pp. 70–82, 2008.
19. Cheng, P., Z. Zhang, H. H. Chen, and P. Qiu, “Optimal Distributed Joint Frequency, Rate and Power Allocation in Cognitive OFDMA Systems”, *IET Communications*, Vol. 2, No. 6, pp. 815–826, 2008.
 20. Hoang, A., Y.-C. Liang, and Y. Zeng, “Adaptive Joint Scheduling of Spectrum Sensing and Data Transmission in Cognitive Radio Networks”, *IEEE Transactions on Communications*, Vol. 58, No. 1, pp. 235–246, 2010.
 21. Rashid, M., M. Hossain, E. Hossain, and V. Bhargava, “Opportunistic Spectrum Scheduling for Multiuser Cognitive Radio: A Queueing Analysis”, *IEEE Transactions on Wireless Communications*, Vol. 8, No. 10, pp. 5259–5269, 2009.
 22. Wang, R., V. N. Lau, L. Lv, and B. Chen, “Joint Cross-Layer Scheduling and Spectrum Sensing for OFDMA Cognitive Radio Systems”, *IEEE Transactions on Wireless Communications*, Vol. 8, No. 5, pp. 2410–2416, 2009.
 23. Liu, Y., S. Xie, Y. Zhang, R. Yu, and V. C. M. Leung, “Energy-Efficient Spectrum Discovery for Cognitive Radio Green Networks”, *Mobile Networks and Applications*, Vol. 17, No. 1, pp. 64–74, 2012.
 24. Su, H. and X. Zhang, “Opportunistic Energy-Aware Channel Sensing Schemes for Dynamic Spectrum Access Networks”, *IEEE Global Telecommunications Conference (GLOBECOM)*, pp. 1–5, 2010.
 25. Su, H. and X. Zhang, “Power-Efficient Periodic Spectrum Sensing for Cognitive MAC in Dynamic Spectrum Access Networks”, *IEEE Wireless Communications and Networking Conference (WCNC)*, pp. 1–6, 2010.
 26. Su, H. and X. Zhang, “Energy-Efficient Spectrum Sensing for Cognitive Radio

- Networks”, *IEEE Conference on Communications (ICC)*, pp. 1–5, 2010.
27. Wu, Y. and D. Tsang, “Energy-Efficient Spectrum Sensing and Transmission for Cognitive Radio System”, *IEEE Communications Letters*, Vol. 15, No. 5, pp. 545–547, 2011.
 28. Pei, Y., Y. Liang, K. Teh, and K. Li, “Energy-Efficient Design of Sequential Channel Sensing in Cognitive Radio Networks: Optimal Sensing Strategy, Power Allocation, and Sensing Order”, *IEEE Journal on Selected Areas in Communications*, Vol. 29, No. 8, pp. 1648–1659, 2011.
 29. Huang, S., H. Chen, Y. Zhang, and F. Zhao, “Energy-Efficient Cooperative Spectrum Sensing with Amplify-and-Forward Relaying”, *IEEE Communications Letters*, Vol. 16, No. 4, pp. 450–453, 2012.
 30. Deng, R., J. Chen, C. Yuen, P. Cheng, and Y. Sun, “Energy-Efficient Cooperative Spectrum Sensing by Optimal Scheduling in Sensor-Aided Cognitive Radio Networks”, *IEEE Transactions on Vehicular Technology*, Vol. 61, No. 2, pp. 716–725, 2012.
 31. Maleki, S., S. Chepuri, and G. Leus, “Energy and Throughput Efficient Strategies for Cooperative Spectrum Sensing in Cognitive Radios”, *IEEE 12th International Workshop on Signal Processing Advances in Wireless Communications (SPAWC)*, pp. 71–75, 2011.
 32. Lee, C.-H. and W. Wolf, “Energy Efficient Techniques for Cooperative Spectrum Sensing in Cognitive Radios”, *5th IEEE Consumer Communications and Networking Conference*, pp. 968–972, 2008.
 33. Peh, E. C., Y.-C. Liang, Y. L. Guan, and Y. Pei, “Energy-Efficient Cooperative Spectrum Sensing in Cognitive Radio Networks”, *IEEE Global Telecommunications Conference (GLOBECOM)*, pp. 1–5, 2011.

34. Chen, Y., Q. Zhao, and A. Swami, "Distributed Spectrum Sensing and Access in Cognitive Radio Networks With Energy Constraint", *IEEE Transactions on Signal Processing*, Vol. 57, No. 2, pp. 783–797, 2009.
35. Sun, X., T. Zhang, and D. Tsang, "Optimal Energy-Efficient Cooperative Sensing Scheduling for Cognitive Radio Networks with QoS Guarantee", *7th IEEE International Wireless Communications and Mobile Computing Conference (IWCMC)*, pp. 1825–1830, 2011.
36. Zhang, T. and D. H. K. Tsang, "Optimal Cooperative Sensing Scheduling for Energy-Efficient Cognitive Radio Networks", *INFOCOM, 2011 Proceedings IEEE*, pp. 2723–2731, 2011.
37. Hao, X., M. H. Cheung, V. W. S. Wong, and V. C. M. Leung, "A Coalition Formation Game for Energy-Efficient Cooperative Spectrum Sensing in Cognitive Radio Networks with Multiple Channels", *2011 IEEE Global Telecommunications Conference - GLOBECOM 2011*, pp. 1–6, 2011.
38. Liang, Y., Y. Zeng, E. Peh, and A. Hoang, "Sensing-Throughput Tradeoff for Cognitive Radio Networks", *IEEE Transactions on Wireless Communications*, Vol. 7, No. 4, pp. 1326–1337, 2008.
39. Cacciapuoti, A. S., I. F. Akyildiz, and L. Paura, "Correlation-Aware User Selection for Cooperative Spectrum Sensing in Cognitive Radio Ad Hoc Networks", *IEEE Journal on Selected Areas in Communications*, Vol. 30, No. 2, pp. 297–306, 2012.
40. Yucek, T. and H. Arslan, "A Survey of Spectrum Sensing Algorithms for Cognitive Radio Applications", *IEEE Communications Surveys & Tutorials*, Vol. 11, No. 1, pp. 116–130, 2009.
41. Zeng, K., P. Paweczak, and D. Cabric, "Reputation-Based Cooperative Spectrum Sensing with Trusted Nodes Assistance", *IEEE Communications Letters*, Vol. 14, No. 3, pp. 226–228, 2010.

42. Hui, P., J. Crowcroft, and E. Yoneki, “Bubble Rap: Social-Based Forwarding in Delay-Tolerant Networks”, *IEEE Transactions on Mobile Computing*, Vol. 10, No. 11, pp. 1576–1589, 2011.
43. Gao, W., Q. Li, B. Zhao, and G. Cao, “Multicasting in Delay Tolerant Networks: A Social Network Perspective”, *Proceedings of the Tenth ACM International Symposium on Mobile Ad Hoc Networking and Computing*, pp. 299–308, 2009.
44. Li, Y., P. Hui, D. Jin, L. Su, and L. Zeng, “Evaluating the Impact of Social Selfishness on the Epidemic Routing in Delay Tolerant Networks”, *IEEE Communications Letters*, Vol. 14, No. 11, pp. 1026–1028, 2010.
45. Chai, W. K., D. He, I. Psaras, and G. Pavlou, “Cache Less for More in Information-Centric Networks”, *NETWORKING 2012*, pp. 27–40, Springer, 2012.
46. Kas, M., S. Appala, C. Wang, K. Carley, L. Carley, and O. Tonguz, “What if Wireless Routers were Social? Approaching Wireless Mesh Networks from a Social Networks Perspective”, *IEEE Wireless Communications*, Vol. 19, No. 6, pp. 36–43, 2012.
47. Güven, C., S. Bayhan, and F. Alagöz, “Effect of Social Relations on Cooperative Sensing in Cognitive Radio Networks”, *First Int. Black Sea Conference on Communications and Networking (BlackSeaCom)*, pp. 247–251, 2013.
48. Chen, X., J. Huang, and H. Li, “Adaptive Channel Recommendation for Opportunistic Spectrum Access”, *IEEE Transactions on Mobile Computing*, Vol. 12, No. 9, pp. 1788–1800, 2013.
49. Bayhan, S. and J. Kangasharju, “Extending Cognitive Radios with New Perspectives”, *The Sixth International Conference on Ubiquitous and Future Networks (ICUFN)*, pp. 363–368, 2014.
50. Li, H., “Customer Reviews in Spectrum: Recommendation System in Cognitive

- Radio Networks”, *IEEE Symposium on New Frontiers in Dynamic Spectrum Access Networks*, pp. 1–9, 2010.
51. Eryigit, S. and T. Tugcu, “Joint Channel and User Selection for Transmission and Sensing in Cognitive Radio Networks”, *Cognitive Radio Oriented Wireless Networks and Communications (CROWNCOM), 7th International ICST Conference on*, pp. 54–59, 2012.
 52. Eryigit, S., G. Gur, S. Bayhan, and T. Tugcu, “Energy Efficiency is a Subtle Concept: Fundamental Trade-offs for Cognitive Radio Networks”, *IEEE Communications Magazine*, Vol. 52, No. 7, pp. 30–36, 2014.
 53. Wang, S., M. Ge, and W. Zhao, “Energy-Efficient Resource Allocation for OFDM-Based Cognitive Radio Networks”, *IEEE Transactions on Communications*, Vol. 61, No. 8, pp. 3181–3191, 2013.
 54. Xing, Y., C. Mathur, M. Haleem, R. Chandramouli, and K. P. Subbalakshmi, “Dynamic Spectrum Access with QoS and Interference Temperature Constraints”, *IEEE Transactions on Mobile Computing*, Vol. 6, No. 4, pp. 423–433, 2007.
 55. Ren, P., Y. Wang, and Q. Du, “CAD-MAC: A Channel-Aggregation Diversity Based MAC Protocol for Spectrum and Energy Efficient Cognitive Ad Hoc Networks”, *IEEE Journal on Selected Areas in Communications*, Vol. 32, No. 2, pp. 237–250, 2014.
 56. Bayhan, S. and F. Alagoz, “Scheduling in Centralized Cognitive Radio Networks for Energy Efficiency”, *IEEE Transactions on Vehicular Technology*, Vol. 62, No. 2, pp. 582–595, 2013.
 57. Kamruzzaman, S. M., E. Kim, and D. G. Jeong, “An Energy Efficient QoS Routing Protocol for Cognitive Radio Ad Hoc Networks”, *13th International Conference on Advanced Communication Technology (ICACT)*, pp. 344–349, 2011.

58. Lan, T., D. Kao, M. Chiang, and A. Sabharwal, “An Axiomatic Theory of Fairness in Network Resource Allocation”, *IEEE INFOCOM*, pp. 1343–1351, 2010.
59. Byun, S.-S., I. Balasingham, and X. Liang, “Dynamic Spectrum Allocation in Wireless Cognitive Sensor Networks: Improving Fairness and Energy Efficiency”, *IEEE Conference on Vehicular Technology (VTC)*, pp. 1–5, 2008.
60. Ge, M. and S. Wang, “Energy-Efficient Power Allocation for Cooperative Relaying Cognitive Radio Networks”, *IEEE Wireless Communications and Networking Conference (WCNC)*, pp. 691–696, 2013.
61. Sun, C. and C. Yang, “Energy Efficiency Analysis of One-Way and Two-Way Relay Systems”, *EURASIP Journal on Wireless Communications and Networking*, Vol. 2012, No. 1, pp. 1–18, 2012.
62. Zhang, X. and K. G. Shin, “E-Mili: Energy-Minimizing Idle Listening in Wireless Networks”, *IEEE Transactions on Mobile Computing*, Vol. 11, No. 9, pp. 1441–1454, 2012.
63. Althunibat, S., V. Sucasas, H. Marques, J. Rodriguez, R. Tafazolli, and F. Granelli, “On the Trade-Off Between Security and Energy Efficiency in Cooperative Spectrum Sensing for Cognitive Radio”, *IEEE Communications Letters*, Vol. 17, No. 8, pp. 1564–1567, 2013.
64. Li, H., *Cognitive Communications: Distributed Artificial Intelligence (DAI), Regulatory Policy, Economics, Implementation*, chapter 10: Social Behaviour in Cognitive Radio, John Wiley, Sons, Ltd, 2012.
65. Mukherjee, A., “Diffusion of Cooperative Behavior in Decentralized Cognitive Radio Networks with Selfish Spectrum Sensors”, *IEEE Journal of Selected Topics in Signal Processing*, Vol. 7, No. 2, pp. 175–183, 2013.
66. Park, S., H. Kim, and D. Hong, “Cognitive Radio Networks with Energy Har-

- vesting”, *IEEE Transactions on Wireless Communications*, Vol. 12, No. 3, pp. 1386–1397, 2013.
67. Ganesan, G. and Y. Li, “Cooperative Spectrum Sensing in Cognitive Radio Networks”, *First IEEE International Symposium on New Frontiers in Dynamic Spectrum Access Networks, 2005*, pp. 137–143, 2005.
68. Eryigit, S., S. Bayhan, and T. Tugcu, “Energy-Efficient Multichannel Cooperative Sensing Scheduling With Heterogeneous Channel Conditions”, *IEEE Transactions on Vehicular Technology*, Vol. 62, No. 6, pp. 2690–2699, 2013.
69. Alouini, M. and A. Goldsmith, “Capacity of Rayleigh Fading Channels Under Different Adaptive Transmission and Diversity-Combining Techniques”, *IEEE Transactions on Vehicular Technology*, Vol. 48, No. 4, pp. 1165–1181, 1999.
70. Conejo, A., E. Castillo, R. Miguez, and R. Garcia-Bertrand, *Decomposition Techniques in Mathematical Programming*, Springer, 2006.
71. Floudas, C. A., *Nonlinear and Mixed Integer Optimization. Fundamentals and Applications.*, Oxford University Press, New York, 1995.
72. Eryigit, S., S. Bayhan, and T. Tugcu, “Channel Switching Cost Aware and Energy-Efficient Cooperative Sensing Scheduling for Cognitive Radio Networks”, *IEEE International Conference on Communications (ICC)*, pp. 2633–2638, 2013.
73. Gozuppek, D., S. Buhari, and F. Alagoz, “A Spectrum Switching Delay Aware Scheduling Algorithm for Centralized Cognitive Radio Networks”, *IEEE Transactions on Mobile Computing*, Vol. 12, No. 7, pp. 1270–1280, 2013.
74. Chen, K.-C., M. Chiang, and H. Poor, “From Technological Networks to Social Networks”, *IEEE Journal on Selected Areas in Communications (JSAC)*, Vol. 31, No. 9, pp. 548–572, 2013.
75. Gonzalez, M. C., C. A. Hidalgo, and A.-L. Barabasi, “Understanding Individual

- Human Mobility Patterns”, *Nature*, Vol. 453, No. 7196, pp. 779–782, 2008.
76. Murawski, R., E. Ekici, V. Chakravarthy, and W. K. McQuay, “Performance of Highly Mobile Cognitive Radio Networks with Directional Antennas”, *IEEE International Conference on Communications (ICC)*, pp. 1–5, 2011.
77. Floudas, C. A. and P. M. Pardalos, *Encyclopedia of Optimization*, Vol. 1, Springer, 2008.
78. Hu, W. and G. Yen, “Adaptive Multiobjective Particle Swarm Optimization Based on Parallel Cell Coordinate System”, *IEEE Transactions on Evolutionary Computation*, 2014.
79. Deb, K., A. Pratap, S. Agarwal, and T. Meyarivan, “A Fast and Elitist Multiobjective Genetic Algorithm: NSGA-II”, *IEEE Transactions on Evolutionary Computation*, Vol. 6, No. 2, pp. 182–197, 2002.
80. Konak, A., D. W. Coit, and A. E. Smith, “Multi-Objective Optimization Using Genetic Algorithms: A Tutorial”, *Reliability Engineering and System Safety*, Vol. 91, No. 9, pp. 992–1007, 2006.
81. Emmerich, M., N. Beume, and B. Naujoks, “An EMO Algorithm Using the Hypervolume Measure as Selection Criterion”, Coello Coello, C., A. Hernandez Aguirre, and E. Zitzler (editors), *Evolutionary Multi-Criterion Optimization*, Vol. 3410 of *Lecture Notes in Computer Science*, pp. 62–76, Springer Berlin Heidelberg, 2005.
82. Chen, R., J.-M. Park, and K. Bian, “Robust Distributed Spectrum Sensing in Cognitive Radio Networks”, *The 27th IEEE Conference on Computer Communications (INFOCOM)*, 2008.
83. Xin, C. and M. Song, “Detection of PUE Attacks in Cognitive Radio Networks Based on Signal Activity Pattern”, *IEEE Transactions on Mobile Computing*, Vol. 13, No. 5, pp. 1022–1034, 2014.

84. Kantrowitz, M. M., Robert Neumann, "Optimization for Products of Concave Functions", *Rendiconti del Circolo Matematico di Palermo*, Vol. 54-2, pp. 291–302, 2005.